DIFFERENTIATED MAFIC-ULTRAMAFIC SILLS IN THE ARCHEAN VERMILION DISTRICT, NORTHEASTERN MINNESOTA

A THESIS
SUBMITTED TO THE FACULTY OF THE GRADUATE SCHOOL
OF THE UNIVERSITY OF MINNESOTA

BY
KLAUS JURGEN SCHULZ

IN PARTIAL FULFILLMENT OF THE REQUIREMENTS
FOR THE DEGREE OF
MASTER OF SCIENCE

FEBRUARY 1, 1974

ABSTRACT

Detailed mapping of part of the Newton Lake Formation north of Ely, Minnesota has shown the presence of numerous sill-like mafic-ultramafic intrusions in the Archean volcanic sequence. Three types of intrusions have been found: layered, differentiated mafic-ultramafic sills ranging from 400 to 1500 feet thick and at least 4 miles long; gabbroic sills of variable thickness and extent; and ultramafic lenses ranging from 75 to 300 feet thick and up to 3000 feet long.

The layered sills were studied in detail. They have a well-developed internal stratigraphy which consists of a lower chilled-margin, peridotite, pyroxenite, bronzite gabbro, and gabbro units and an upper chilled-margin. Petrographic studies indicate that the units formed by gravitational accumulation of mineral grains. The stratigraphic succession reflects the general order of crystalization: 1) chromite, 2) chromite + olivine, 3) clinopyroxene + orthopyroxene, 4) clinopyroxene + orthopyroxene + plagioclase, 5) clinopyroxene + plagioclase. Microprobe analyses of cumulus pyroxenes has shown cryptic variations exist between units.

The gabbroic sills are generally similar to the upper gabbroic parts of the layered sills. The ultramafic lenses consist of a central peridotite unit surround by a complex chilled-margin. Textural and structural features of

the ultramafic lenses suggest intrusion of an olivine bearing liquid, with flowage differentiation forming the peridotite unit and rapid chilling of a crystal free liquid forming the chilled-margin.

Differentiation trends of whole rock samples and calculated liquid compositions of the layered intrusions are generally in close agreement and show a general iron but minimal alkali enrichment with differentiation. Chemical analyses of chilled-margins are low in Al_2O_3 (10 wt%) and high in MgO (11 wt%) with a high CaO/Al_2O_3 ratio (0.85). The calculated bulk composition is distinctly ultrabasic in nature (MgO= 17 wt%). Mixing calculations utilizing least square methods suggest that the magma was partially differentiated at the time of intrusion. The bulk composition for the layered sills is very similar to high-MgO basalts from the Archean of Western Australia.

An inital magma temperature for the layered intrusions of between 1200°C and 1100°C is inferred from element partitioning between coexisting mineral phases. Textural relations and phase equilibria suggest that crystallization of both sills and lenses probably did not take place under pressures greater than about 1 kb. (2.7 km) and may have been even lower.

Metamorphism of the lower grades of the greenschist facies has affected all rocks of the Newton Lake Formation. The ultramafic rocks are serpentinized to varying degrees with olivine often the only altered phase.

Serpentinization appears to have occurred along small microfractures which cut the peridotite. The mafic rocks typically have actinolite, sausseritized plagioclase, chlorite, epidote, and rare sphene. Relict grains are common in both ultramafic and mafic units suggesting that metamorphic reactions were retarded perhaps by low H_2O and CO_2 availability and pressure.

The layered sills and lenses of the Newton Lake Formation apparently formed penecontemporaneously with the surrounding basic volcanic rocks. The layered sills probably formed as high level synvolcanic intrusions, some of which may have also acted as magma chambers for gabbroic liquids which formed sills and/or flows. The ultramafic lenses could be smaller injections of the same magma which formed the larger layered sills.

TABLE OF CONTENTS

Page

ABSTRACT.....i
TABLE OF CONTENTS.....iv
LIST OF ILLUSTRATIONS.....vi
INTRODUCTION.....1
Location.....1
Purpose.....1
Acknowledgements.....3
REGIONAL GEOLOGY.....3
Regional Setting.....3
Previous Work.....4
Newton Lake Formation.....8
Structure.....9
Metamorphism.....11
PRESENT STUDY.....12
Field Methods.....12
Laboratory Methods.....12
IGNEOUS GEOLOGY OF THE MAFIC-ULTRAMAFIC SILLS.....14
Form and Structure.....14
Terminology.....16
Layering.....16
Alteration.....24
Petrography of the Layered Sills.....24
Chilled-Margins.....24
Peridotite.....37
Pyroxenite.....49
Bronzite Gabbro.....57
Gabbro.....65
Residual Segregations.....70
Petrography of the Wholly Gabbroic Sills.....73
Petrography of the Ultramafic Lenses.....76
Description of Individual Intrusions.....82
Little Long Lake Sill.....82
Cedar Lake Sill.....83
Picketts Lake Sill.....85
PETROLOGY.....87
Formation of the Layered Sequence in the Differentiated Sills.....87
Peridotite.....91
Pyroxenite.....96
Bronzite Gabbro and Gabbro.....100
Formation of the Chilled-Margins.....104
Chilled-Margins of the Ultramafic Lenses.....109
PETROCHEMICAL ASPECTS OF NEWTON LAKE SILLS.....110
Mineral Chemistry for the Layered Sills.....110
Olivine.....110
Orthopyroxene.....113
Augite.....116
Chromian Spinels.....119
Amphibole.....120
Plagioclase.....126
Major Element Geochemistry of the Layered Sills.....130

Cedar Lake Sill.....130
Silica.....137
Aluminum.....137
Iron (Fe_2O_3 + FeO).....137
Magnesium.....138
Calcium.....138
Sodium.....139
Potassium.....139
Titanium.....139
Manganese.....139
Phosphorus.....140
Picketts Lake Sill Peridotite.....140
Differentiation Trends.....141
FeO_t - MgO - CaO Variation.....141
Alk - FeO_t - MgO Variation.....142
Oxides Versus MgO.....142
Successive Magmatic Liquid Compositions in a Differentiated Layered Sill.....147
Bulk Compositions of the Layered Sills.....153
Comparison of the Bulk and Chilled-Margin Compositions with other mafic rock types.....159
Order of Crystallization in the Layered Sills..167
Temperature and Pressure of Formation of the Layered Sills based on Mineral Composition and Textural Relations.....175
Temperature.....175
Orthopyroxene-Clinopyroxene.....175
Olivine-Chromian Spinel.....176
Ca/Ca + Mg Ratios in Pyroxenes.....178
Evaluation.....178
Pressure.....180
METAMORPHISM OF THE NEWTON LAKE SILLS.....182
General Preservation of Textures.....182
Ultramafic Rocks.....183
Mafic Rocks.....189
PETROGENESIS AND GEOLOGIC HISTORY FOR NEWTON LAKE SILLS.....191
Classification.....191
Origin of the Newton Lake Sills and Lenses.....193
Summary of the Geologic History of the Newton Lake Formation.....196
ECONOMIC GEOLOGY.....198
SUMMARY AND CONCLUSIONS.....200
REFERENCES.....205

LIST OF ILLUSTRATIONS

Plates

I Geologic Map of a Portion of the Newton Lake Formation.....Pocket
II NW-SE Structural Section of a Portion of the Newton Lake Formation.....Pocket

Tables

1. Rock-type Classification.....17
2. Alteration products for layered sill minerals..25
3. Modal compositions for chilled-margin zone.....30
4. Modal compositions for peridotite unit.....41
5. Modal compositions for pyroxenite unit.....50
6. Modal compositions for bronzite gabbro unit....59
7. Modal compositions for gabbro unit.....67
8. Chemical composition and structural formulas for analyzed olivines.....111
9. Chemical composition and structural formulas for analyzed pyroxenes.....115
10. Chemical composition and structural formulas for analyzed chromian spinels.....122
11. Chemical composition and structural formulas for analyzed primary amphiboles.....125
12. Chemical analyses from the Newton Lake layered sills.....133
13. Recalculated chemical analyses.....134
14. C.I.P.W. norms for recalculated chemical analyses.....135
15. Bulk analyses for relevant igneous rock types.165

Figures

1. Location map and geologic setting.....2
2a. General geologic map for the western portion of the Vermilion District.....5
2b. General geologic map of the central portion of the Vermilion District.....6
3. Major zones and units for a typical layered differentiated sill.....18
4. Stratigraphic columns for some of the Newton Lake sills.....20
5. Rhythmic layering in a bronzite gabbro.....23
6. Lamination in peridotite.....23
7. Ideal chilled-margin sequence.....28
8. Photomicrograph: Unit A, chilled-margin.....32
9. Photomicrograph: amygdule, Unit B, chilled-margin.....32
10. Photomicrograph: skeletal clinopyroxene, Unit B, chilled-margin.....32
11. Camera-lucid drawing of skeletal pyroxenes.....34
12. Photomicrograph: branching clinopyroxene, Unit B, chilled-margin.....36

13. Hand sample showing variolites.....36
14. Photomicrograph: skeletal plagioclase, Unit C, chilled-margin.....36
15. Pyroxene oikocrysts in peridotite.....39
16. Serpentinized peridotite.....39
17. Photomicrograph: embayed olivine; peridotite....43
18. Photomicrograph: fluid inclusion in olivine; peridotite.....43
19. Photomicrograph: embayed chromite; peridotite...47
20. Photomicrograph: euhedral elinopyroxene; peridotite.....47
21. Hand sample, pyroxenite.....53
22. Photomicrograph: twinned augite; pyroxenite.....53
23. Photomicrograph: interference texture; pyroxenite.....53
24. Photomicrograph: orthopyroxene phenocryst with embayed augite inclusions; pyroxenite.....56
25. Photomicrograph: exsolution in orthopyroxene phenocryst.....56
26. Hand sample, bronzite gabbro.....62
27. Photomicrograph: orthopyroxene phenocryst with enclosed plagioclase; bronzite gabbro.....62
28. Photomicrograph: poikilitic orthopyroxene; bronzite gabbro.....62
29. Photomicrograph: augite; bronzite gabbro.....64
30. Photomicrograph: poikilitic augite; bronzite gabbro.....64
31. Hand sample, gabbro.....69
32. Photomicrograph: ferro augite; gabbro.....69
33. Photomicrograph: micrographic texture; gabbro...72
34. Photomicrograph: iron-titanium oxide; gabbro...72
35. Photomicrograph: granophyric gabbro.....74
36. Cross section of an ultramafic lens.....77
37. Photomicrograph: zoned hornblende; ultramafic lens peridotite.....81
38. Branching clinopyroxene ultramafic lens chilled-margin.....81
39. Photomicrograph: zoned augite; Picketts Lake sill peridotite.....81
40. Shape of plagioclase with varying degrees of supercooling.....107
41. Comparison of olivine compositions from mafic and ultramafic intrusion types.....112
42. Pyroxene crystallization trend.....118
43. Plot of Cr/(Cr + Al) vs Mg/(Mg + Fe^{++}) for analyzed spinels.....123
44a. Photomicrograph: hollow plagioclase; Unit C, chilled-margin.....128
44b. Potassium microprobe scan.....128
44c. Calcium microprobe scan.....128
45. Ab-An-Or diagram showing plagioclase lamellae compositions.....129
46. Major element variation for the Cedar Lake sill.....136

47. FeO_t - MgO - CaO variation diagram.....143
48. FeO_t - MgO - Alk variation diagram.....144
49. Major oxides versus MgO diagram.....145
50. FeO_t - MgO - CaO variation diagram for Cedar Lake sill liquids.....150
51. FeO_t - MgO - Alk variation diagram for Cedar Lake liquids.....151
52. Major oxides versus MgO for Cedar Lake sill liquids.....152
53. Alkali-silica plot for chilled-margin compositions.....160
54. MgO - CaO - Al_2O_3 diagram.....161
55. $CaO/(CaO + Al_2O_3)$ vs $FeO_t/(FeO_t + MgO)$ plot for Newton Lake rocks.....163
56. Ol-Cpx-Pl-Q phase diagram model.....170
57. Ol and Cpx projections from Ol-Cpx-Pl-Q phase diagram.....174
58. Equilibrium relations along the join $MgSiO_3$ - $CaMgSi_2O_6$.....179
59. Equilibrium curves for serpentine reactions.....188
60. ACF diagram.....190

INTRODUCTION

Location

The area investigated is located in the Vermilion District, about four miles north of the town of Ely in St. Loius County, Minnesota. The area mapped encompasses, in part or whole, 19 sections in the Ely 7.5 minute quadrangle (T.63-64N., R.11-12W.) and four sections in the Shagawa Lake 7.5 minute quadrangle (three in T.63N., R.12W. and one in T.63N., R.13W.). (See Figure 1 for outline of area and Plate 1).

Access to the area is provided by two roads: the Echo Trail (County Highway 116), which crosses the western portion of the project area and an old, converted railroad grade, locally called the "Old Cloquet Line", which crosses the eastern portion. Numerous lakes and portage trails also provide access to many parts of the map area.

Purpose

Layered mafic-ultramafic bodies have been described from many Early Precambrian metavolcanic-metasedimentary complexes throughout the world (see MacRae, 1969; Williams and Hallberg, 1973). The occurrence of such bodies in the Vermilion District of northeastern Minnesota has just recently been discovered (Green, 1970 a,b). The purpose of this investigation was three fold: 1) to map in detail some of these mafic-ultramafic bodies, 2) to

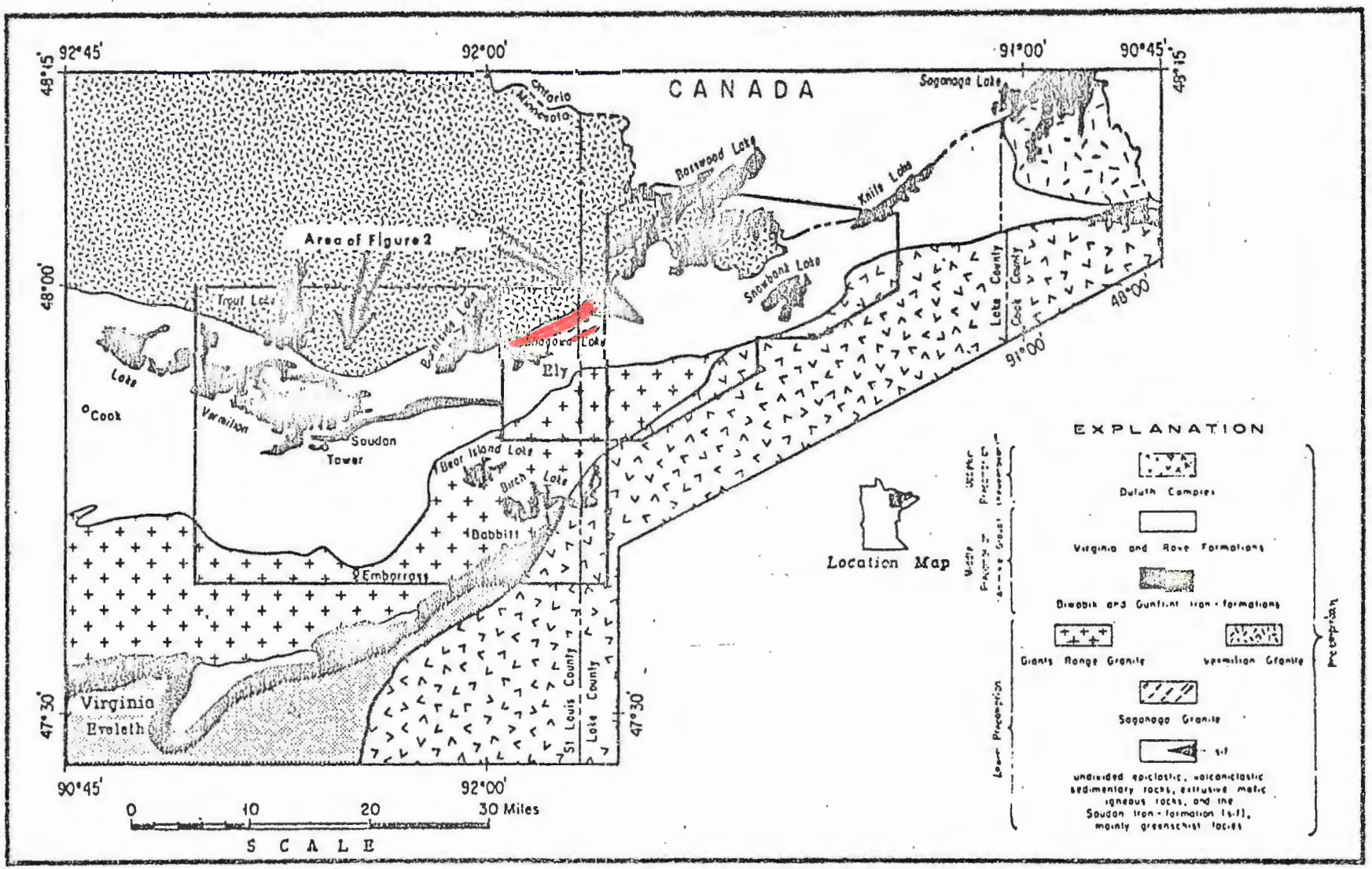

Figure 1. Location map and geologic setting of the project area (in red) within the Vermilion district of northeastern Minnesota (after Sims and others, 1972).

determine the structural relations between the bodies and the surrounding rocks and 3) to conduct a petrologic study of the bodies, compare them to described Precambrian mafic-ultramafic bodies and attempt to determine their origin.

Acknowledgments

The writer is indebted to Dr. John C. Green, who suggested the project and supervised the investigation, and to Dr. Paul W. Weiblen for his helpful suggestions and guidance in the use of the electron microprobe. The Minnesota Geological Survey provided financial assistance for the field work and for eight chemical analyses and this support is greatfully acknowledged. Special thanks go to my wife Charlene, whose patience and typing skills were important to the completion of this thesis.

REGIONAL GEOLOGY

Regional Setting

The Vermilion District lies at the southern edge of the Superior (structural) Province of the Canadian Shield, and all bedrock is Precambrian in age. The region has an extensive cover of Pleistocene sand, gravel and till, however in the area investigated, outcrop averages about 30 percent and is as high as 60 percent locally in some sections. The outcrops form many prominent ridges

and smaller knobs. Many of the linear topographic lows, which are generally drift-covered, are eroded in shear zones and faults.

Previous Work

The Vermilion District is a volcanic-sedimentary complex of Early Precambrian (Archean) age and is bordered by granitic batholiths on the north and south. The general geology of the district was first described by Clements (1903). He concluded that the sequence consisted mainly of an older mafic volcanic succession, the Ely Greenstone, and a younger sedimentary succession dominated by the "Knife Lake Slates". The work of Clements was subsequently refined by Grout (1926) and Gruner (1941).

Goldich and others (1961) developed a time framework for the Vermilion District, based on K-Ar ages. This work showed only one important igneous-tectonic event at about 2400 - 2750 m.y. (the Algoman Orogeny, Goldich, 1968).

In 1962 the Minnesota Geological Survey began a restudy of the geology of northeastern Minnesota. Work done by Green, Phinney and Weiblen (1966), Green (1970 a), Griffin and Morey (1969), Griffin (1969) and Morey and others (1970) shows the geology to be more complex than indicated by earlier workers. Morey and others (1970) revised the stratigraphy as shown in Figure 2. Available information indicates that the metavolcanic-metasedimentary sequence constitutes a complex volcanic pile, deposited

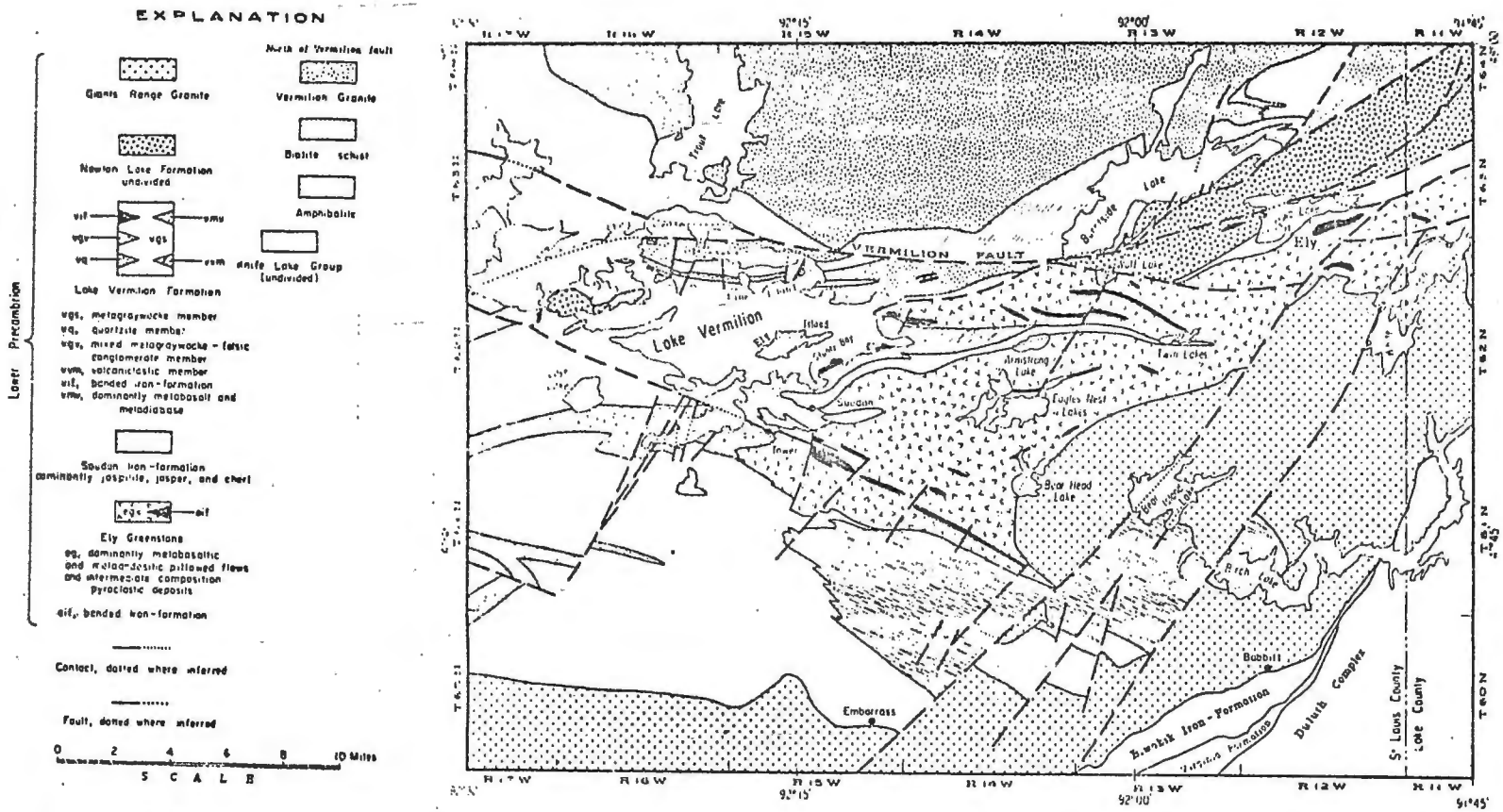

Figure 2 a. General geologic map for the western portion of the Vermilion district (after Morey and others, 1970).

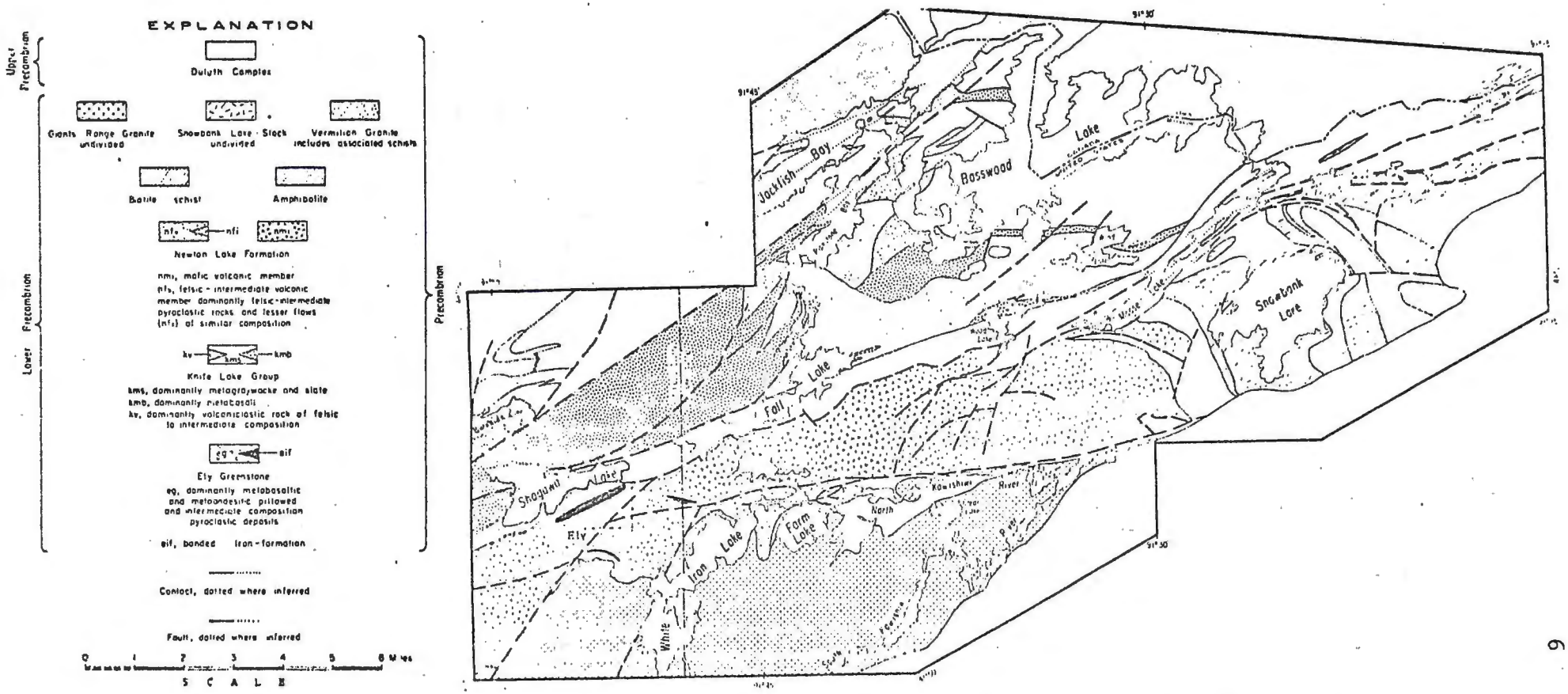

Figure 2 b. General geologic map for the Central portion of the Vermilion district (after Morey and others, 1970).

largely in a subaqueous environment (Sims and others, 1972).

Much work has been done to better define the geological history of the Early Precambrian rocks of northeastern Minnesota. Work by Anderson (1965), Hanson and others (1971), Hart and Davis (1969), Jahn and Murthy (1971), Goldich and others (1972), Peterman and others (1972) and Prince and Hanson (1972) have attempted to resolve ages for the two possible orogenic periods, Laurentian and Algoman, recognized by the early workers. Studies based on K-Ar and Rb-Sr have been unsuccessful, but U-Pb data suggests that structural deformation and igneous activity were more or less continuous from 2700 to 2750 m.y. and that two separate periods do not exist (Peterman and others, 1972). Work on the rare earth elements from the major igneous-rock types of the area is being done (Arth, 1973 and Arth and Hanson, 1972) in an effort to determine the nature and origin for these rocks.

John C. Green (Green and others, 1966, and Green,1970a,b) was the first to describe ultramafic rock from the Vermilion District. In the Gabbro Lake quadrangle five metaperidotite bodies bordered by metagabbros were found intruding a dominantly pillowed metabasaltic Archean sequence. Recent mapping shows that several similar bodies, some considerably larger, also exist to the west in the Ely quadrangle (Green, Minnesota Geological Survey open file map, Ely 7 1/2 minute quadrangle, 1972). The mafic-ultramafic bodies were mapped as concordant structures in sur-

rounding rocks and interpreted as synvolcanic in nature (Green, 1970 a).

Newton Lake Formation

The mafic-ultramafic bodies investigated occur within the Newton Lake Formation as defined by Morey and others (1970). The Newton Lake Formation was originally considered part of the Ely Greenstone by Clements (1903) but was renamed since recent work (Green, 1970 a) has shown it to be stratigraphically younger than at least part of the Knife Lake group and not equivalent to the Ely Greenstone, which is older than the Knife Lake (see Figure 2).

The Newton Lake Formation is divided into two informal members by Morey and others (1970), a mafic metavolcanic member west of Newton Lake and a felsic-intermediate metavolcanic member east of Newton Lake. The area investigated lies within the mafic member, so discussion will be restricted to this member. The reader is referred to Green (1970 a) for a detailed description of the felsic-intermediate member. No mafic-ultramafic bodies have been reported to occur in the felsic member.

The Newton Lake Formation, in the area investigated, is composed of about 60 percent mafic-ultramafic bodies and 40 percent mafic-metavolcanics and minor sediments. The common mafic metavolcanic is a dark colored, pillowed to massive and sometimes variolitic metabasalt. Textures are fine-grained diabasic or ophitic with a common mineral assemblage of albite, quartz, chlorite, calcite, sericite,

epidote, magnetite, sphene and some tremolite-actinolite. A minor type of greenstone occurs on the south side of Cedar Lake in the SE 1/4, Sec. 13, T.65N., R.12W. and SE 1/4, Sec. 7, T.63N., R.11W. and the northeast end of Picketts Lake in the SE 1/4, Sec. 6, T.63N., R.11W. This rock is black, commonly pillowed, and shows 4 mm. long radiating amphiboles. In thin section, the rock contains thin skeletal pyroxenes, now largely actinolite, set in a groundmass of tremolite-actinolite and feldspar. The common occurrence of pillows in both types of metavolcanics indicates a submarine origin.

Sedimentary rocks are rarely exposed, but several small outcrops of laminated, mafic to intermediate metagraywacke are located on the north shore and to the north and northeast of Camp Lake, Sec. 28, T.64N., R.11W., and outcrops of metagraywacke and metatuff occur south of Little Long Lake in Sec. 16, T.63N., R.12W. Drilling in this area has encountered considerable amounts of sedimentary rocks which suggests that sediments and tuffs may be more common than is indicated by surface mapping.

Structure

Foliations and stratigraphic units of the area have a general northeast strike with dips varying from vertical to steeply dipping to the northwest. The gabbroic portions of the mafic-ultramafic bodies and the mafic metavolcanics are relatively competent units compared to the ultramafics and sediments. The abundance of gabbro

and mafic metavolcanics in the area, has resulted in deformation primarily by localized shearing and faulting, with only rare and widely-spaced folds.

Numerous faults have been mapped based on offsets in rock units, shearing and topographic lineaments. Two sets of high-angle faults have been recognized as having either longitudinal or transverse trends. A major longitudinal fault, the Vermilion fault, seperates the Vermilion batholith from the Newton Lake Formation (see Plate 1). Sims and others (1972) indicate a possible horizontal displacement of several miles and a verticle displacement on the order of a mile for this fault. Other longitudinal faults lie south of the Vermilion fault (see Figure 2 and Plate 1). Exact displacement on these faults is unknown but is probably less than for the Vermilion fault.

Northwestward or north-northeastward trending transverse faults with a dominantly left-lateral displacement cut up the area into a number of blocks or segments. A number of these faults appear to be the result of a horse-tailing effect of the longitudinal faults as they terminate. The transverse faults are generally earlier than the longitudinal faults as offsets by the latter appear common. Later movements along some faults has occurred and helped to complicate the structural relations.

Numerous sheared zones in the metavolcanics, metagabbros, and more commonly in the ultramafics appear to be related to nearby faults along which some displacement

can be demonstrated. The ultramafic rocks often show abundant, throughgoing, parallel microfractures, that appear unrelated to any primary igneous fabric, cutting otherwise massive outcrops. Serpentinization can be seen to have followed these fractures in many samples indicating that the serpentinization post dates intrusion and crystallization (Green, 1970 b).

Folding in the area is marked by broad isoclinal anticlines and synclines (Green, Minnesota Geological Survey open file map, Ely 7.5 minute quadrangle, 1972). Evidence for this folding consists mainly of top-sense indicators such as abundant pillows in the mafic metavolcanics and differentiation and layering in the mafic-ultramafic bodies (discussed below). An isoclinal syncline is located north of Shagawa Lake, with an axial trace trending northeastward through the NW 1/4 of Sec. 22 and SE 1/4 of Sec. 15, T.63N., R.12W. Both ends of this fold are truncated by faulting. An anticline is inferred to exist to the northwest of the syncline based on a change in top directions, but the location of the axis for this fold is still undetermined. An isoclinal anticlinal fold is also found near Cedar Lake. The axis of the fold is marked by a longitudinal fault trending northeast through the center of Cedar Lake (Sec. 7, T.63N., R.11W.).

Metamorphism

The rocks of the area have all been altered by low-

grade regional metamorphism to the greenschist facies. The mafic rocks commonly contain a mineral assemblage characteristic of the chlorite zone of the greenschist facies (Turner, 1968), that includes chlorite, tremolite-actinolite, epidote, albite, quartz and calcite. The peridotites contain abundant serpentine and small amounts of talc and tremolite. Relict igneous minerals are common even though metamorphic recrystallization has been pervasive in the rocks, indicating that recrystallization was not complete. Igneous textures are also generally well preserved unless the rock is strongly sheared.

PRESENT STUDY

Field Work

Six weeks of field mapping were conducted in August and September of 1972. Mapping was done on a scale of 1 to 12,000 on enlargements of the Ely and Shagawa Lake 7.5 minute quadrangles. Mapping was carried out by means of pace-and-compass traverses and by walking obviously continuous ridges. Air photos were used to help plan traverses and locate outcrops. Plate 1 is a geologic map of the investigated area based on this mapping and that of Green (Minnesota Geological Survey open file map, Ely 7.5 minute quadrangle, 1972).

Laboratory Methods

Laboratory work included petrographic, electron microprobe and x-ray studies. A total of 160 thin-sections

were examined in the study. An attempt was made to obtain thin-sections from each mafic-ultramafic body mapped to best determine variations present in the bodies. Point counts of 1000 or more points were carried out on 30 of the least altered samples in an attempt to obtain the best estimate of the original mineralogy of the rocks.

Microprobe mineral analyses were made on twelve rock samples, in order to determine mineral compositional variations through a particular body. This work was carried out at the University of Minnesota, Department of Geology using a MAC Model 400 electron microprobe.

The electron microprobe analyses were made on polished thin section covered with a thin carbon film. An accuracy of 1 to 5% of the actual amount present is assumed for the microprobe data obtained, with the least accuracy obtained for the minor elements especially Na_2O and K_2O. Microprobe data was corrected for background and reduced with the aid of a computer program provided by the Department of Geology, University of Minnesota, Minneapolis. For a more detailed discussion of the data collection and reduction procedures used see Grant and Weiblen (1971).

X-ray analysis was mainly used to help identify alteration minerals (see Table 2).

A total of eight chemical analyses of rock samples were also obtained and were chosen to show whole-rock chem-

ical variations upward through a layered, differentiated mafic-ultramafic body. Samples were prepared by crushing and grinding (in a steel motor) slabs sawn through homogeneous hand samples.

IGNEOUS GEOLOGY OF THE MAFIC-ULTRAMAFIC SILLS

Form and Structure

The intrusions of the area may be catergorized into three types. The first, represented by the Ceder Lake sill, (Plate 1), consists of a sequence of peridotite, pyroxenite and gabbro. The second, represented by lenses southwest of Bright Lake, consists wholly of peridotite surrounded by a complex chilled zone. The third, represented by Bass Lake gabbroic sill, consists wholly of gabbroic rocks. The exact number of bodies present in the mapped area is impossible to determine with certainty because of the complex structural relations present; however, at least nine layered, differentiated mafic-ultramafic bodies, threee wholly peridotite bodies and several gabbroic bodies are thought to be present.

The mafic-ultramafic bodies appear as intrusive units conformable to the surrounding metavolcanics and are interpreted as layered, differentiated sills. Lower contacts are commonly highly sheared and fault-bounded and where contacts are observed, dips are very steep to verticle, as are the contacts within the country rocks.

The general form of the sills is lens-like. No feeder dikes have been recognized in the mapped area.

The principal mafic-ultramafic sills range in thickness from about 400 to 1500 feet (133 - 500 meters). The wholly ultramafic lenses are thinner, ranging from 75 to about 300 feet (25 to 100 meters). Because of the folding and complex faulting the sills are now highly segmented and their original lengths cannot be estimated with certainty. Two bodies are estimated, however, to be at least 4 miles (6.5 kilometers) long. The ultramafic lenses range from about 2000 to 3000 feet (660 to 1000 meters) long.

Most of the sills consist of layers of peridotite, pyroxenite and gabbro, which tend to occur in that stratigraphic succession. Both lower and upper margins are characteristically marked by complex chilled zones. The great extent of the major internal layers and their textures (discussed below) indicate that they formed by gravitational accumulation of mineral grains with the order of succession apparently reflecting the general order of crystallization: olivine; clinopyroxene and/or orthopyroxene; clinopyroxene, orthopyroxene and plagioclase; clinopyroxene and plagioclase. The stratigraphic sequence is structurally supported by top determinations based on pillows in surrounding metavolcanic rocks. The contacts between peridotite and pyroxenite layers are sharp, while other contacts between layers are somewhat

gradational. Layers are grossly uniform in composition, although in places, size grading and small-scale (rhythmic) layering are present.

Terminology

In describing the petrogrphy and petrology of these sills the terminology developed by Wager, Brown and Wadsworth (1960) and Jackson (1967 and 1971), for rocks formed by accumulation of minerals, has been used. The term cumulate, originally proposed by Wager and others in 1960, refers to any rock formed by crystal accumulation. The term cumulus refers to a texture produced by a crystal forming outside of and previously to, the magmatic sediment in which it now occurs, while postcumulus material refers to primary material that formed in situ (Jackson, 1967). Postcumulus overgrowth and postcumulus replacement refer to processes that modify cumulus crystals (Jackson, 1971).

The rock-type classification used for this study has been adapted from MacRae (1969) and is given in Table 1.

Layering

The typical complete sequence for the differentiated mafic-ultramafic sills is shown in Figure 3. The typical sill can be divided into four "zones" or mappable units; a lower chilled zone followed by ultramafic, mafic and upper chilled zones. The ultramafic and mafic zones can be

Table 1: Rock-type Classification (adopted from MacRae, 1969).

Rock Name	Cumulus	Intercumulus
Peridotite	30-90% Olivine (Minor Chromite)	40-10% Pyroxene 30-0% Plagioclase 20-0% Hornblende
Pyroxenite	70-90% Pyroxene 10-0% Olivine	30-10% Pyroxene, Plagioclase
Bronzite Gabbro	30-50% Plagioclase 30-50% Clinopyroxene 1-20% Orthopyroxene	20-5% Plagioclase 20-5% Pyroxene 0-5% Quartz 0-5% Oxides, Sulfides
Gabbro*		40-60% Plagioclase 20-50% Pyroxene 0-5% Olivine 0-5% Quartz 0-5% Oxides, Sulfides
Quartz Gabbro*		40-60% Plagioclase 20-50% Pyroxene 5-15% Quartz + Granophyric Intergrowths 0-5% Oxides, Sulfides

* Does not have cumulus texture.

ZONES	UNITS	MINERALS	
Upper chilled zone*		Plagioclase-Pyroxene	
Mafic Zone	Gabbro	Plagioclase Clinopyroxene Iron-titanium Oxides Quartz	
		Cumulus	Intercumulus
	Bronzite Gabbro	Plagioclase Clinopyroxene Orthopyroxene	Quartz Iron-titanium Oxides
Ultramafic Zone	Pyroxenite	Climopyroxene Orthopyroxene	Plagioclase
	Peridotite	Olivine Chromite	Clinopyroxene Orthopyroxene Plagioclase Hornblend
Lower Chilled Zone*		Plagioclase - Pyroxene	

Figure 3. Major zones and units for a typical layered differentiated Newton Lake sill. Also shown are major minerals for each of the units. *, units of the chilled-zone shown on Figure 7.

further subdivided into units based on mineral association and composition. The typical sequence so determined is: a lower chilled zone followed by peridotite, pyroxenite, bronzite gabbro and gabbro units and an upper chilled zone. Figure 4 shows stratigraphic columns for some of the major sills.

The contacts between layers are generally marked by the appearance or disappearance of a cumulus mineral. The contact between the peridotite and pyroxenite units is generally quite sharp, occurring within a few inches. It marks the disappearance of olivine and appearance of pyroxene as the major cumulus phase. This contact can also be mapped by magnetometer since magnetite is quite abundant in the peridotites but generally absent in the pyroxenite. The contact between the pyroxenite and bronzite gabbro units is gradational in nature occurring over a distance of about 20 feet. In passing from the pyroxenite to the bronzite gabbro, plagioclase first becomes a cumulus phase and increases in amount at the expense of pyroxene upwards through the sill. The contact between the bronzite gabbro and gabbro units is also gradational over a distance of about 50 feet and is marked by the disappearance of orthopyroxene and the development of a hypidiomorphic granular texture in the gabbros. The lower chilled zone is generally in sharp contact with peridotite while the upper chilled zone is gradational downward into gabbro over a distance of about 20 feet.

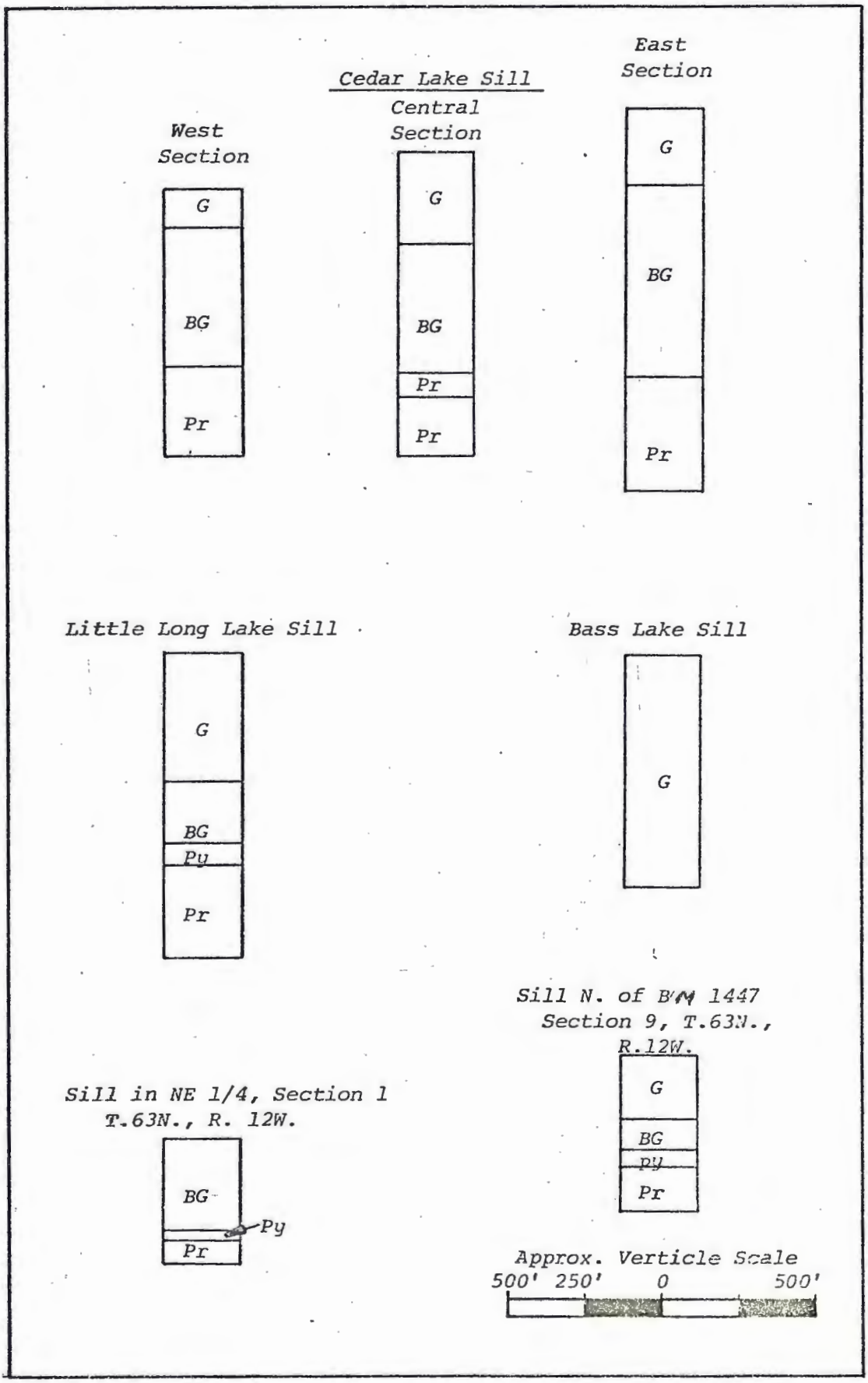

Figure 4. Stratigraphic columns for some of the Newton Lake sills. Pr = peridotite, Py = pyroxenite, BG = bronzite gabbro, G = gabbro.

Cryptic or chemical-graded layering (Jackson, 1971) is not directly determinable in most sills because of metamorphic alteration of original minerals, but it can be demonstrated using normative mineral compositions (Table 14). Determination of relict pyroxene compositions by electron microprobe analyses does show a progressive increase in iron with increasing height (see Figure 42). It is inferred that plagioclase increases in sodium upwards through a sill based on the normative compositions; however, direct determination has not been possible because of extreme alteration.

Though phase and cryptic layering are both well developed in the sills, rhythmic layering is rare or absent. Size-graded layers were observed in drill core from a thick peridotite unit located in the SE 1/4, SE 1/4 of Sec. 36, T.64N., R.12W. Occasional rhythmic layering has also been observed in the bronzite gabbro unit of some sills (Figure 5). Igneous lamination has only been observed in a few peridotite units where elongate olivines show a slight preferred orientation (Figure 6). The general lack of rhythmic layering may indicate that convection was not very strong in the magma chambers and possibly lacking except for the thicker intrusive bodies.

Cyclic units, which appear to be a feature of the ultramafic zone of many layered intrusions (Jackson, 1967) appear to be generally absent in these bodies. One pos-

Key to Figures

Figure 5. Rhythmic layering in a bronzite gabbro. White is plagioclase, black and gray are pyroxene. Layering is a result of changes in the pyroxene to plagioclase ratio. Sample SEN-326 NW 1/4 of NW 1/4 Sec. 11, T.63N., R.12W.

Figure 6. Peridotite showing faint lamination due to orientation of olivines (indicated by arrow). Note also the weathering of olivine in relief. Sample SEN-106, NE 1/4 of NW 1/4, Sec. 32, T.64N., R.11W.

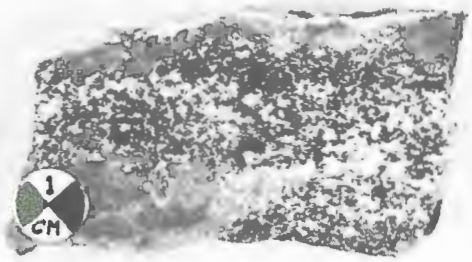

5

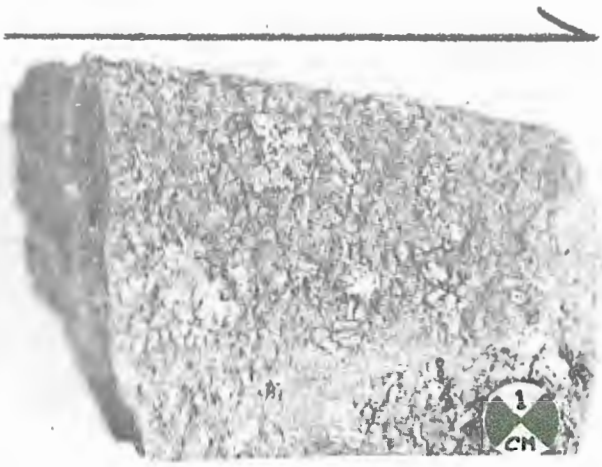

6

sible cyclic unit does occur in the Cedar Lake sill where a peridotite-pyroxenite sequence is repeated at least once.

Alteration

Though a detailed examination of the secondary minerals was not conducted it was necessary, in studying these extensively altered igneous rocks with preserved original textures, to establish criteria for distinguishing the pseudomorphs of different primary minerals. The methods used for identification are based on recognition of relict textures, the form of the pseudomorphs and on the morphology, identity and pattern of development of the secondary minerals. Comparisons with similar altered rocks described from other areas (e.g. Williams, 1971) have been helpful. Unaltered relics of primary minerals have, in many cases aided as controls in the identification. Table 2 shows the main alteration products found in the ultramafic, mafic and chilled zones of the layered sills. Details of the alteration are discussed in the section dealing with metamorphism of the sills (see page 182).

Petrography of the Layered Sills

Chilled Margins

Complex chilled margins have been located on many of the layered sills of the area. It is probable that most or all the layered sills developed such chilled margins but that many have not been preserved in out-

Table 2: Common alteration products for minerals of the layered, differentiated sills produced during metamorphism.

Ultramafic Zone	
Olivine	Serpentine (s) → Antigorite + Magnetite
	Tremolite (?) + Talc
Orthopyroxene	Talc + Tremolite → Chlorite
	Bastite (s) → Chlorite
Clinopyroxene	→ Tremolite - Actinolite ± Magnetite
Plagioclase	→ Chlorite
Mafic Zone	
Orthopyroxene	Chlorite + Tremolite
	Talc + Tremolite
Clinopyroxene	→ Actinolite
Plagioclase	→ Saussurite
Iron-titanium oxides	→ Sphene + Leucoxene
Chilled Zone	
Plagioclase	→ Saussurite
Clinopyroxene	→ Actinolite

→ common alteration
-→ less common alteration
s-serpentinization

crop. Chilled margins are found both at the lower and upper contacts, however the lower contact is less often preserved in outcrop because of the common occurrence of shearing in the peridotite and faults at the base of the sills. It is also possible that intrusion of underlying sills may have partially engulfed the lower chilled margins of some overlying sills. The absence of good outcrop at contacts has made it difficult to reconstruct any one complete chilled margin sequence. However, by combining data collected from various sills a reconstruction has been attempted and is presented in Figure 7. Ripley (1973), working on the Deer Lake Ultramafic Complex in Itasca County, Minnesota, has observed similar chilled margins on sills in that area. His reconstruction for the chilled margins is based largely on drill core evidence and is almost identical to that shown in Figure 7.

Though it is difficult to determine accurately the thickness of the chilled zones, it appears that the lower chilled zone is about 10 to 20 feet thick whereas the upper chilled zone is somewhat thicker (20 to 50 feet). The lower zone is in sharp contact with the overlying peridotite; the upper zone is gradational down into the underlying gabbro. Rock types for both zones are the same, though the upper zone is generally somewhat coarser-grained.

As shown in Figure 7, each chilled margin can gen-

Figure 7. Idealized chilled margin sequence for Newton Lake layered sills and lenses based on a compilation of field observation. The sketch depicts the relations for the chilled margins between two concordant sills (i.e. lower chilled margin of one in contact with upper chilled margin of another layered sill). Dashed lines indicate gradational contacts between units and the solid line shows the sharp contact found between peridotite and Unit C of the chilled margin. Plumose is used as a general descriptive term for the skeletal and branching nature of the pyroxene and plagioclase found in Units B and C (see Figures 8 - 14).

IDEAL CHILLED MARGIN SEQUENCE

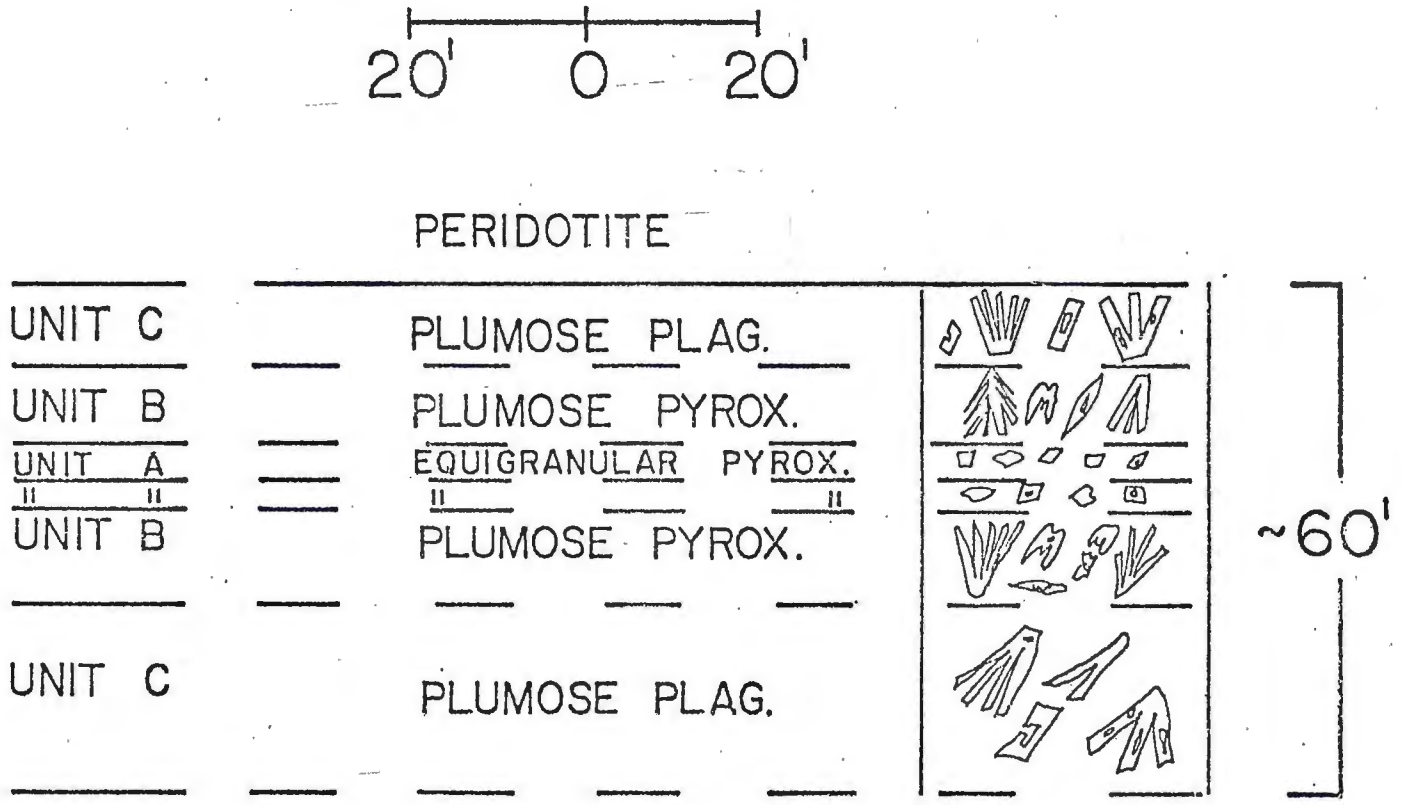

Fig. 7

erally be divided into 3 units, based on thin section examination. These units are completely gradational and are difficult though not everywhere impossible to differentiate in outcrop. While the sequence as shown appears to be typical for many sills it is not representative of all. A reversal in the sequence has been noted in at least one sill based on an outcrop in the NW 1/4, NW 1/4, Sec. 11, T.63N., R.12W. Modes for seven chill margin samples are presented in Table 3.

The first unit encountered (nearest the contact; "Unit A") is typically about 5 feet thick. It is a fine-grained, dark green basaltic appearing rock, consisting of about 50% small (1 mm) blocky amphibole pseudomorphs after clinopyroxene surrounded by a fine groundmass of intergrown altered plagioclase and pyroxene (Figure 8). The pyroxene pseudomorphs often have chlorite-filled centers suggesting that they were originally hollow, skeletal crystals possibly filled with glass. Small rounded grains of sulfide and oxide minerals are locally quite abundant in this unit forming up to 4 or 5% of the rock. The higher concentration appears more commonly in the lower chilled zone where the unit is characteristically highly oxidized and limonite stained. Amygdules are quite common toward the inner part of the unit and may be present in amounts up to 3%. They are about 1 mm in diameter and are filled with amphibole and altered plagioclase. They are also generally partially or com-

Table 3: Modal Compositions for Rocks of the Chilled Margin Zone.

Mineral	SES-22	SEN-271	SEN-323	SEN-324	SEN-211+	SEN-212+	SEN-213+
Plagioclase + Alteration	44.1	---	69.3	---	---	---	---
Clinopyroxene + Alteration	15.4	36.6	5.2	39.6	29.1	38.8	52.1
Groundmass*	36.5	59.3	22.1	59.3	69.7	55.7	40.9
Opaques	4.0	0.5	3.4	1.1	0.2	1.0	1.7
Amygdules	---	3.6	---	---	1.0	4.5	5.3
Total Points Counted	1000	1000	1000	1000	1000	1000	1000

+, Samples of Chilled Margin from Ultramafic Lens.
*, Plagioclase + Clinopyroxene Intergrowth.

Key to Figures

Figure 8. Photomicrograph of a sample from Unit A of the chilled margins. Note blocky amphibole pseudomorphs after clinopyroxene in groundmass of altered plagioclase and pyroxene (and/or glass). Sample SEN-268, NE 1/4 of NW 1/4, Sec. 1, T.63N., R.12W. Scale 1mm ~15μ (75x).

Figure 9. Photomicrograph of sulfide rimmed amygdule from Unit A of chilled margins. Amygdule filled with chlorite, amphibole and epidote. Surrounding material same as in Figure 8. Sample SEN-268, same as Figure 8. Scale 1mm ~15μ (75x).

Figure 10. Photomicrograph of skeletal clinopyroxene (now amphibole) from Unit B of chilled margins. Note variety of shapes present. Sample SEN-324, NW 1/4 of NW 1/4, Sec. 11, T.63N., R.12W. Scale 1mm ~15μ (75x).

8

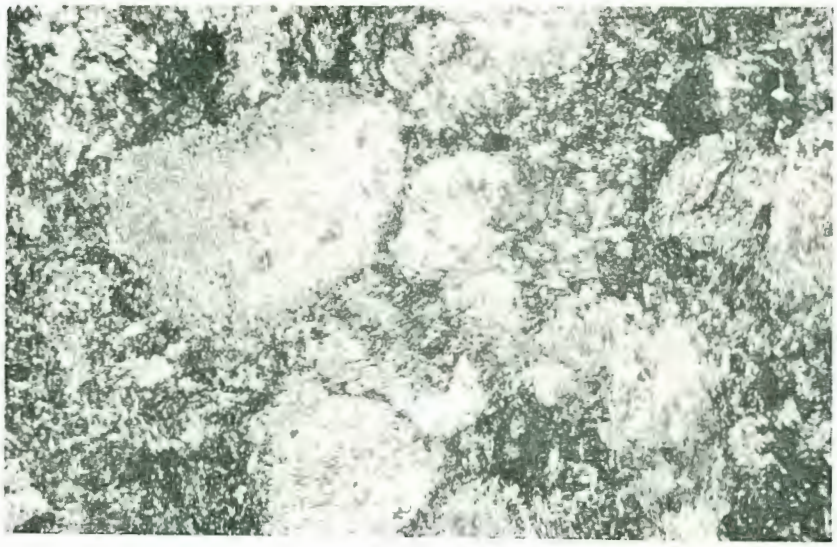

9

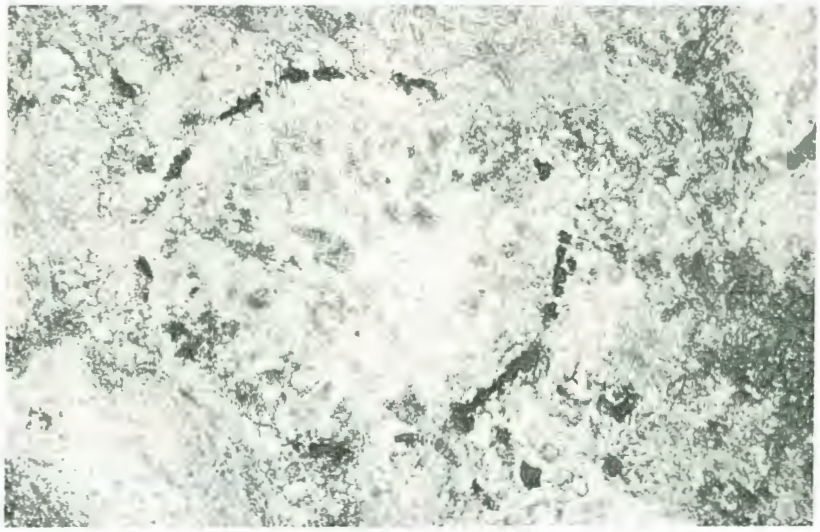

10

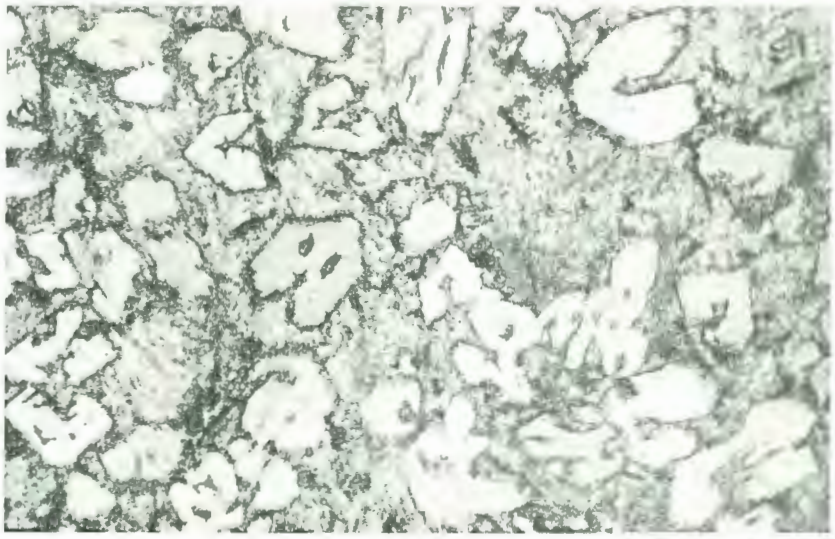

pletely rimmed by opaques (Figure 9).

Gradationally inwards towards the sill Unit A passes into a fine-to-coarse-grained dark green rock with megascopically conspicuous amphibole needles ("Unit B"). In thin section the rock is seen to consist of highly skeletal, radiating actinolite pseudomorphs after clinopyroxene (50%) surrounded by a distinctively textured intergrowth of altered plagioclase and pyroxene. The altered pyroxene shows a large variety of skeletal forms and grain size ranging from small (1 mm) highly irregular shaped grains (Figures 10 and 11) to large fan like, branching crystals several centimeters long (Figure 12). The groundmass has fine, branching actinolite after clinopyroxene intergrown with altered plagioclase. Opaques are present in generally smaller amounts than in Unit A. Amygdules are also widepread but are less abundant than in Unit A. Locally, unit B is highly variolitic (Figure 13).

Unit B is gradational inwards into Unit C which is similar in appearance to Unit B but has long, thin, fan-like altered plagioclase crystals with only a few altered pyroxenes also present. The plagioclase occurs as blocky, hollow crystals or as thin branching crystals up to 2 cm. long (Figure 14). The pyroxene occurs either as long, thin crystals or as blocky, subhedral or subophitic grains. The groundmass, as in Unit B, consists of intergrowths of altered plagioclase and pyroxene. Opaques are gen-

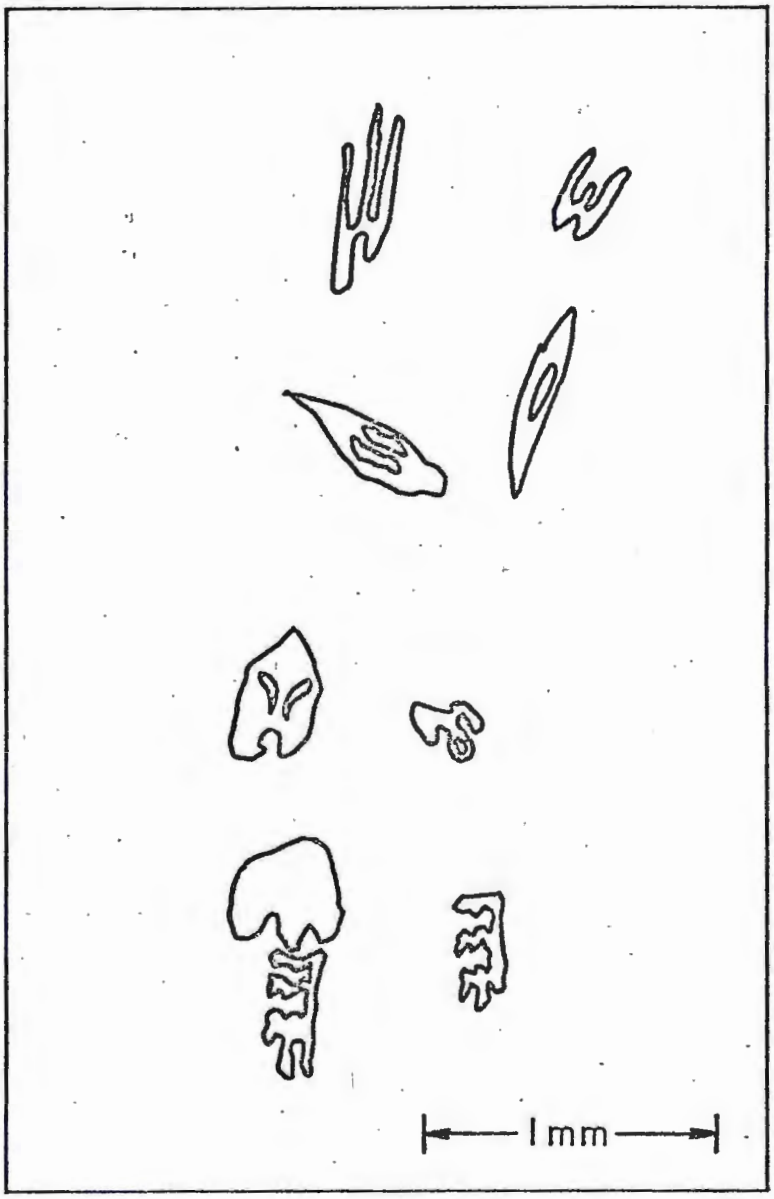

Figure 11. Camera-lucid drawings of skeletal pyroxene shapes found in Unit B of the chilled margins.

Key to Figures

Figure 12. Photomicrograph of branching clinopyroxene (now amphibole) from Unit B of chilled-margins. Note skeletal nature of the pyroxene. Sample SEN-347, SW 1/4 of SW 1/4, Sec. 9, T.63N., R.12W., Scale 1 mm ~15μ (75x).

Figure 13. Sample showing variolites developed in Unit B of some chilled-margins. Variolites are composed largely of branching pyroxene (now amphibole). Sample SEN-324, NW 1/4 of NW 1/4, Sec. 11, T.63N., R.12W.

Figure 14. Photomicrograph showing branching plagioclase of Unit C of chilled-margins. Note hollow cores of some plagioclase laths. White is actinolite-chlorite. Black grains are opaques. Sample SES-22, NE 1/4 of NW 1/4, Sec. 18, T.63N., R.11W. Scale 1 mm ~ 15μ (75x).

12

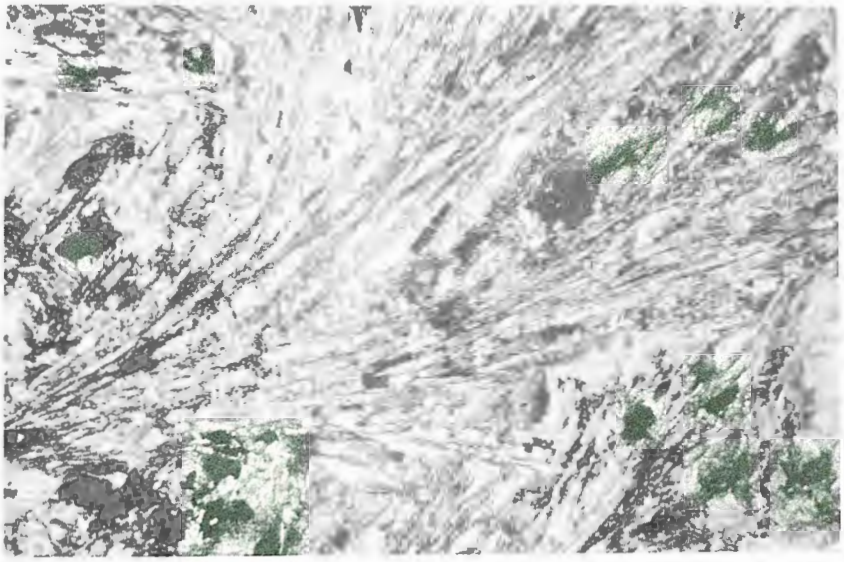

13

14

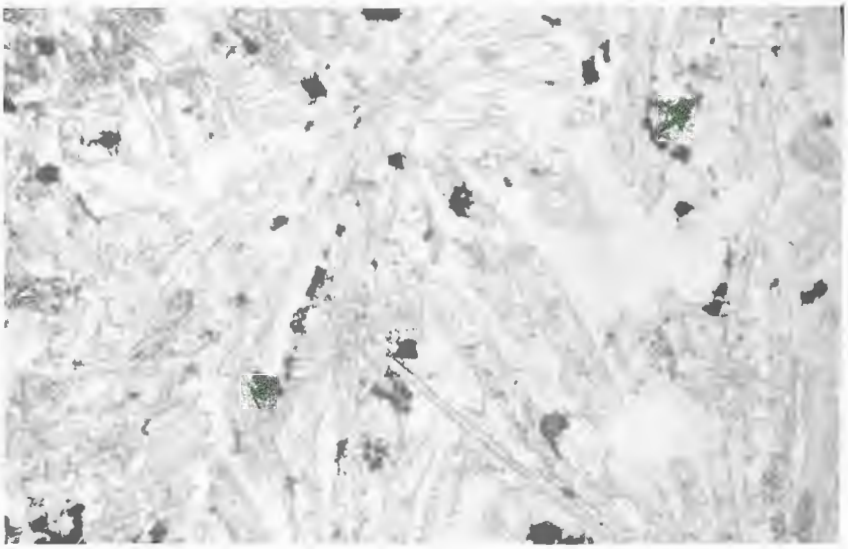

erally present in small amounts (1%) and amygdules are generally not present.

Peridotite

The peridotite unit is in sharp contact with the lower chilled-margin. This is the basal unit of the layered mafic-ultramafic sills ranging from 50 to 400 feet thick in the various sills (Figure 4). In the field the peridotite is black or greenish black and commonly massive. Weathering has commonly produced a thin (2-4 mm) rusty rind on the peridotite giving outcrops a characteristic reddish-brown appearance. The olivine grains can be seen in the weathered rind, with the cleavage faces of pyroxene oikocrysts generally visible on fresh fracture surfaces. Where weathering has been deeper than usual the oikocrysts tend to stand in relief (Figure 15). Outcrops tend to be low and somewhat blocky, commonly occurring in low swampy areas. Small veins of tremolite and serpentine are generally present, and where shearing has been extensive blue-green serpentine may be present on the slickensides. Abundant, through-going parallel microfractures that are unrelated to the primary igneous fabric cut many outcrops of otherwise massive ultramafic rock. In thin section, where these microfractures cut relict olivine grains, at least some of the serpentinization can be seen to have followed this fracturing (Figure 16).

Key to Figures

Figure 15. Sample of peridotite with pyroxene oikocrysts weathered in relief. Sample SEN-42, SW 1/4 of SE 1/4, Sec. 29, T.64N., R.11W.

Figure 16. Photomicrograph of serpentinized peridotite. Note parallel fractures (going N - S) cutting olivine surrounding by serpentine. Magnetite (black) commonly outlines fractures. Sample E-89, SE 1/4 of SW 1/4, Sec. 36, T.64N., R.12W. Scale 1 mm ~15μ (75x).

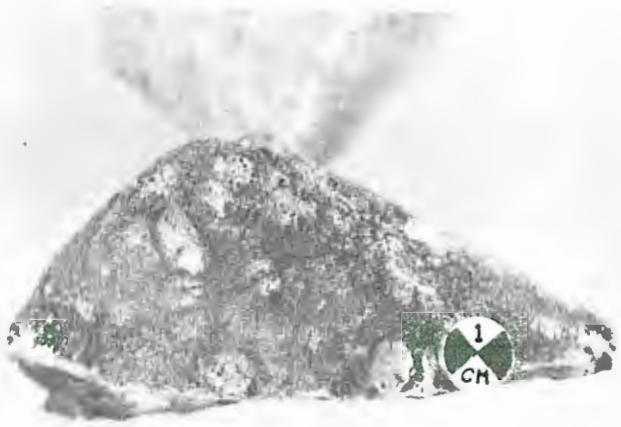

15

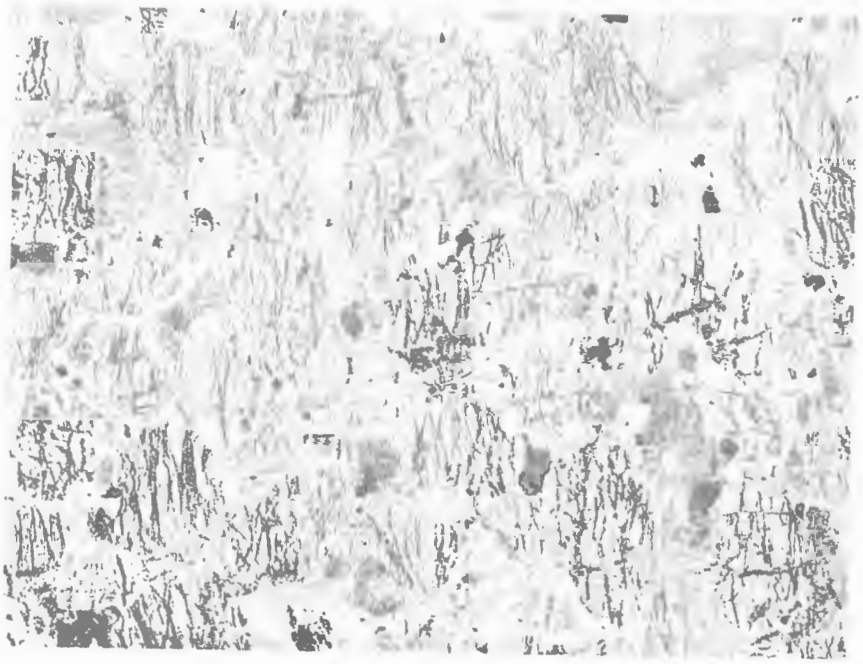

16

The peridotite shows excellent preservation of textures in all but the most sheared samples, even though the primary minerals may be completely destroyed. The original minerals were principally olivine, orthopyroxene, clinopyroxene and plagioclase, with smaller amounts of chromite and magnetite, variable amounts of pale brown hornblended and generally traces of biotite and apatite. Olivine and minor chromite are generally subhedral or euhedral, with the other minerals interstitial to them. Modes for nine peridotite samples are given in Table 4.

The olivine occurs as subhedral to euhedral grains 0.2 to 7 mm in length (average about 2 mm) and constitutes from 35 to 85% of the rock (average about 65%). Though a statistical study of olivine grain size variation has not been conducted it appears that a wide range in size may be present, even within a single thin section, beyond what is expected from a randomly cut section. Furthermore, where olivines are poikilitically enclosed by pyroxene they are commonly smaller than grains enclosed by plagioclase and appear rounded with occasional embayments (Figure 17). The above relationship is especially evident where the enclosing grain is clinopyroxene. Where olivine is enclosed by plagioclase it is generally subhedral to euhedral showing relatively flat crystal faces and angular corners.

Olivine grains are generally free from inclusions except for occasional chromite grains and small, round

Table 4: Modal Compositions for Rocks of the Peridotite Unit.

Mineral	E-466	E-145	SEN-37	SEN-73	SEN-75	SEN-247	SEN-253	SEN-310	SEP-8*
Olivine	28.1	5.6	---	---	16.0	---	---	5.0	---
Olivine Alteration	35.2	57.6	60.5	85.8	40.6	73.5	59.5	51.7	47.6
Orthopyroxene + Alteration	14.0	2.9	---	---	---	7.8	10.0	10.4	16.6
Clinopyroxene + Alteration	4.2	7.9	23.5	7.5	---	4.9	---	12.5	6.6
Cumulus Clinopyroxene + Alt.	---	7.7	---	---	---	---	---	---	---
Hornblende	1.3	9.3	---	---	34.2	3.6	1.8	4.1	1.2
Plagioclase Alteration	13.0	7.4	15.0	6.2	8.8	9.8	26.9	14.5	22.0
Chlorite	1.3	1.3	0.5	---	---	---	---	---	1.2
Biotite	2.0	---	Tr	Tr	Tr	---	0.8	Tr	Tr
Chromite	0.9	0.3	0.5	0.5	0.4	0.4	1.0	1.8	3.2
Apatite	---	Tr	---	---	---	---	---	Tr	Tr
Total Points Counted	1000	1000	1000	1000	1000	1000	1000	1000	1000

*, Ultramafic lens.

Key to Figures

Figure 17. Photomicrograph of peridotite showing rounding and embayment of olivine (light gray) enclosed in augite (dark gray). Also note radiating fractures extending out from the altered olivines suggestive of expansion during alteration. Sample SEN-310, SW 1/4 of SE 1/4, Sec. 9, T.63N., R.12W. Scale 1 mm~15μ (75x).

Figure 18. Photomicrograph of two possible melt inclusions (center of photo) in olivine. Inclusions contain serpentine, amphibole and opaques. Sample E-56, Ne 1/4 of NW 1/4, Sec. 10, T.63N., R.12W. Scale 1 mm~15μ (75x).

17

18

melt inclusions (?). The later are quite common in the olivines of some peridotite samples and are generally composed of serpentine, amphibole and fine dusty opaques (Figure 18). No unaltered examples have been observed. In view of the ellipsoidal shape and mineralogy it is possible that they represent devitrified and altered melt inclusions similar to those found in lunar olivines and recent terrestial basalts (Roedder and Weiblen, 1971).

Three unaltered relict olivine grains from three different sills were analyzed with the electron microprobe. The analyzed compositions range from Fo_{74} to Fo_{81} (Table 8). No evidence of zoning was found in the samples examined. Mineral variations for all analyzed samples are discussed further in a later section (page 110).

Chromite, occurring as euhedral to rounded grains, constitutes no more than 3% of any sample. Grains occur within olivine but are more commonly enclosed in the interstitial minerals. Occasional signs of embayment are present in some samples (Figure 19). Microprobe analyses of chromites from four sills showed the Cr_2O_3 content to be quite variable, ranging from 15% to 47% (Table 10). Reconnaissance microprobe analyses by Green (1970 a), on chromites from other peridotites within the Newton Lake Formation, indicates that the Cr/Fe ratio tends to decrease outwards towards the margins of the grains. Magnetite has been found to rim many of these grains.

Orthopyroxene, clinopyroxene, plagioclase and hornblende all appear interstitial to olivine and chromite. The orthopyroxene is poikilitic with grains as large as 1 to 2 cm. in diameter present in some samples, and it ranges in amounts from 0 to 20% of the rock. Relict orthopyroxene shows the presence of fine exsolution lamellae parallel to {100} and is thus a "Bushveld type" orthopyroxene (Hess, 1960). Microprobe analysis of one relict orthopyroxene shows it to be bronzite with a composition of $Ca_4Mg_{81}Fe_{15}$ (Table 9).

Augite occurs principally as interstitial poikilitic grains about 5 mm. across but also less commonly as small (1-2 mm.) equant crystals (Figure 20). It is present in amounts ranging from 0 to 20% of the rock. Augite is generally the least altered major mineral in the peridotites and appears light green in thin section. Strong parting and exsolution lamellae are visible both in the poikilitic and equant grains, with some grains showing development of two sets of lamellae. The composition of the exsolved phases is not presently known. The interstitial pyroxene from one sample is diopsidic augite ($Ca_{40}Mg_{53}Fe_7$, Table 9).

A pale reddish-brown hornblende forms as much as 40% of some samples but is absent or rare in most. It occurs principally as primary interstitial poikilitic grains and rarely as small subhedral to euhedral crystals. Some interstitial hornblende also shows euhedral cores.

Key to Figures

Figure 19. Photomicrograph of chromian spinel in peridotite. Note embayments in the left central grain. Both grains are enclosed in altered pyroxene. Sample SEN-101, NE 1/4 of NW 1/4, Sec. 32, T.64N., R.11W. Scale 1 mm ~15μ (75x).

Figure 20. Photomicrograph of euhedral clinopyroxene in peridotite. Note simple twinning of the augite. These augites are interpreted as cumulus in nature. Sample E-145, NE 1/4 of NW 1/4, Sec. 18, T.63N., R.11W. Scale 1 mm ~15μ (75x).

19

20

A common feature of the hornblende is a color zoning from a pale reddish-brown core to a clear margin. Microprobe analysis indicates that this zoning is related to a decrease in the Ti/Al ratio outwards toward the margin from about 0.25 at the core to 0.03 at the margins. Microprobe analyses are given in Table 11 of five grains from five samples; the hornblende could be called a kaersutitic pargasite.

No fresh plagioclase was found in any of the 30 peridotite samples examined, but pseudomorphs and partly replaced grains are present in a few samples. The common replacement is a fine, dense mat of almost isotropic chlorite, with the chlorite forming 5 to 30% of the rock. It occurs as interstitial patches which were probably poikilitic crystals. The interpretation of the chlorite as a replacement of plagioclase is somewhat uncertain; however, plagioclase is present in the norm in amounts about equal to that determined for the chlorite. Also this type of replacement has been described from other Precambrian peridotites by MacRae (1969) and Williams (1971).

Apatite and biotite are common minor accessories in many peridotites. The apatite is generally clouded with dust-like particles and occurs as short, stubby, subhedral grains commonly enclosed by hornblende. The biotite, which is pale and evidently magnesian, occurs as interstitial flakes generally in association with

magnetite.

Using normal igneous rock classification the peridotites could be classified as plagioclase lherzolites and augite harzburgites.

Pyroxenite

In the layered, differentiated sills pyroxenite stratigraphically overlies the peridotite with the transition occurring over a few inches. The upper contact is gradational, involving an increase in plagioclase content upwards. The gradational nature of the upper contact has made thickness determinations imprecise, however, the unit is generally about 50 feet thick and is not more than 100 feet thick in any sill examined. Outcrops in association with peridotite are mostly low and grass-covered, whereas the upper portions are often encountered on topographically higher outcrops of the overlying bronzite gabbro.

The rock is characterized by its medium to dark green color on fresh and weathered surfaces, medium grain size and essentially monomineralic composition, consisting of small, stubby pyroxene crystals. Small amounts of plagioclase are also generally visible in hand specimens. Table 5 contains modes for 8 samples from the pyroxenite units. The pyroxenite commonly has a porphyritic texture because of the presence of dark green phenocrysts of orthopyroxene (Figure 21). Plagioclase

Table 5.: Modal Compositions for Rocks of the Pyroxenite Unit.

Mineral	E-146	E-147	SES-26	SEN-40	SEN-199	SEN-200	SEN-309	SEN-352
Clinopyroxene	69.9	47.6	9.9	80.5	46.5	49.2	69.8	77.8
Clinopyroxene Alteration	---	---	---	---	37.2	29.2		
Orthopyroxene	15.2	---	56.8	---	---	---	---	---
Orthopyroxene Alteration	---	22.9	---	---	10.5	5.7	6.4	2.9
Plagioclase Alteration	13.8	26.8	24.6	18.8	1.4	15.6	19.6	15.6
Hornblende	---	1.9	---	---	3.4	---	2.2	---
Opaques	1.0	0.6	0.7	0.7	0.4	0.3	0.3	0.8
Chlorite	---	0.2	---	---	---	---	Tr	2.0
Olivine Alteration	Tr	---	8.0	---	0.6	---	---	---
Quartz	---	---	---	Tr	---	---	1.7	0.9
Total Points Counted	1000	1000	1000	1000	1000	1000	1000	1000

often forms thin rims around these phenocrysts (Figure 21).

In thin section the pyroxenites are found to be composed primarily of augite, plagioclase and orthopyroxene with minor magnetite, sulfide, quartz and hornblende. Textures vary from panidiomorphic granular to porphyritic with crystals of augite and orthopyroxene surrounded by interstitial plagioclase, quartz and hornblende. A few altered olivine grains are generally present near contacts of the pyroxenite with peridotite.

The augite occurs as small (1 to 2 mm) subhedral to euhedral grains, generally light greenish brown, which constitute about 70 to 90% of the rock. Simple twinning on $\{100\}$ is a common feature (Figure 22). Fine exsolution lamellae and exsolved rounded blebs are also common. Alteration of augite is usually restricted to rims of tremolite-actinolite.

In pyroxenites with small amounts of interstitial material, augite grains tend to show mutual interference textures (Figure 23). The interference texture is restricted to those parts of augite crystals which are in contact with neighboring augite crystals, whereas those parts in contact with other interstitial minerals retain their crystal faces.

Three augite grains from pyroxenites were analyzed with the electron microprobe. They have a diopsidic augite composition ranging from $Ca_{42}Mg_{48}Fe_{10}$ to $Ca_{45}Mg_{48}Fe_{7}$ (Table 9). Figure 42 shows the compositional

Key to Figures

Figure 21. Sample of pyroxenite showing orthopyroxene phenocrysts. Note plagioclase rimming some phenocrysts. Sample SEN-309, SW 1/4 of SE 1/4, Sec. 9, T.63N., R.12W.

Figure 22. Photomicrograph of twinned augite from pyroxenite unit. Note slight alteration to actinolite at grain margins (dark gray is altered plagioclase). Sample E-131 b, pyroxenite unit of Little Long Lake sill. Scale 1 mm ~ 15μ (75x).

Figure 23. Photomicrograph showing interference texture developed where augite grains are in contact. Note sharp crystal faces where augite is in contact with plagioclase (upper left of photo). Sample E-146, NE 1/4 of NW 1/4, Sec. 18, T.63N., R.11W. Scale 1 mm ~ 15μ (75x).

21

22

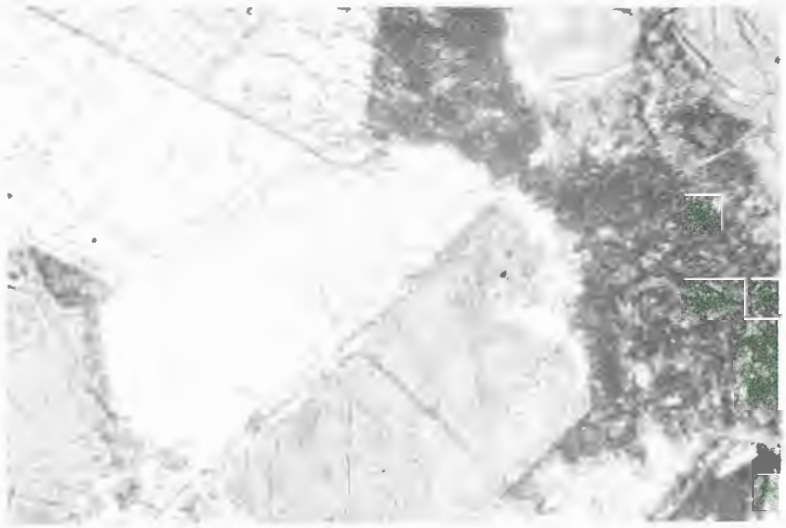

23

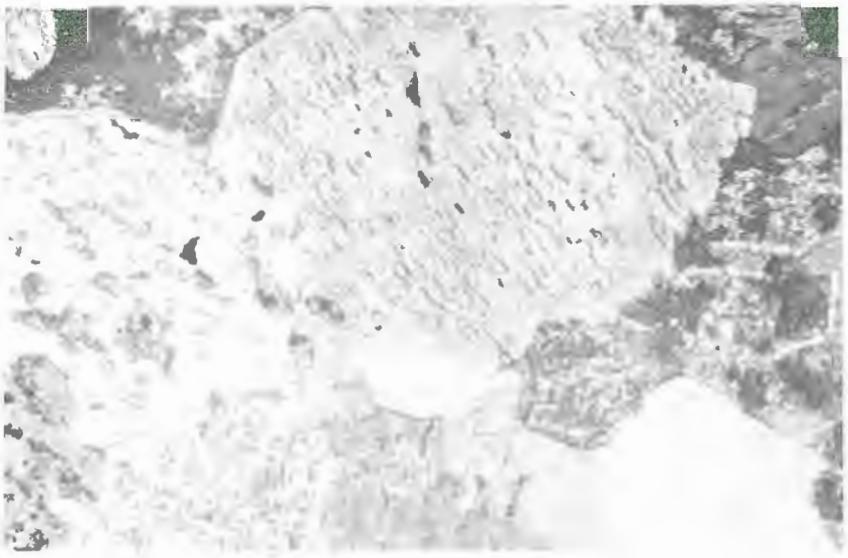

trend of the pyroxenes.

Orthopyroxene is present mostly as 5 to 10 mm phenocrysts, now in the form of tremolite-chlorite pseudomorphs. The pseudomorphs have a lamellar habit similar to that observed in the peridotites suggesting that they are replacements of Bushveld-type orthopyroxene. The orthopyroxene is usually blocky in habit, with small rounded and embayed clinopyroxene inclusions present in some specimens (Figure 24). A few phenocrysts have also been found to have subhedral cores.

The only unaltered orthopyroxene was found in a sample of pyroxenite from the Cedar Lake sill. It occurs as blocky grains slightly larger than accompanying diopsidic augite and forms about 50% of the rock. Fine Bushveld-type exsolution of diopsidic augite (see Table 9 for lamellae analysis) is common (Figure 25) and where orthopyroxene and augite are in contact, augite shows rounding and embayments. The orthopyroxene in this sample was found to have a bronzite composition, slightly enriched in iron compared to the orthopyroxene from the peridotite unit (see Table 9 and Figure 42).

Plagioclase is the major interstitial phase in most samples of pyroxenite, forming 2 to 25% of the rock. It is typically extremely altered to an opaque saussuritic assemblage, however, where it has been found less altered it can be seen to occur as poikilitic grains with albite twinning and a slightly zoned extinction.

Key to Figures

Figure 24. Photomicrograph showing orthopyroxene phenocrysts (gray) with enclosed augite grains (white) from the pyroxenite unit of the Cedar Lake sill. Note embayment of the enclosed augite grains. Also note lamellar habit of orthopyroxene pseudomorph (compare with Figure 25). Sample E-146, same as for Figure 23. Scale 1 mm ~15μ (75x).

Figure 25. Photomicrograph of a largely unaltered bronzite from the Cedar Lake sill pyroxenite. Note fine exsolution lamellae of diopsidic augite. Sample SES-26, same as for Figure 23. Scale 1 mm ~15μ (75x).

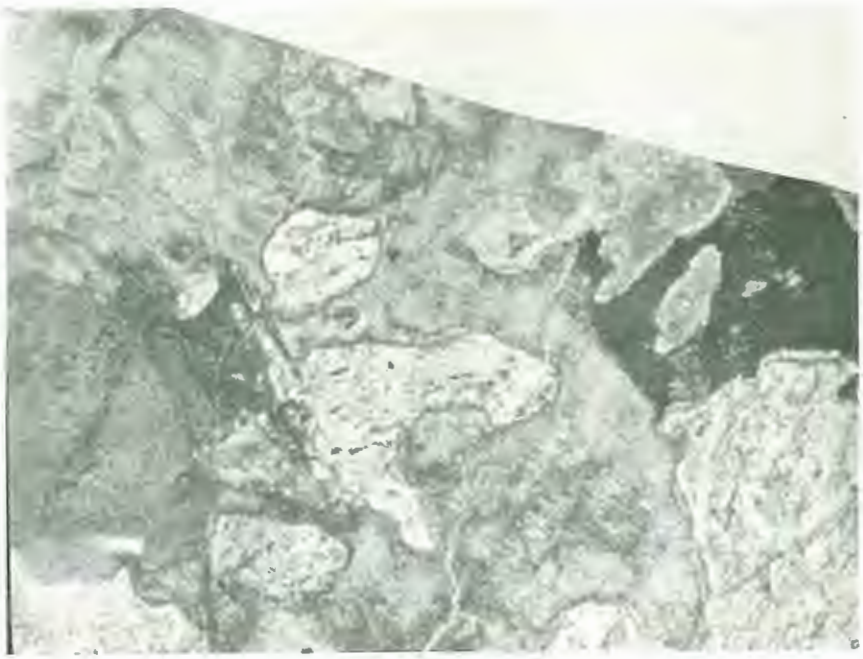

24

25

Quartz, magnetite, sulfide and hornblende form minor interstitial phases, together making up no more than 3 to 4% of any rock sample.

The pyroxenites would be termed websterite, augitite and feldspathic augitite using an igneous mineral classification.

Bronzite Gabbro

The appearance of plagioclase as a major phase marks the base of the bronzite gabbro unit above the pyroxenite in the layered, differentiated sills. Since both the upper and lower contacts of the unit are gradational, thickness determinations are only approximate; however, the unit is generally about 100 to 200 feet thick. It appears that in some sills this unit is the thickest unit present (see Cedar Lake sill column, Figure 4). Outcrops are massive to widely jointed and tend to form fairly high and extensive hills. A few thin, white, quartz-feldspar veins are present locally. Fine rhythmic layering on a scale of 1 to 2 cm. has been observed locally within this unit in some sills (see Figure 5).

The bronzite gabbro can be divided into two subunits based on textural relations. The lower part is grey to greenish grey, medium grained and characterized by 2 to 10 mm orthopyroxene phenocrysts and 1 to 2 mm blocky plagioclase laths (Figure 26). The general appearance is very similar to that of the pyroxenite except that plagioclase

and orthopyroxene phenocrysts are more abundant and that the plagioclase appears as larger, subhedral grains. Modally the rock is a bronzite gabbro with quartz, iron-titanium oxides and minor biotite occurring interstitially (see Table 6).

The upper part of the bronzite gabbro is dark grey to greenish grey, medium grained and is characterized by 1 to 4 mm plagioclase laths and interstitial subophitic augite and poikilitic, not porphyritic, orthopyroxene. Minor amounts of quartz, iron-titanium oxides, ~~and~~ apatite and biotite are also present (see Table 6). The contact between the subunits is completely gradational with the upper unit generally thicker. The transition from the lower to the upper part of the bronzite gabbro reflects a change in pyroxene crystallization from subhedral crystals to ophitic-subophitic grains. The unit as a whole marks the final stages of orthopyroxene crystallization in the sills.

Plagioclase occurs as small (1 to 2 mm) blocky laths throughout the bronzite gabbro and generally forms from 40 to 50% of the rock. They tend to be larger in the upper portion of the unit. Alteration is generally intense; however, where alteration has not been complete albite and carlsbad twinning can be seen.

Orthopyroxene in the lower portions of the unit is very similar to that described from the pyroxenite unit. Grains are 2 to 5 mm in diameter, blocky and altered to

Table 6: Modal Compositions for Rocks of the Bronzite Gabbro Unit.

Mineral	E-47	SES-28	SES-29	SES-33	SEN-201	SEN-240	SEN-308
Plagioclase Alteration	38.0	45.6	46.0	48.5	39.5	43.1	43.3
Clinopyroxene	46.7				11.4	----	
Clinopyroxene Alteration	----	37.5	35.6	32.1	44.5	39.4	36.1
Orthopyroxene "Phenocrysts"	13.2	----	----	17.0	----	15.4	16.4
Orthopyroxene Oikocrysts	----	7.5	7.2	----	1.9	----	----
Quartz	0.6	5.0	7.2	0.6	1.4	----	1.9
Chlorite	1.1	1.6	1.5	1.6	1.1	1.1	1.5
Oxides	0.4	2.8	2.5	0.2	0.2	1.0	0.8
Total Points Counted	1000	1000	1000	1000	1000	1000	1000

pseudomorphs showing a lamellar habit. The phenocrysts comprise about 15 to 20% of the rock and may have small, altered inclusions of plagioclase and/or rounded augite (Figure 27).

Orthopyroxene in the upper portions of the unit is poikilitic, though subhedral cores are present in some grains. Grain boundaries tend to be irregular with numerous plagioclase laths enclosed in the poikilitic grains (Figure 28). Orthopyroxene is fairly scarce in most samples, comprising only 1 to 8% of the rock.

Augite in the lower bronzite gabbro occurs as small, 1-2 mm grains, light green in plane-polarized light with moderate to high birefringence under crossed nicols. Good parting and commonly some fine exsolution lamellae of undetermined composition are also present. Grains tend to have anhedral outlines (Figure 29) and comprise about 40 to 45% of the rock. Exsolution lamellae often do not extend to the margin of the grain (see Figure 29). In the upper portions of the unit augite has a similar appearance but occurs as interstitial and partly poikilitic grains (Figure 30). It is present in slightly smaller amounts than lower in the unit, averaging about 35% of the rock. Microprobe analyses of three augites from this unit show a range in composition from $Ca_{44}Mg_{46}Fe_{10}$ to $Ca_{47}Mg_{47}Fe_{6}$ (Table 9).

Quartz is a common accessory mineral in this unit, comprising up to 7% of the rock. It generally occurs

Key to Figures

Figure 26. Sample of bronzite gabbro. Note orthopyroxene phenocrysts (light gray) and small clusters of tubular plagioclase (white). Sample SES-33, SW 1/4 of NW 1/4. Sec. 8, T.63N., R.11W.

Figure 27. Photomicrography showing altered plagioclase inclusion (dark gray) in orthopyroxene phenocryst (gray, lamellar habit). Sample SES-33, same as for Figure 26. Scale 1 mm ~15μ (75x).

Figure 28. Photomicrograph shows poikilitic orthopyroxene enclosing plagioclase laths (outlined in black) from the upper portion of a bronzite gabbro unit. Saple SES-28, NE 1/4 of NW 1/4, Sec. 18, T.63N., R.11W. Scale 1 mm ~15μ (75x).

26

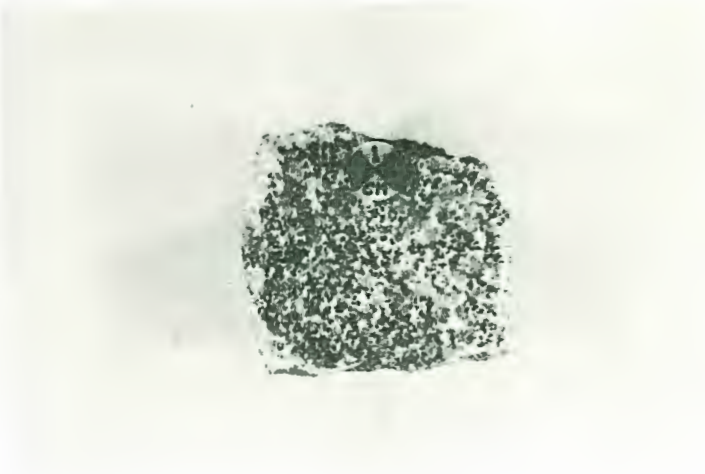

27

28

Key to Figures

Figure 29. Photomicrograph of augite from lower portion of bronzite gabbro unit. Note strong parting, exsolution lamellae and irregular outline of grain. Exsolution often dies out before reaching the margins of grains supporting the interpretation that adcumulus growth has enlarged the augite grains. Sample SES-33, same as for Figure 27, Scale 1 mm ~15μ (75x).

Figure 30. Photomicrograph of poikilitic augite enclosing altered plagioclase laths (black) from the upper portion of bronzite gabbro unit. Note interstitial quartz (white). Sample SES-28, same as for Figure 28. Scale 1 mm ~15μ (75x).

29

30

as interstitial, poikilitic grains around plagioclase laths and in the upper portions of the unit is ~~in~~ occasionally in micrographic intergrowths with plagioclase. Quartz shows an increase in abundance upwards through the unit.

Iron-titanium oxides (~~see foot note, Table 6~~) are additional common accessory minerals. They also show an increase in abundance upwards through the bronzite gabbro to a maximum of about 3%. The grains are equant to skeletal and are generally altered except for lamellae. These grains were not studied in reflected light, but their appearance in transmitted light is strikingly similar to oxides described by Ripley (1973, pp. 99 and 102) from the sills of the Deer Lake Complex, Minnesota. He has interpreted the oxide as originally being magnetite containing abundant exsolved ilmentite with complete removal (oxidation-hydration) of the magnetite during the alteration process.

Gabbro

Gabbro forms the upper unit for many of the sills examined and ranges from 100 to greater than 400 feet in thickness. Outcrops tend to form topographic highs and the rock is massive except for widely spaced joints.

The gabbroic rocks show a wide diversity in textures and grain size, both in outcrop and in thin section. The minerals present, while variable in amount are essentially

plagioclase and augite with lesser amounts of quartz and iron-titanium oxide. Modes for 6 gabbro samples are given in Table 7. The transition from the bronzite gabbro unit to the gabbro unit is gradational and marked by an increase in the size of the plagioclase laths and development of prismatic pyroxene grains. Much of the gabbro unit shows a medium- to coarse-grained, hypidomorphic granular texture with interlocking plagioclase and augite (Figure 31). The rest of the gabbro has predominantly subophitic texture with ophitic texture present locally.

Plagioclase, in amounts ranging from 40 to 55%, occurs as thin laths 1 to 3 mm long in the ophitic and subophitic gabbros and as blocky laths 2 to 5 mm long in the hypidiomorphic granular gabbro. Alteration is usually intense but margins are commonly unaltered indicating that some zoning to less calcic compositions may exist. Twinning of the laths on the albite and carlsbad laws is evident in some samples.

Augite is greenish brown, twinned, and in the upper portions of the unit shows simple twinning and exsolution (Figure 32). It occurs as interstitial 2 to 3 mm ophitic to subophitic grains or as distinct 3 to 6 mm prismatic grains and is present in amounts ranging from 35 to 50% of the rock. Ripley (1973) analyzed similar pyroxenes from gabbro units in the strikingly similar Deer Lake Complex and found them to be ferroaugites (about $Ca_{38}Mg_{29}Fe_{35}$). It is likely that the augite from

Table 7; Modal Compositions for Rocks of the Gabbro Unit.

Mineral	E-134	SEN-104	SEN-238	SEN-327	SEN-348	SEN-375
Plagiclase + Alteration	38.9	52.3	41.7	50.8	43.7	41.0
Clinopyroxene + Alteration	47.3	40.8	39.8	38.0	33.9	40.9
Chlorite	---	5.3	4.7	2.7	1.3	4.7
Epidote	---	---	---	---	10.9	---
Quartz	10.3	---	10.8	6.5	5.7	7.1
Oxides	3.5	1.6	3.0	2.0	4.5	6.4
Total Points Counted	1000	1000	1000	1000	1000	1000

Key to Figures

Figure 31. Sample of gabbro showing interlocking plagioclase laths and prismatic augite. Sample SEN-411, SE 1/4 of SE 1/4, Sec. 24, T.63N., R.13W.

Figure 32. Photomicrograph of probable ferroaugite showing simple twinning and possible exsolution lamellae. Sample SEN-327, SE 1/4 of SW 1/4, Sec. 2, T.63N., R.12W., scale 1 mm ~15μ (75x).

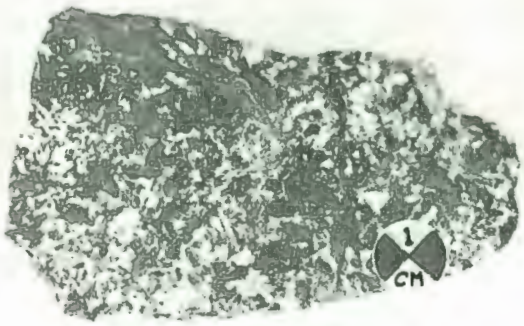

31

32

the upper gabbro unit of these sills in the Newton Lake Formation are also ferroaugite in composition.

Quartz is a common component in many of the gabbroic rocks and constitutes 5 to 15% of the rock. It occurs as distinct interstitial grains or as micrographic intergrowths with sodic (?) plagioclase (Figure 33).

Iron-titanium oxides are generally present in amounts ranging from 2 to 6% of the rock. Most grains are skeletal showing well developed octahedrally oriented ilmenite (?) lamellae (Figure 34).

Apatite and sphene occur as common minor accessory minerals in the gabbro unit.

Residual Segregation

Many of the sills show evidence of residual liquid segregation. Three main types of segregations are found: veins, pegmatitic zones and granophyric gabbros. Of these three types the veins are the most common.

The veins occur as thin (1 to 3 cm wide) veinlets up to a few feet long cutting the bronzite gabbro and gabbro units. The veins have sharp contacts with the surrounding rock and cross cut the strike of the units. The veins have never been found to cut the peridotite or pyroxenite units. The veins in the bronzite gabbro unit are generally white and composed of plagioclase, quartz and epidote. Plagioclase is the predominant mineral forming about 70 to 80% of the veinlets. In the gabbro

Key to Figures

Figure 33. Photomicrograph showing micrographic texture developed between plagioclase and quartz in the gabbro unit. Sample SEN-348, SE 1/4 of SW 1/4, Sec. 9, T.63N., R.12W. Scale 1 mm ~ 15μ (75x).

Figure 34. Photomicrograph of an irregularly shaped iron-titanium oxide grain showing oriented ilmenite (?) lamellae. Magnetite (?) generally is replaced by a whitish residue. Sample SEN-348, same as for Figure 33, scale 1 mm ~15μ (75x).

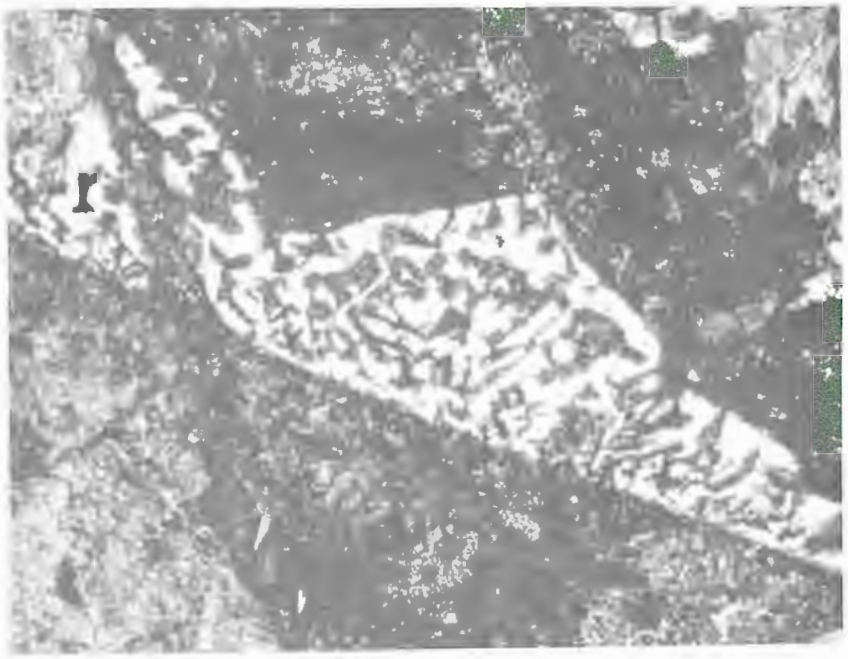

33

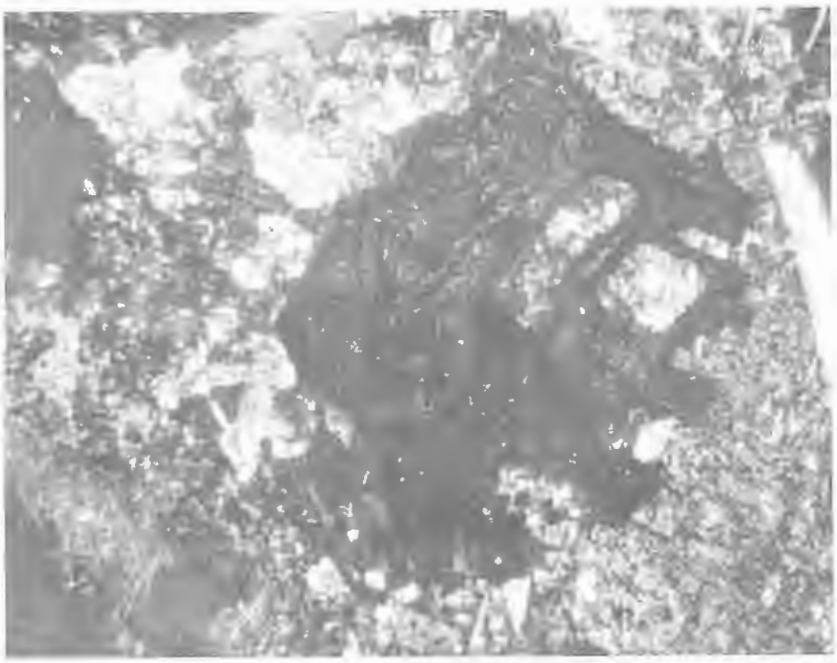

34

unit the veins are pink and composed of potassium feldspar, quartz and epidote. Many of the smaller veinlets from this unit are 90 to 95% feldspar. In some outcrops these veins have also been found to cut the lower unit (Unit C) of the upper chilled zone.

Pegmatitic zones are locally developed in the upper portion of some gabbro units. The pegmatitc zones have gradational contacts with surrounding gabbro and vary in size from small pods to lenses 50 feet or more in length. Augite and plagioclase, with some quartz are the major minerals. Augite occurs as long (up to several centimeters) twinned crystals now represented largely by actinolite pseudomorphs. Plagioclase is present as thin laths up to 2 cm long. Quartz is interstitial, occurring either as distinct grains or in granophyic intergrowths with plagioclase. Low-grade metamorphism has usually altered the pegmatoids to blue-green actinolite (after augite) and epidote group minerals (after plagioclase).

Granophyric gabbros are also locally present. They are generally similar to normal gabbro but contain from 15 to 30% of granophyric intergrowths of quartz and plagioclase. Plagioclase grains are commonly at the centers of the granophyric areas (Figure 35).

Petrography of the Wholly Gabbroic Sills

Several wholly gabbroic sills have been located in the map area. The sills range from 500 to 1200 feet thick and are of lengths ranging from 1/2 mile to several

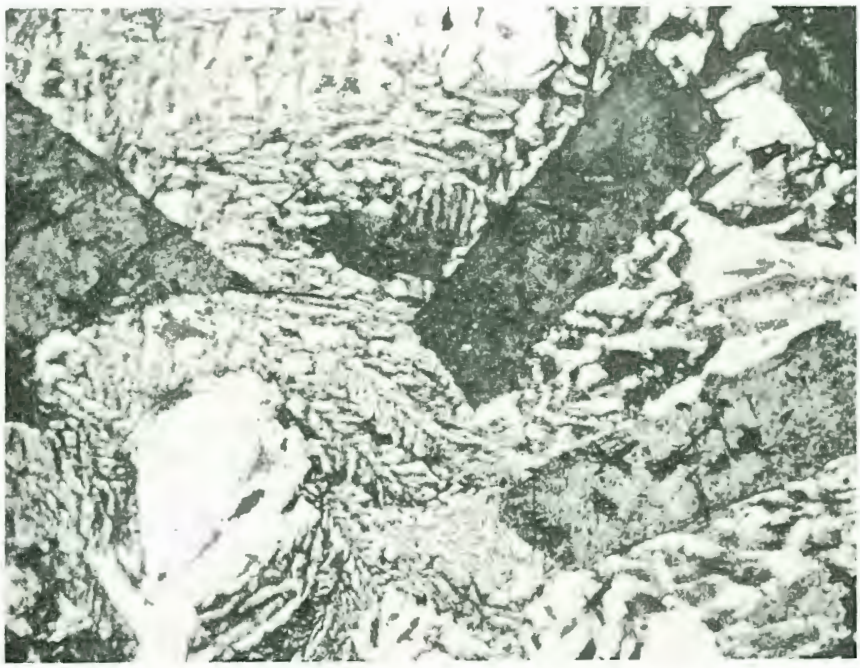

35

Figure 35. Photomicrograph of granophyric gabbro. Note plagioclase laths (dark grey) are surrounded by granophyric quartz-plagioclase. Sample E-198, NW 1/4 of SW 1/4, Sec. 29, T.64N., R.11W., Scale 1 mm ~15μ (75x).

miles long. Peridotite and pyroxenite units have not been found directly associated with these gabbro sills with the possible exception of the Picketts Lake sill (discussed below, see page 85).

The mineral composition of the gabbro sills is almost identical to the gabbroic portions of the layered, differentiated sills described above. Both bronzite gabbro and gabbro are commonly present, however the bronzite gabbro typically does not show the orthopyroxene phenocrysts so commonly found in the layered sills; the orthopyroxene is poikilitic and these rocks are thus similar to the upper portion of the bronzite gabbro unit in the layered sills (see above). Where both bronzite gabbro and normal gabbro are present, the bronzite gabbro underlies the gabbro. The gabbro generally shows a hypidiomorphic-granular texture with interlocking plagioclase and augite as described above. Quartz and iron-titanium oxides are commonly present as interstitial minerals. The transition between the two units, as in the layered sills, is gradational in nature.

In a few of the gabbro sills the bronzite gabbro unit is not present and its place in the sequence is taken by a rock having large (5 mm) ophitic grains of augite enclosing small blocky plagioclase. This rock shows a characteristic lumpy surface in outcrop because of differential weathering of the pyroxene oikocrysts.

Petrography of the Ultramafic Lenses

At least three wholly ultramafic lenses have been identified in the map area (see map, Plate 1). The lenses southwest of Bright Lake (NE 1/4, NW 1/4, Sec. 6, T.63N., R.11W.) are the best examples of this type. Others are located northeast of Bright Lake in the NW 1/4, Sec. 32, T.64N., R.11W.

The two ultramafic lenses southwest of Bright Lake are about 75 feet thick and extend laterally for at least several hundred feet with a NE-SW strike. The lenses are composed of about 30 feet of peridotite surrounded by a thick complex chilled margin which is thicker (30 feet) on the top of the lense. Figure 36 shows a cross section for one of the ultramafic lenses from southwest of Bright Lake.

The rocks of the lenses are very similar to those described from the layered sills. The peridotite is fine-grained, black and weathers to a reddish brown. It is composed of small (1/8 - 1 mm) altered olivine and hornblende crystals surrounded by altered pyroxene and plagioclase. The olivine is euhedral to rounded with small melt (?) inclusions commonly present. Hornblende is subhedral with euhedral cores (Figure 37) and shows a strong zoned extinction and zoning from a red center to a clear rim. Pyroxene is poikilitic and generally extensively altered, but it appears that both ortho- and clinopyroxene were originally present. Plagioclase

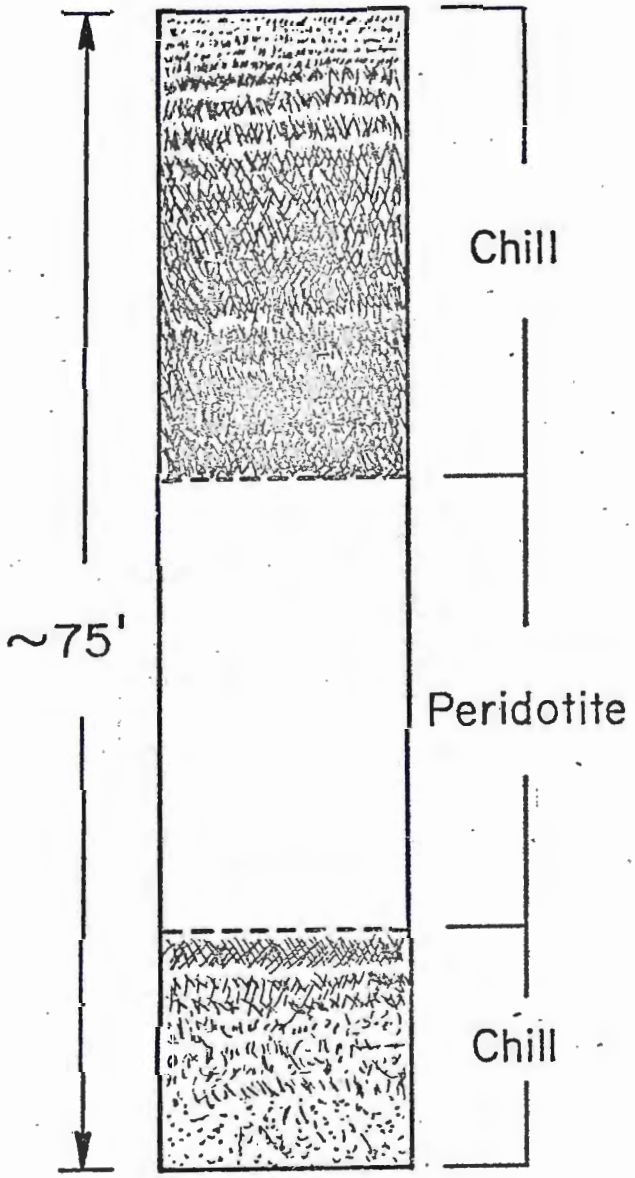

Figure 36. Diagramatic cross section of an ultramafic lens. Lines in chilled portion depict plumose plagioclase and pyroxene.

is also intensly altered but appears to have formed as poikilitic grains. Magnetite, chromite, biotite and apatite are generally present in minor amounts. Alteration has been intensive in the peridotites examined with only relict hornblende remaining among the silicates.

The complex chilled margin is very similar to that from the layered sills and can be divided into the same three units. Contacts between the units are gradational with the contact between the chilled zone and peridotite generally being sharp, occurring over a few inches. Modes for three samples from the chilled zone are given in Table 3.

Amygdules are common in the chilled zone. The amygdules increase in amount present outwards from the peridotite contact from less than 1% to about 5% at the upper contact of the lens. Amygdules are filled with chlorite, plagioclase and actinolite and are generally rimmed by opaques.

Textures found in the chilled zone are similar to those previously described for the chilled zones of the layered sills. Pyroxenes show the same skeletal shapes as shown in Figure 11. In Unit B the pyroxenes show an increase in size inwards toward the peridotite. They form branching, bladed crystals several centimeters long (Figure 38) which can be seen to fan out inward from the upper (or lower) contact. The pyroxenes in these cases are horizontal and lie perpendicular to the vertical contacts.

Differential weathering has commonly given the rock a ribbed or lined appearance which is quite distinctive in outcrop.

Plagioclase in Unit C of the ultramafic lens chilled zones occurs as thin, radiating laths and also a small (1 mm, diameter) hollow crystals. It is generally altered but has carlsbad twins and shows zoned extinction.

Interstitial to pyroxene in Unit A is a nondescript, light brown material with little or no birefringence. This material has low relief relative to balsm and may represent altered glass and/or plagioclase. In Unit B interstitial, branching pyroxene can be seen surrounded by this light brown material. In Unit C the brown material is no longer present being replaced by an intergrowth of pyroxene and plagioclase with some fine chlorite or serpentine patches also present.

Texturally the ultramafic lenses are very similar to lenses described by Naldrett and Mason (1968) from the Dundonald area of Ontario. It is interesting to note that in Ontario the chilled zone of the ultramafic lenses contains abundant skeletal olivine whereas in the chilled zones of the Newton Lake ultramafic lenses no olivine appears to have been present.

Key to Figures

Figure 37. Photomicrograph of primary hornblende from peridotite unit of an ultramafic lens. Note zoning and euhedral core of the hornblende. Sample SEN-210, NE 1/4 of NW 1/4, Sec. 6, T.63N., R.11W., scale 1 mm ~ 15μ (75x).

Figure 38. Sample from chilled portion of an ultramafic lens showing branching of pyroxene crystals. Sample SEN-422, same as for Figure 37.

Figure 39. Photomicrograph of a strongly zoned augite from the Picketts Lake sill. Sample SEP-10, SW 1/4 of SW 1/4, Sec. 6, T.63N., R.11W., scale 1 mm ~ 15μ (75x).

37

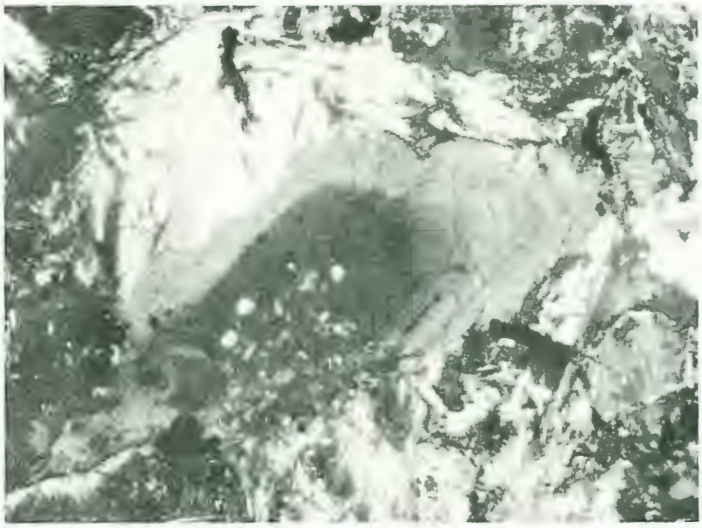

38

39

Description of Individual Intrusions

Little Long Lake Sill

The Little Long Lake sill is located in the Shagawa Lake quadrangle at the southwest end of Little Long Lake. The sill is about 1000 feet thick and extends for at least 2 miles in a NE-SW direction. Greenstone has been found to underlie the sill with the upper contact cut off by the Vermilion fault (see map, Plate 1). Contacts, where visible in the sill, are vertical. The sequence of layering in the sill indicates that the top is to the northwest. This agrees with top directions in the underlying greenstone. Though the contact between the sill and the underlying greenstone is not exposed, greenstone 50 feet from the basal peridotite shows no evidence of contact metamorphism.

The sill shows a complete sequence from peridotite through quartz gabbro with only outcrops of the chilled margins missing. Figure 4 shows a stratigraphic column for the Little Long Lake sill.

Peridotite forms the basal portion of the sill and is about 200 to 300 feet thick. It is black, medium-grained and commonly shows large (1 cm) oikocrysts of pyroxene on freshly broken surfaces. The peridotite is in sharp contact upwards with a porphyritic pyroxenite which is about 75 feet thick. The pyroxenite is medium-grained with 5 to 8 mm blocky orthopyroxene phenocrysts present in amounts from 5 to 10% in a groundmass made up

principally of equant augite crystals. The pyroxenite is gradational into a bronzite gabbro unit which is porphyritic initially but becomes ophitic upwards. The bronzite gabbro is about 200 feet thick. Orthopyroxene phenocrysts are present in amounts ranging from 15 to 25% in the lower part of the unit. In the upper portion orthopyroxene oikocrysts form about 10 to 15% of the rock. The bronzite gabbro in turn grades into a gabbro unit. The gabbro is dark green and changes from medium-grained at the base of the unit to coarse-grained at the top. Augite crystals 2 to 3 cm long are locally developed in the upper portion. Quartz and granophyre are quite common, especially in the upper portion of the sill. Locally thin quartz-feldspar veinlets and felsic pods and lenses, similar to those described above, are also present.

Cedar Lake Sill

The Cedar Lake sill is located south of Cedar Lake in the Ely quadrangle. It trends NE-SW and is about 3 miles long and 1000 feet thick. The sill is conformable to underlying and overlying volcanic rocks and is lens-shaped, tapering at both ends. Contacts, where exposed, are largely vertical and pillows in surrounding greenstone indicate tops to the southeast. This is also the direction of differentiation in the sills, as indicated by the sequence of its internal units.

At least four faults have cut the sill into segments (Plate 1). The faults have either NE or NW trends and have either left-lateral or right-lateral displacement. It is possible that vertical displacement is also present. The sill lies on the south limb of an isoclinal anticline, with the axis of the fold being marked by a fault trending the length of Cedar Lake (Plate 1).

The Cedar Lake sill shows a complete sequence from peridotite through quartz gabbro, with a partially exposed upper chilled margin also present (see Figure 4 for a stratigraphic column). Within the peridotite unit of the sill a pyroxenite layer has been found but is apparently only locally developed. In the NE 1/4, NW 1/4, Sec. 18, T.61N., R.11W., a low outcrop of peridotite occurs near the road (near spot elevation 1388). The peridotite contains a ten-foot thick layer of porphyritic pyroxenite. The outcrop is small and the pyroxenite layer cannot be traced more than 30 feet. The layer has not been found to occur elsewhere in the sill, although a regular pyroxenite unit is present above the peridotite in this sill. There is no evidence that this local repetition of units in the ultramafic zone is the result of faulting.

The peridotite unit is about 200 feet thick. It is black to greenish-black, medium-grained and commonly shows 1 to 2 cm pyroxene oikocrysts on freshly broken surfaces. Small, subhedral augite grains are present in some parts of the peridotite. The peridotite, in the central portion

of the sill, is in sharp contact upwards with a medium- to coarse-grained pyroxenite, however on the ends of the sill the peridotite is in sharp contact upwards with bronzite gabbro.

The pyroxenite is a dark green websterite with large (2-3 mm) bronzite crystals as well as smaller diopsidic augite grains (see Table 5, Sample 26 for mode). This unit is only about 50 feet thick and is present only in the central portion of the sill. Where it is present it is gradational upwards into the bronzite gabbro unit.

Bronzite gabbro forms the largest unit of the sill and averages about 400 feet thick. Textural changes in this unit are as described for the general case of differentiated sills above. The bronzite gabbro unit is gradational upwards into a hypidiomorphic-granular gabbro or quartz gabbro. The gabbro unit is about 150 feet thick and appears to pinch out laterally.

The Cedar Lake sill appears to have a deficiency in normal gabbro from what would be expected to be associated with the large volume of ultramafic rock present. This is supported by a discrepancy found between the calculated bulk composition for the sill and that obtained from the analysis of the chilled margin (see page 153).

Picketts Lake Sill

The Picketts Lake sill is located along the north shore of and beneath Picketts Lake in the Ely quadrangle

(Plate 1). The sill is variable in thickness (50 to 300 feet) and extends for a length of at least 1.5 miles. Contacts are generally vertical and the sill is generally concordant though it may be locally discordant with the surrounding greenstones.

The sill appears to contain peridotite, pyroxenite and gabbro units with no chilled zone found in outcrop. The peridotite is fine-to-medium-grained and may have some layering as suggested by lineations on weathered surfaces. The peridotite is composed of about 50% olivine, 20% pyroxene and 25% plagioclase with minor hornblende, chromite, biotite and apatite (see Table 5, SEP-8 for mode). The peridotite is in sharp contact upwards with pyroxenite.

The pyroxenite is at least locally porphyritic and similar to that described from the other layered sills. The pyroxenite locally forms the upper portion of the sill while in other areas it is gradational into a light green, fine-grained rock with small (1-2 mm) blocky pyroxenes surrounded by small blocky plagioclase laths. The pyroxenes show strong normal zoning with some sector zones also developed (Figure 39). These microphenocrysts form about 40% of the rock. This augite-rich microgabbro appears to be gradational upwards into another fine-grained, light green microgabbro that shows a diabasic texture.

The exact relationship between the microporphyritic gabbro and the underlying ultramafics and the relationship

between the fine-grained diabasic gabbroic rock to the sill are uncertain. The texture of the gabbroic rocks is unlike that found in other layered sills in the area. The common occurrence of pillowed greenstone above the gabbro could indicate that the gabbros where intruded below a contemporaneous pillow-basalt cover and are unrelated to the underlying ultramafic units. More field work is required to determine which interpretation is correct.

PETROLOGY

Formation of the Layered Sequence in the Differentiated Sills

Large-scale compositional layering, as has been described above, is a characteristic feature of many of the sills within the Newton Lake Formation. The lack of internal chilled zones or other evidence indicative of intrusive relations between layers suggests that the compositional units of the sills have developed as the result of a continuous sequence of crystallization. This inference is further supported by the facts that (1) the same sequence or at least most of it is represented in each sill without reversals, and (2) the units have the same outer limits as the sill as a whole.

It has become widely accepted that fractional crystal-

lization by gravity settling of early formed crystals is a major mechanism in producing layered mafic igneous sequences (see Wager, and others, 1960; Wager and Brown, 1967; Jackson, 1971). The rocks formed by this mechanism are termed cumulates (Wager and others, 1960) and can be described and interpreted in terms of classical sedimentary petrology (see Irvine, 1965; Jackson, 1967 and 1971; Wadsworth, 1973).

A number of characteristic features have been observed in well-studied cumulate sequences around the world and these can be used to help determine if a particular sequence of rocks has formed by crystal accumulation. Some of the more important features of cumulates are given below.

1. Presence of extensive layering.
2. Contacts marked by abrupt changes in mineralogy.
3. Presence of rhythmic layering (small-scale stratification marked by change in mineralogy).
4. Development of common sedimentary structures such as graded bedding, slump structures, scour and fill, etc.
5. Cryptic layering marked by a gradual change in composition in mineral solid solutions (e.g. the anorthite content of plagioclase).
6. Development of cyclic units (repeated sequences) in ultramafic portions.
7. Lineation and lamination expressed by igneous

mineral alignment in cumulus.

8. Presence of rocks having compostions far removed from known igneous melts (e.g. dunite, pyroxenite).
9. Textures that can be interpreted in terms of sedimentary accumulation of euhedral crystals, with variously formed interstitial material.

Determining whether or not a particular rock sample is a cumulate can be very difficult. As pointed out by Wager and others (1960), "the fewer the number of cumulus minerals in a rock, the greater the likelihood that its texture will reflect its origin". With increasing numbers of cumulus phases, on the other hand, distinctive settling features are less likely to be maintained and a cumulate composed of plagioclase, olivine, augite, and magnetite forming from a gabbroic liquid could develope a normal gabbro texture. A number of criteria can be used, however, to help determine if a particular sample is a cumulate. These include:

1. the presence of many euhedral crystals surrounded by interstitial poikilitc grains,
2. evidence of preferred mineral orientation,
3. a monomineralic composition,
4. a general lack of zoning in the large crystals and interstitial phases,
5. presence of a granular texture with few interlocking textures (except for poikilitic), and

6. the presence of interstitial phases which together give unreasonable melt compositions.

Not all the above features are always present in any one sample, but combinations of two or more are commonly observed in known cumulates. The one principal feature of all rocks of this type, especially the ultramafic types, is that they are sedimentary in nature, having sedimentary textures, layering on a grain-by-grain scale, obey laws of superposition and can be recognized and classified in much the same way as ordinary sediments (Jackson, 1971).

Examination of the layered sills from the Newton Lake Formation has found that many of the characteristic features of rocks formed by crystal accumulation are indeed present. These features include:

1. extensive compositional layering with layers obeying the law of superposition as outlined by known principals of fractional crystallization,
2. presence of occasional rhythmic and graded layering,
3. presence of cryptic layering,
4. presence of largely monomineralic rocks (e.g. pyroxenite), and
5. compositional units defined by the appearance or disappearance of a mineral or an abrupt change in ratios between minerals.

In the discussion that follows an attempt has been made to interpret the rocks of the layered sills in terms of

cumulus textures. The relationships so described are of critical importance in understanding the formation and differentiation of the sills, which will be discussed in the succeeding sections.

Peridotite

As previously described (page 37) the peridotites are composed of olivine, ortho- and clinopyroxene and plagioclase with lesser amounts of chromite, iron-titanium oxide, hornblende and generally traces of biotite and apatite. Because olivine and chromite are generally the only euhedral or subhedral minerals, they are interpreted to be cumulus minerals, with the other minerals forming as intercumulus poikilitic grains. Occasional cumulus pyroxene and hornblende grains may also be present at least locally. The formation of the peridotite is attributed to crystal accumulation for the following reasons: (a) the presence of many euhedral to subhedral crystals surrounded by large poikilitic grains; (b) the olivine grains themselves form an "open framework" similar to the clasts in a coarse sand deposit; (c) occasional mineral orientation and size grading can be observed; (d) some samples are almost monomineralic; (e) the composition is dissimilar to normal igneous melts.

The coprecipitation of olivine and chromite as cumulus minerals is a common feature in layered mafic intrusions and suggests that they crystallize along a cotectic boundary. Irvine (1967) has shown that only a small content

of Cr_2O_3 in liquids rich in potential olivines or pyroxene will lead to early precipitation of a spinel phase. He also states that during fractional crystallization, only a small proportion (~2%) of spinel would coprecipitate with forsterite or a magnesium-rich pyroxene. The small proportion of chromite in the peridotites of the layered sills (see Table 4) is in agreement with Irvine's conclusions.

As described earlier, the poikilitic grains tend to be quite large (up to ~2cm) with pyroxene oikocrysts generally larger than plagioclase oikocrysts. Jackson (1971) has pointed out that coarse poikilitic textures are typical features of ultramafic cumulates. It appears that where a mineral, not present as a cumulus phase, begins to crystallize from the intercumulus liquid, nucleation centers tend to be rather widely spaced and poikilitic textures are well developed.

In the peridotite, intercumulus minerals are thought to have formed not only by direct crystallization from intercumulus liquid but also by reaction with olivine. This is indicated by rounding and embayment of olivine where it is enclosed by pyroxene, especially augite. Olivines, where enclosed by plagioclase are generally euhedral or subhedral, suggesting that poikilitic plagioclase formed prior to the reaction of olivine to pyroxene. This is supported by no reaction products being included in the plagioclase. Williams and Hallberg (1973)

have recently described the same relations in Archean layered sills from Western Australia. The reason for plagioclase forming prior to pyroxene from the intercumulus liquid is not known.

The presence of hornblende in the peridotite largely as poikilitc grains but occasionally as cumulus grains indicates that sufficient water was present in the magma to allow its formation. In some peridotites it appears to have formed to the exclusion of pyroxene and plagioclase (?). MacRae (1969) has attributed the formation of hornblende in sills from the Abitibe region of Ontario to water being supplied from country rocks at the time of crystallization of the peridotite. Such a mechanism does not appear applicable to the Newton Lake sills as no primary hornblende is seen in the chilled margins. Also the chilled margins would have formed a fairly impervious zone making it unlikely that water could migrate into the liquid during the period that the peridotite crystallized. It appears therefor, that the water required for the crystallization of hornblende in the peridotite was present in the initial magma.

The average ratio of cumulus to intercumulus minerals is about 65:35 in most peridotite samples from the Newton Lake layered sills. This may not represent the original crystal to liquid ratio in the cumulate however, as reaction between olivine and interstitial liquid may have increased the amount of intercumulus

material. The general presence of olivine relicts within the pyroxene grains indicates that the reaction was not complete however and that the ratio of 65:35 may be fairly close to the initial ratio.

Wager and others (1960) suggest that 35 to 45% intercumulus material is typical of cumulates formed simply by crystal settling. The percentages were obtained from an experiment preformed to simulate settling of plagioclase in the lower portion of the Skaergaard intrusion. Hess (1960) estimated that 26 to 29% intercumulus material was typical of cumulates from the Stillwater Complex, while Jackson (1961) estimated an average of 25 to 40% for the ultramafic rocks of the Stillwater Complex. Experimental studies by Cameron (1969) of settling of bronzite grains gave a minimum value of about 28% and with loose packing ranging up to 45%. These values also indicate that the ratio of cumulus crystals to intercumulus liquid in the Newton Lake peridotites may not be far removed from the initial ratio.

A few peridotites examined have ratios as high as 85:15 cumulus to intercumulus minerals. As can be seen from the discussion above such a low percentage for intercumulus material can not be accounted for by normal gravity settling of olivine grains. Jackson (1961) has pointed out that three main factors can reduce porosity (i.e. percent intercumulus liquid) in cumulates: (a) an increase in the size of cumulus crystals after settling, (b) an

increase in tabular habit, making close packing easier, and (c) a poor degree of size sorting. No evidence for post cumulus growth of olivine has been seen in the peridotites under discussion. Olivines are generally euhedral to subhedral with no interference textures present. A common feature in these peridotites is the tabular habit of olivine and it is probable that the tabular habit has allowed closer packing of grains. Some lack of size sorting is also present and may have helped in reducing the amount of intercumulus liquid.

Wager and others (1960) have developed a classification for cumulates based largely on the relationship between cumulus grains and intercumulus material. Using this classification the peridotites from the Newton Lake sills could be named olivine-chromite heteradcumulates. Wager and others give as characteristics for heteradcumulates a lack of zoning in the intercumulus minerals and the presence of minerals not found as cumulus phases in that particular zone of the intrusion. The poikilitic pyroxenes of the Newton Lake peridotites show no zoning in thin section and this has been confirmed by microprobe analysis. The lack of zoning in poikilitic plagioclase can not be confirmed due to the extensive alteration of this mineral. The presence of plagioclase as an intercumulus mineral in the peridotite, while it is not present as a cumulus phase untill higher in the sequence, is in agreement with the heteradcumulate nature of the peridotites.

Wager and others (1960) and Hess (1960) have attributed the formation of heteradcumulates to diffusion of material between the trapped intercumulus liquid and the main magma above. Such diffusion would explain development of unzoned interstitial minerals. Hess (1960) has pointed out that rate of crystal settling will largely determine if a heteradcumulate will form or some other type (i.e. orthocumulate, mesocumulate). It appears that slow settling rates are required for heteradcumulates to form as only with slow settling would there be time for diffusion of material to take place.

One complication in classifying the peridotites as heteradcumulates is the reaction relation observed between olivine and liquid (to pyroxene). This relation suggests that intercumulus pyroxene did not form completely by diffusion. Jackson (1961) has described similar features from the Stillwater Complex where olivine was found to have reacted to orthopyroxene in some peridotites. Wager and Brown (1968) feel that such a reaction relation between cumulus minerals and trapped pore liquid indicates orthocumulus or mesocumulus processes. It may be that the peridotites of the Newton Lake sills formed too fast for constant diffusion between trapped liquid and the main magma to take place.

Pyroxenite

The pyroxenite approaches a monomineralic rock composed of augite with lesser amounts of plagioclase, ortho-

pyroxene, minor magnetite, sulfide, quartz and hornblende. Augite and orthopyroxene are cumulus minerals with the other minerals occurring as intercumulus material. A few altered cumulus olivine grains are also locally present at peridotite-pyroxenite contacts. A number of features indicate an origin by crystal settling for the pyroxenite unit and include: (a) nearly monomineralic rock composition, (b) textures similar to a sandstone with a complex cement, (c) unreasonable bulk composition for an igneous melt, (d) interference textures developed between adjacent pyroxene grains.

Augite is the most abundant cumulus mineral and occurs as small euhedral to subhedral grains which commonly show mutual interference surfaces where in contact with other pyroxene, but where in contact with interstitial material they retain their crystal faces. The presence of the interference texture implies considerable adcumulus overgrowth on the cumulus augite crystals.

Orthopyroxene is present as large subhedral phenocrysts, commonly rimmed by plagioclase which occurs as anhedral interstitial material (see Figure 21). Enclosed in some phenocrysts are rounded augite relics. The presence of orthopyroxene as phenocrysts suggests that few nuclei were present, resulting in the large growth by intercumulus diffusion of those that did form. The presence of plagioclase rims around the phenocrysts appears difficult to relate to a cumulus origin. Williams and Hallberg (1973)

have observed similar rims on orthopyroxene phenocrysts from norite gabbro portions of Western Australian mafic-ultramafic sills. They suggest that settling orthopyroxene crystals collected small, slowly settling plagioclase crystals as they sank downward through the magma. In the Newton Lake sills such a mechanism appears unlikely as plagioclase was not yet a cumulus phase. It appears possible however, that the plagioclase rims formed as the result of a reaction between orthopyroxene and the interstitial liquid.

Plagioclase is the major intercumulus mineral though quartz and hornblende are locally important. The plagioclase occurs as small poikilitic grains showing albite twins and zoned extinction. The presence of quartz interstitially suggests that advanced fraction of the trapped intercumulus liquid may have occurred.

The lack of chromite in most pyroxenite contrasts with its presence in the peridotite. Its disappearance may be related to a peritectic reaction with chromite going to diopsidic augite as suggested by Irvine (1967). Textural evidence for such a peritectic reaction is seen in the commonly embayed and irregular margins of chromite grains from the upper part of the peridotite unit (see Figure 19).

As previously discussed (see page 94) crystal settling alone can not produce largely monomineralic rocks because 28 to 40% intercumulus liquid should be trapped in the

settling process. Jackson (1961) in discussing pyroxenites from the Stillwater Complex attributed the low percentage of intercumulus material to continued growth of settled crystals subsequent to deposition. Such growth would force out trapped liquid as pyroxenes grew into the interstitial spaces. As evidence for such growth Jackson points to the interference textures commonly displayed between pyroxene grains. As previously described the augite from the pyroxenites of the Newton Lake layered sills commonly show such a texture and it suggested that continued growth of augite crystals has occurred after settling. The presence of crystal faces where augite is in contact with intercumulus material indicates that the secondary enlargement was completed prior to precipitation of new minerals from most of the interstitial liquid (Jackson, 1961).

Using the terminology of Wager and others (1960) the pyroxenites would be named augite-orthopyroxene mesocumulates. The lower contact of the pyroxenite with peridotite would be a "phase contact" (Jackson, 1971) since it is marked by the disappearance of olivine and chromite as cumulus phases and the new appearance of pyroxene. The upper contact with the bronzite gabbro is both a phase contact and a ratio contact (Jackson, 1971) as plagioclase becomes a cumulus phase and increases with concommitant decrease in pyroxene.

Bronzite Gabbro and Gabbro

The basal portion of the bronzite gabbro is interpreted as a cumulate for the following reasons: (a) there are no interlocking textures between plagioclase and pyroxene, which are common in normal gabbros; (b) plagioclase occurs as segregations of many small laths rather than dispersed throughout the rock; (c) subhedral cores can be seen in some pyroxene grains which have irregular outlines suggesting adcumulus growth; (d) occasional rhythmic layering is locally present. The base of the bronzite gabbro is thus marked by the appearance of plagioclase as a major cumulus phase. The basal portion of the unit is a plagioclase-augite-orthopyroxene cumulate with quartz, iron-titanium oxide and minor biotite occurring as postcumulus phases.

Based on the grain size of individual plagioclase laths (1 to 2 mm) it appears that they cannot be in hydraulic equilibrium with pyroxene which are larger (2 x 4 mm). Much of the plagioclase occurs as clots or segregations and it appears that the plagioclase may have settled in small aggregates rather than as individual crystals. However, a detailed hydrodynamic analysis has not been attempted in this study.

The presence of orthopyroxene as phenocrysts suggests that few nuclei formed compared to those forming augite crystals. The reason for this lack of nucleation in orthopyroxene is not presently known. Although porphyritic cumulus rocks are not abundant they are not unknown

and have been described by Willemse (1969) from the Bushveld Complex, by Viljoen and Viljoen (1970) from the Kaapmuiden area, South Africa and by Williams and Hallberg (1973) from Early Precambrian layered sills from Western Australia. In all the above cases the phenocrysts are orthopyroxene occurring in either pyroxenites, norites or noritic gabbros. The relations described by Williams and Hallberg (1973) are especially interesting in that they are from layered sills very similar to those studied in this investigation. They attribute the orthopyroxene phenocrysts to formation during the waning stages of orthopyroxene crystallization, at which time plagioclase crystals were enclosed. It is possible that such a mechanism may also be applicable to the phenocrysts of the bronzite gabbro described above. It is still unclear however, why the larger orthopyroxene crystals did not settle out into a distinct layer. They are probably of the same density as the augite grains but should be heavier owing to their size and are more dense than the associated plagioclase grains also. It may be that the large number of slowly settling augite and plagioclase impeded the downward progress of the phenocrysts. It may also be that the phenocrysts nucleated slighlty above the zone crystallizing augite and plagioclase and grew while falling into that zone. Such a mechanism has been proposed by Jackson (1961) to account for differences in grain size between olivine and bronzite

crystals from certain layers of the ultramafic zone of the Stillwater Complex. It is unclear however, what would cause orthopyroxene to crystallize above augite and plagioclase in the Newton Lake sills.

The lower bronzite gabbro has very little intercumulus material that cannot be attributed to adcumulus growth of the three cumulus phases after crystal settling. Textural evidence of subhedral to euhedral cores in pyroxene grains which now have anhedral forms suggests that they continued to grow after settling, filling in the open spaces around them. Quartz and biotite also crystallized from the intercumulus liquid and occupy the spaces between the cumulus overgrowths.

In the terminology of Wager and others (1960) the lower bronzite gabbro would be a plagioclase-augite-orthopyroxene mesocumulate. Hess (1960) as well as others have attributed adcumulus growth of crystals to diffusion of material between trapped intercumulus liquid and the main magma. Such a mechanism requires fairly slow rates of crystal settling and it appears therefore, that both the pyroxenite and lower bronzite gabbro formed slowly enough to allow some diffusion to occur. The lack of zoning in any of the cumulus phases indicates addition of material of the same composition and supports this model for adcumulus growth.

Plagioclase is generally 1 to 2 mm in length at the base of the bronzite gabbro unit but increases in size

stratigraphically upwards. It also increases in amount upwards through the gabbro units with the texture becoming ophitic to subophitic as augite and orthopyroxene change from cumulus to interstitial grains. It appears that the upper bronzite gabbro as well as the gabbro unit above have crystallized largely in place without any significant crystal settling having occurred.

Wadsworth (1973) has indicated that the vital ingredients for the successful accumulation of a sediment of any kind are: (a) the presence of solid particles dispersed in a fluid medium; (b) a density contrast between the particles and the fluid; (c) the operation of gravitational forces; (d) adequate time for sedimentation to occur. Other important factors include the density of the fluid, the degree of density contrast between phases, the size and shape of the particles and the presence of currents within the fluid.

The presence of normal interlocking textures in the upper gabbroic portions of the Newton Lake sills suggests that a framework of crystals had developed after formation of the lower bronzite gabbro unit and that there was little time for crystal settling to occur. Increasing viscosity of the magma (e.g. enrichment in silica with differentiation) also probably helped curtail crystal settling in the upper gabbro units. Increasing silica enrichment in the magma is expressed by changes in the crystallizing phases with differentiation and in the increase in quartz content upwards through the sill.

Formation of the Chilled Margins

The chilled margins of the layered, differentiated sills (as well as those of the lenses), are dissimilar to those generally ascribed to layered mafic intrusions (see Hess, 1960 and Irvine, 1970). Their texture is, however, very similar to those described by Williams (1972) for some Archean high-Mg basalts from Western Australia, by Wood and others (1971) (see especially page 190) for some lunar basalts and by Nesbitt (1971) and Naldrett (1972) for certain ultramafic lenses of Archean age (in the ultramafic lenses the skeletal phase is largely olivine with the resulting texture termed "spinifex" after its similarity to the Australian grass of that name (Nesbitt, 1970)). A detailed mineralogic description of a texturally similar lunar vitrophyre has also recently been published by Weigand and Hollister (1973).

The development of the chilled margins of the Newton Lake layered sills is attributed to rapid cooling or quenching resulting in in situ rapid crystallization of a crystal-free liquid after intrusion at a shallow depth. This interpretation is based on the following features of the chilled margins:

A. They contain highly skeletal pyroxene and plagioclase crystals.

B. Devitrification textures are developed in interstitial material.

C. Branching, fan-like crystals oriented perpendicular

to the contact and reaching several centimeters in length are developed inwards toward the sill, away from the contact.

D. Variolites are locally present.

E. Amygules rimmed by opaques are common in parts of the border zone.

F. The textures observed are analogous to experimentally formed textures in rapidly cooled slags and are also similar to textures described from other rocks in similar geologic environments.

As has been pointed out by many authors (e.g., Nesbitt, 1971 and Williams, 1972), rapid cooling alone can not account for the skeletal habit common in the chilled zones as many rapidly chilled basalts lack this feature. It appears that in addition to rapid cooling some degree of supercooling is also required. Taubeneck and Poldervaart (1960) have pointed out the supercooling would result in very rapid crystallization, elongation of crystals, development of curved and branching forms, and growth at right angles to the cooling surface. All these features are commonly observed in the chilled zones of the layered sills and lenses. The cause of the supercooling was probably rapid chilling caused by shallow intrusion into still wet sediments and volcanics. Such fast cooling could produce overshooting of the liquids surface, resulting in supercooling (Nesbitt, 1971). The amount of supercooling which took place is difficult to determine; however,

recent work by Lofgren (1972 and 1973) on the crystallization of plagioclase seem applicable. Lofgren found that the shape of crystallizing plagioclase varies with the degree of supercooling of the liquid (see Figure 40). Applying his conclusions to plagioclase from the chilled margins of the layered sills it appears that crystallization took place between 100 and 200°C below the equilibrium liquidus temperature.

Though crystallization must have been fairly rapid in the chilled zone the absolute rate of crystallization is unknown. The presence of a finer-grained chill at the upper surface, the continual increase in the size of pyroxene crystals inwards and away from the upper contact, and the compositional zoning of plagioclase (and pyroxene ?) indicate that the conditions of formations probably did not involve an instantaneous quench (Pyke and others, 1973). It appears that crystallization took place in a rapidly cooled environment in which heat was lost from the upper surface and crystals grew downward into the underlying liquid, attached to crystal nuclei above. Pyke and others (1973) suggest that the systematic variation in grain size of the skeletal crystals is related to a lower heat loss downwards toward the base allowing for growth of crystals in that direction. Nesbitt (1971) points out that it is also related to growth in the direction of maximum supersaturation of the components of the crystallizing minerals. It is probably that each of the large prismatic-branching

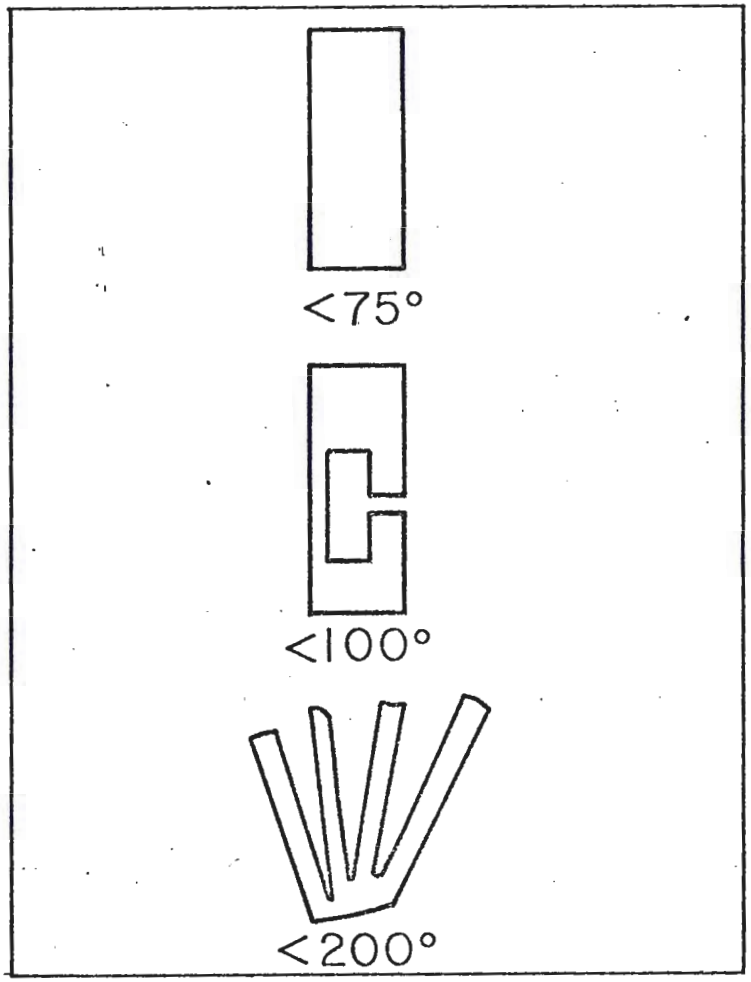

Figure 40. Variation in the shape of crystallizing plagioclase with varying degrees of supercooling (after Lofgren, 1972).

crystals in the inner zone could be traced to tiny nuclei in the outer margin and that after formation of the nuclei the crystals grew downwards with crystallization becoming slower as the liquid became better insulated. With slower crystallization growth would continue on a decreasing number of crystals as they became completely isolated from the liquid.

The formation of large single crystals rather than many small ones seems to require that nucleation be centered on few sites. This requires an absence of crystal nuclei prior to nucleation. Nesbitt (1971) relates the lack of nuclei in skeletal textural development to the presence of superheat (that is, temperatures above the liquidus surface) in the initial liquid. It is possible that rapid ascent of the liquid from relatively deep to fairly shallow levels could account for any superheating that may have occurred.

The development of layering in the chilled zone in terms of a change from pyroxene to plagioclase crystallization, such as has been described above for the Newton Lake sills, has not been described for any of the major mafic intrusions. However, a similar sequence has been described by Travis and others (1971) from the Kalgoorlie Goldfields in Australia. The sequence they describe is generally the same as for the chilled margins of the Newton Lake sills except that their sequence is 100 to 200 feet thick, whereas that in the Newton Lake sills is

only about 30 feet thick. Textures are similar in the Australian sequence but are generally less skeletal than seen in the Newton Lake chilled zones. What the Australian example points out is that liquids having compositions similar to those obtained for the Newton Lake chilled margin samples (see Table 13) exist elsewhere and have produced somewhat similar sequences.

The crystallization of branching pyroxene followed by plagioclase is similar to that observed in the Willow Lake Intrusion in Oregon (Taubeneck and Poldervaart, 1960) and called Willow Lake layering. The layers in the Willow Lake Intrusion are repeated many times and the authors relate their formation to supercooling accompanied by an increase in water pressure. Yoder (1954) has shown increased water pressure may shift four-phase points in three component systems such as the diopside-anorthite-water system allowing crystallization of alternate phases to take place. It may be that streaming of volatiles towards the margins of the sills of the Newton Lake formation helped increase water pressure enough to cause a shift in the eutectic and allow plagioclase, rather than pyroxene, to crystallize.

Chilled Margins of the Ultramafic Lenses

The chilled margins of the ultramafic lenses have the same features as those described for chilled margins of the layered sills (see above) and probably formed in much the same manner. In the case of the lenses no dif-

ferentiation has occurred and the chilled zone is in sharp contact with peridotite both above and below the unit. The lack of any olivine in the chilled zone suggests that the olivine of the peridotite layer may have been carried in suspension upon intrusion and that through flow differentiation and gravity settling was concentrated toward the lower portion of the lens. A similar model was proposed by Naldrett and Mason (1968) for ultramafic lenses found associated with the Dundonald sill of Canada.

PETROCHEMICAL ASPECTS OF NEWTON LAKE SILLS

Mineral Chemistry for the Layered Sills

Olivine

Three olivine analyses were obtained with the electron microprobe (Table 8). The samples have a forsterite content of 77.4, 78.9 and 80.3. Comparison of the forsterite content of these olivines with olivines from other mafic layered intrusions (Figure 41) shows them to be very similar in composition to many olivines found in similar environments, with the exception of some of the Phanerozoic orogenic olivines which tend to be more magnesian.

The minor elements Ni, Mn, and Ca fall in the fields found by Simkin and Smith (1970) in plots of olivine minor elements against Mg content. Their results indicate that while Mn and Ni in olivines are related to major-element fractionation Ca may be related to depth (pressure) of

Table 8: Chemical Composition and Structural Formulas for Analyzed Olivines.

	1	2	3
SiO_2	44.80	40.72	39.16
Fe as FeO	18.20	18.81	18.93
MnO	0.28	0.23	0.23
MgO	34.70	39.59	43.22
CaO	0.10	0.22	0.20
Cr_2O_3	0.15	0.03	0.03
NiO	0.13	0.18	0.23
	98.36	99.78	102.00
Fe	22.56	21.10	19.72
Mg	77.44	78.90	80.28

Structural Formula Based on 4 Oxygens.

Si	1.140	1.039	0.984
Fe	0.388	0.402	0.398
Mg	1.319	1.507	1.619
Mn	0.007	0-006	0.005
Ca	0.003	0.006	0.006
Cr	-----	0.001	0.005
Ni	0.003	0.004	0.005
	2.850	2.965	3.018

All analyses are an average of two spots.

1. Peridotite, Cedar Lake Sill, SE1/4, NE1/4, Sec. 7, T. 63 N., R. 11 W., Sample No. E-46b.
2. Peridotite, NW1/4, SE1/4, Sec. 29, T. 64 N., R. 11 W., Sample No. SEN-75.
3. Peridotite, SW1/4, SE1/4, Sec. 9, T. 63 N., R. 12 W., Sample No. SEN-310.

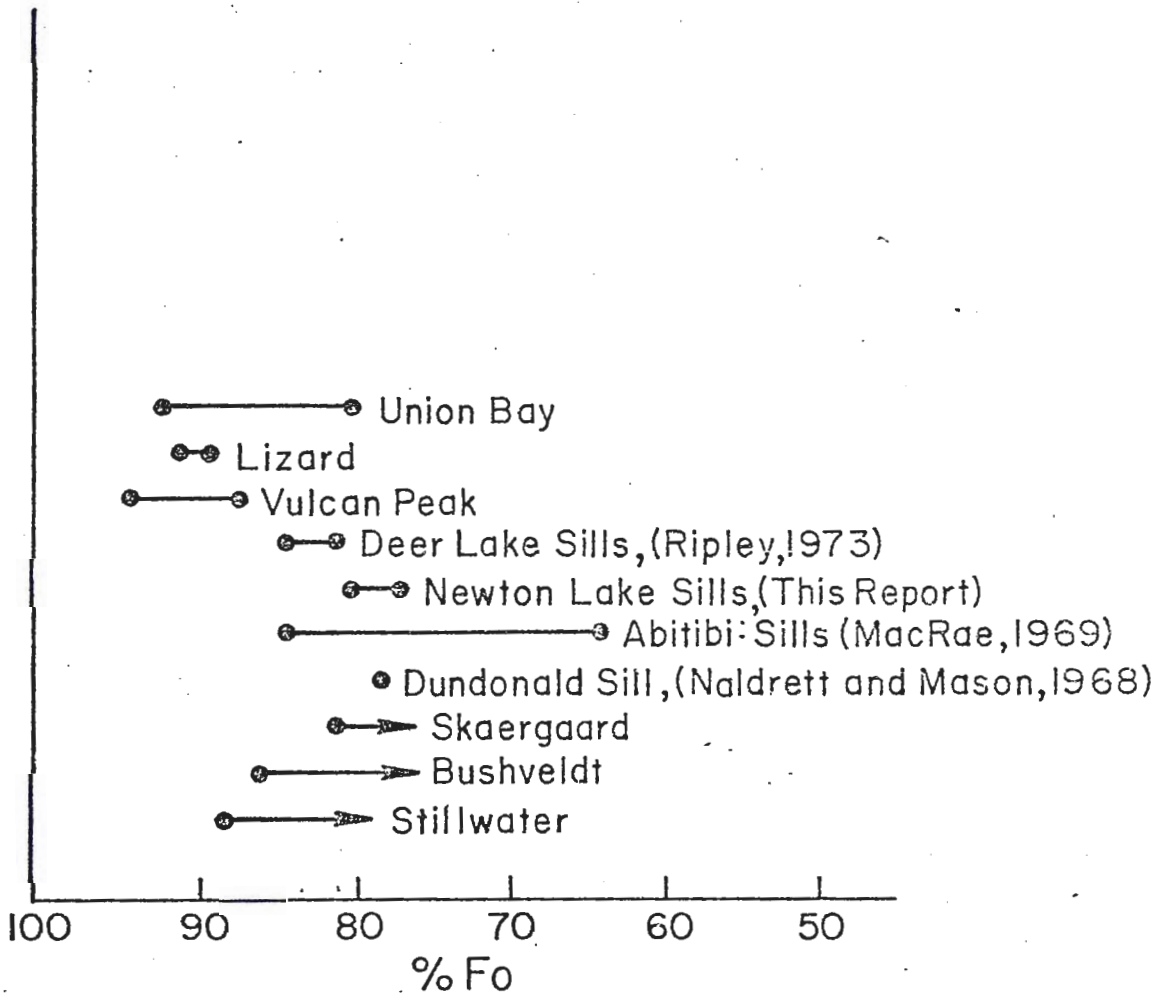

Figure 41. Comparison of olivine data from Newton Lake layered sills with olivine data from other mafic and ultramafic intrusions. (Unless otherwise indicated data taken from Lewis, 1973).

crystallization. The three olivine analyses obtained from the Newton Lake peridotites plot in the field for hypabyssal olivines suggesting crystallization at shallow depths (Simkin and Smith, 1970, p. 318).

Orthopyroxene

Although orthopyroxene is generally quite altered in the samples examined, two analyses were obtained, one from a peridotite and one from a pyroxenite (Table 9). Both orthopyroxenes analyzed have bronzite compositions and show the fine exsolution lamellae of augite (Table 9) parallel to {100} characteristic of "Bushveld" type orthopyroxene. The major difference in the composition of the two orthopyroxenes is a higher Mg:Fe ratio in the orthopyroxene from the peridotite sample, which is poikilitic and has a composition of $Ca_{3.5}Mg_{81.2}Fe_{15.3}$ and a lower ratio in the orthopyroxene from the pyroxenite in which it occurs as cumulus grains with the composition $Ca_{3.5}Mg_{75.6}Fe_{20.9}$. Although based on only two samples, the trend toward iron enrichment is that expected with fractional crystallization (Figure 42) (Poldervaart and Hess, 1951). The fairly constant percentage of Ca in the orthopyroxene is also typical.

The significance of observed differences of the minor elements analyzed is questionable because only two analyses are available, however some general comments may be made. The Al_2O_3 content appears to increase with fractional crystallization but is substantially lower in

Key to Analyses

Table 9

1. Peridotite, Cedar Lake Sill, SE 1/4, NE 1/4, Sec. 7, T. 63 N., R. 11 W., Sample No. E-46b.
2. Pyroxenite, Cedar Lake Sill, NE 1/4, NW 1/4, Sec. 18, T. 63 N., R. 11 W., Sample No. SES-26.
3. Peridotite, Picketts Lake Lens, SW 1/4, SW 1/4, Sec. 6, T. 63 N., R. 11 W., Sample No. SEP-8.
4. Peridotite, SW 1/4, SE 1/4, Sec. 9, T. 63 N., R. 12 W., Sample No. SEN-310.
5. Pyroxenite, SW 1/4, SE 1/4, Sec. 9, T. 63 N., R. 12 W., Sample No. SEN-309.
6. Pyroxenite, Cedar Lake Sill, same as No. 2., Sample No. SES-26.
7. Pyroxenite, Cedar Lake Sill, same as No. 2., Sample No. SES-26.
8. Pyroxenite, SW 1/4, SE 1/4, Sec. 29, T. 64 N., R. 11 W., Sample No. SEN-40.
9. Bronzite Gabbro, Cedar Lake Sill, same as No. 2., Sample No. SES-27.
10. Bronzite Gabbro, Cedar Lake Sill, NW 1/4, SE 1/4, Sec. 13, T. 63 N., R. 12 W., Sample No. SES-14.
11. Bronzite Gabbro, Cedar Lake Sill, SW 1/4, NW 1/4, Sec. 8, T. 63 N., R. 11 W., Sample No. SES-33.

Table 9: Chemical Composition and Structural Formulas for Analyzed Pyroxenes.

	1	2	3	4	5	6	7	8	9	10	11
	Opx.	Opx.+	Cpx.	Cpx.	Cpx.+	Cpx.°	Cpx.+	Cpx.+	Cpx.+	Cpx.+	Cpx.+
SiO_2	51.51	55.41	55.09	53.39	52.85	55.40	53.74	53.88	56.60	52.82	51.98
TiO_2	0.17	0.46	0.40	0.11	0.55	0.13	0.52	0.08	0.14	0.24	0.45
Al_2O_3	0.44	1.01	3.35	1.60	1.45	0.48	2.28	1.54	0.75	2.72	1.68
Fe as FeO	11.34	13.60	5.90	4.51	6.47	4.28	5.59	4.20	3.28	5.54	6.66
MnO	0.35	0.28	0.18	0.14	0.25	0.10	0.19	0.18	0.22	0.20	0.22
MgO	33.74	27.59	15.40	19.56	17.37	17.80	17.12	16.86	16.06	15.18	16.25
CaO	2.06	1.78	19.08	20.73	21.46	21.29	21.10	21.62	22.34	22.35	21.75
Cr_2O_3	0.36	0.12	0.62	0.64	0.35	0.11	0.48	0.38	0.18	0.68	0.90
NiO	0.03	0.45	0.05	---	---	0.04	0.04	0.03	0.04	0.03	0.03
	100.00	100.70	100.07	100.68	100.75	100.63	101.60	98.77	99.61	99.76	99.92
Fe	15.3	20.9	10.2	6.8	9.9	6.8	8.9	6.8	5.6	9.0	9.9
Ca	3.5	3.5	42.3	40.3	42.4	43.1	42.8	44.7	47.3	46.8	43.7
Mg.	81.2	75.6	47.5	52.9	47.7	50.1	48.3	48.5	47.1	44.2	46.4
				Structural Formula Based on 6 Oxygens.							
Si	1.848	1.981	1.992	1.928	1.931	2.020	1.940	1.988	2.048	1.948	1.923
Al	0.018	0.019	0.008	0.068	0.063	---	0.060	0.012	---	0.052	0.073
Cr	0.010	2.000	2.000	1.996	1.994	2.020	2.000	2.000	2.048	2.000	1.996
Fe	0.124										
	2.000										
Al	---	0.024	0.135	---	---	0.021	0.037	0.055	0.032	0.066	---
Ti	0.005	0.013	0.011	0.003	0.015	0.004	0.014	0.003	0.004	0.007	0.013
Fe	0.216	0.407	0.179	0.136	0.198	0.131	0.169	0.130	0.100	0.171	0.207
Cr	---	0.004	0.018	0.018	0.010	0.003	0.014	0.011	0.006	0.020	0.026
Mg	1.804	1.470	0.830	1.053	0.946	0.967	0.921	0.927	0.867	0.835	0.895
Mn	0.011	0.008	0.006	0.004	0.008	0.003	0.006	0.006	0.007	0.007	0.007
Ca	0.079	0.068	0.739	0.802	0.840	0.832	0.816	0.853	0.867	0.884	0.863
Ni	0.001	0.001	0.001	---	---	0.-01	0.001	---	0.001	0.001	0.001
	2.116	1.995	1.919	2.016	2.017	1.962	1.978	1.985	1.884	1.987	2.012

+Analyses average of two or more pts. °,Clinopyroxene lamellae in orthopyroxene.
Opx. = Orthopyroxene Cpx. = Clinopyroxene

the orthopyroxene than in associated augites (see Table 9). The Al_2O_3 content of both analyzed orthopyroxenes is also lower than that normally found in orthopyroxenes of this type (see Hess, 1960, Table 3, page 25). The reason for the low aluminum contents may be the result of early crystallization of plagioclase which would deplete the liquid in aluminum (Bence and Papike, 1972, page 467). It may also be related to crystallization under low-pressure conditions (Green, 1964).

The other minor constituents show less apparent variation than aluminum. The TiO_2 content shows an increase in the orthopyroxene from the pyroxenite over that from the peridotite. Both MnO and Cr_2O_3 show a decrease in the pyroxenite orthopyroxene while NiO shows an increase. The increase in NiO and decrease in MnO (if not analytical) is at variance with trends found by Hess (1960) in Stillwater orthopyroxenes, however more analyses are required to establish pyroxene trends in the Newton Lake sills.

Augite

Nine microprobe analyses for augites from the Newton Lake layered sills are given in Table 9. Two analyses are of poikilitic augites in peridotite, three are of cumulus augites in pyroxenite, three in bronzite gabbro and one is of an augite lamallae in a cumulus orthopyroxene (in pyroxenite).

With fractional crystallization the major variable in chemical composition of the augites is the change in the Ca:Mg:Fe ratio. Figure 42 shows the augite analyses plotted in the pyroxene quadrilateral with augite analyses from Hess (1960), MacRae (1969) and Williams and Hallberg (1973) given for comparision. Analyses of augites from the Deer Lake Complex (Ripley, 1973) have also been plotted and used to help define the trend shown by the Newton Lake pyroxenes. As can be seen from the figure the augite trend from the Newton Lake layered sills (and the Deer Lake Complex) is similar to that shown by those plotted for comparison.

An important feature of this trend is the initial increase in the calcium content with fractional crystallization. Such an initial increase in calcium is at variance with trends drawn by Wager and Brown (1968) for Skaergaard pyroxenes and by Boyd and Schairer (1964) for pyroxenes from layered intrusives. More recent experimental work on the pyroxene solidus at one atmosphere shows however, that an initial increase in calcium occurs in the crystallization trend of diopsidic pyroxenes (Huebner, 1973, in preparation).

The rest of the trend shown for the Newton Lake pyroxenes is also inferred to be identical to that of the Deer Lake Complex (Ripley, 1973), and Deer Lake pyroxenes were used to help define the trend. The calcium content shows a decline after the formation of the pyroxenites,

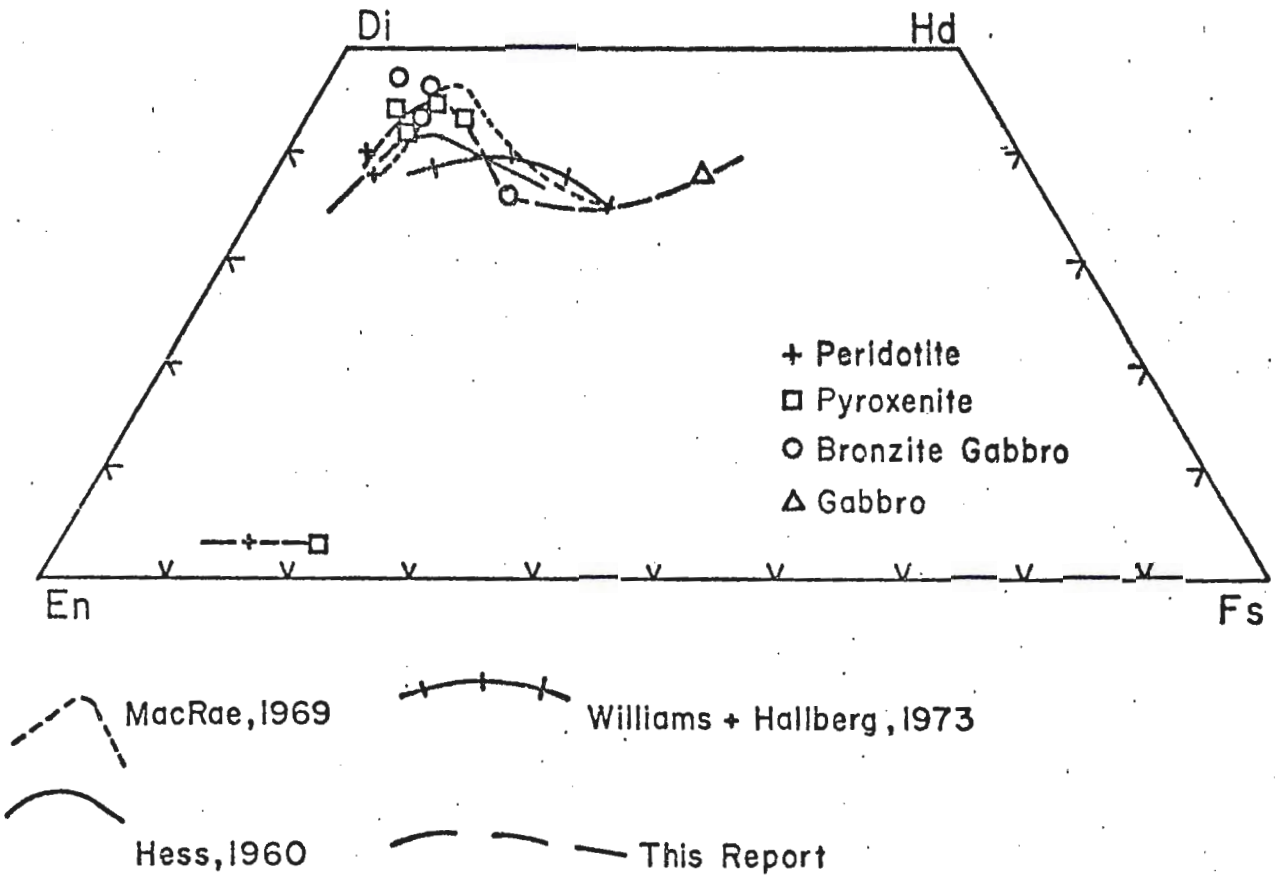

Figure 42. Crystallization trend on pyroxene quadrilateral for pyroxenes from Newton Lake (and Deer Lake Complex) layered differentiated sills. Plotted for comparison are pyroxene crystallization trends for the Abitibi sills, Canada (MacRae, 1969) Western Australian sills (Williams and Hallberg, 1973) and the Stillwater Complex (Hess, 1960).

and increases slightly again with the crystallization of the bronzite gabbro and gabbro units as the Fe/Mg ratio increases.

The minor elements show variations similar to those described for augites from other layered intrusives. The TiO_2 and MnO show a slight increase with fractionation whereas the Cr_2O_3 shows a general decline. The Cr_2O_3 content of two augites from the bronzite gabbro unit of the Cedar Lake sill is quite high in comparison to the other analyses. The high values may be related to the lack of crystallization of pyroxenite in the area of the two anomalous samples. Where the bronzite gabbro unit is underlain by pyroxenite the augites of the former unit show lower Cr_2O_3 values (see Table 9, No. 9.).

The Al_2O_3 content of the Newton Lake augites is lower than for the augites of the Stillwater or Bushveld Complexes (Hess, 1960). This may in part be due to the analytical accuracy obtained or the availability of aluminum and the pressures of crystallization as discussed above for the orthopyroxenes. The Al_2O_3 content of the augites is higher, however, than in associated orthopyroxene.

Chromian Spinels

Electron microprobe analyses for five chromian spinels are given in Table 10. As seen in the table the analyses all show low oxide totals. This is probably related to oxidation of the FeO and errors in determination of the

Al_2O_3 content. Also the low totals and differences between analyses (two of which are from the same sample) may be due to surface conditions and size variations of the grains analyzed. More work is necessary to accurately determine spinel compositions in the layered sills. Based on the present analyses for FeO, the amount of FeO and Fe_2O_3 was inferred from the general spinel formula ($R^{++}R_2^{+++}O_4$) and by setting R^{++} equal to one.

The present data suggests that the spinels may have a considerable range in chemical composition. This can be seen in the range of cation ratios of $Mg/(Mg + Fe^{++})$ (0.41 to 0.05) and $Fe^{+++}/(Fe^{+++} + Cr + Al)$ (0.70 to 0.07). The $Cr/(Cr + Al)$ ratio is more constant and ranges from 0.65 to 0.80. A plot of the $Cr/(Cr + Al)$ and $Mg/(Mg + Fe^{++})$ ratios (Figure 43) shows all but one of the chromian spinels falls within the field of chromites from stratiform intrusions.

Amphibole

Six primary brown amphiboles were analyzed (Table 11). The analyses are fairly similar and show little variation in major elements (except for analysis 6, which is from the Cedar Lake sill pyroxenite and has lower silica). The analyses show the primary brown amphiboles to have a composition similar to pargasite except for having high TiO_2 and lower Al_2O_3 and K_2O (see Deer and others, 1963, Table 43, pages 286-287). In these elements the amphiboles resemble kaersutite (see Deer and others, 1963, Table 50, pages

Key to Analyses

Table 10

1. Peridotite, Picketts Lake Lens, SW 1/4, SW 1/4, Sec. 6, T. 63 N., R. 11 W., Sample No. SEP-8.
2. Peridotite, same as No. 1., Sample No. SEP-8.
3. Peridotite, SW 1/4, SE 1/4, Sec. 9, T. 63 N., R. 12 W., Sample No. SEN-310.
4. Peridotite, Cedar Lake Sill, SE 1/4, NE 1/4, Sec. 7, T. 63 N., R. 11 W., Sample No. E-46b.
5. Pyroxenite, Cedar Lake Sill, NE 1/4, NW 1/4, Sec. 18, T. 63 N., R. 11 W., Sample No. SES-26.

Table 10: Chemical Composition and Structural Formulas for Chrome Spinels.

Sample	1	2	3	4	5
SiO_2	0.28	0.40	1.66	3.13	0.35
TiO_2	5.21	1.68	0.64	6.68	1.10
Al_2O_3	7.00	10.99	12.92	2.54	14.40
Fe as FeO	46.62	35.01	24.95	59.60	33.69
MnO	2.13	0.66	0.64	1.84	0.68
MgO	0.80	4.72	7.91	4.73	6.00
Cr_2O_3	33.99	38.88	46.65	15.01	39.58
NiO	0.10	0.10	0.14	0.15	0.10
	96.16	92.47	95.51	93.71	95.91
	Structural Formula Based on 4 Oxygens.				
Fe^{++}	0.883	0.703	0.573	0.646	0.661
Mg	0.047	0.266	0.408	0.290	0.318
Mn	0.070	0.021	0.019	0.064	0.021
	1.000	1.000	1.000	1.000	1.000
Fe^{+++}	0.629	0.403	0.148	1.405	0.341
Cr	1.043	1.161	1.275	0.489	1.113
Al	0.320	0.490	0.527	0.123	0.603
Ti	0.152	0.048	0.017	0.207	0.029
	2.144	2.102	1.967	2.224	2.096
$\frac{Fe^{+++}}{Fe^{+++}+Cr+Al}$	0.314	0.197	0.076	0.696	0.169
$\frac{Mg}{Mg + Fe^{++}}$	0.051	0.266	0.408	0.290	0.318
$\frac{Cr}{Cr + Al}$	0.765	0.703	0.708	0.799	0.648

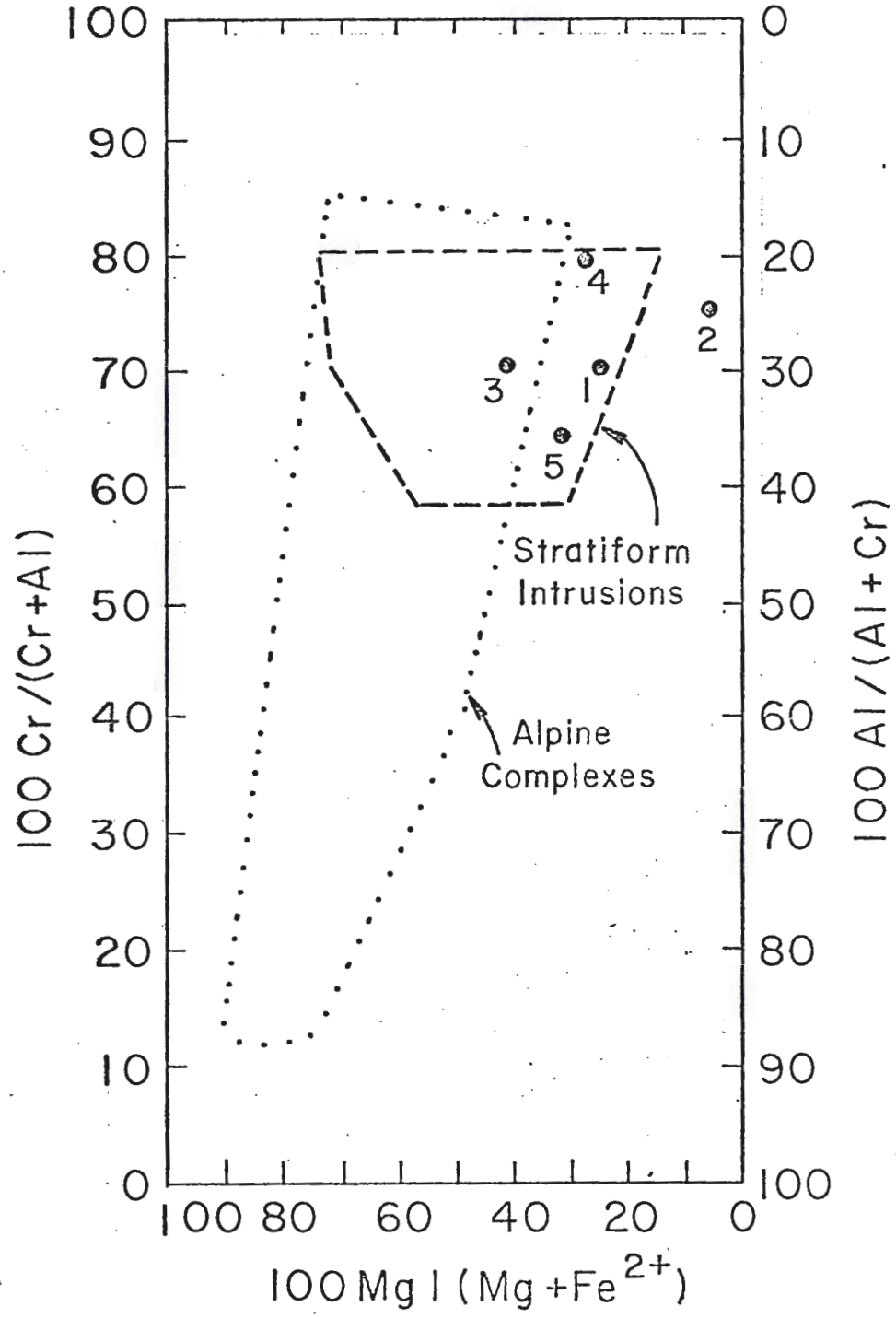

Figure 43. Plot of Cr/(Cr + Al) verses Mg/(Mg + Fe^{++}) for Newton Lake spinels. (Adapted from Irvine and Findlay, 1972).

Key to Analyses

Table 11

1. Peridotite, Picketts Lake Lens, SW 1/4, SW 1/4, Sec. 6., T.63N., R.11W., Sample No. SEP-8.
2. Peridotite, Cedar Lake Sill, SE 1/4, NE 1/4., Sec. 7., T.63N., R.11W., Sample No. E-46b.
3. Peridotite, NW 1/4, SE 1/4, Sec. 29., T.64N., R.11W., Sample No. SEN-75.
4. Peridotite, SE 1/4, SE 1/4, Sec. 9., T.63N., R.12W., Sample No. SEN-310.
5. Peridotite, same as No. 4., Sample No. SEN-310.
6. Pyroxenite, Cedar Lake Sill, NE 1/4, NW 1/4, Sec. 18., T.63N., R.11W., Sample No. SES-26.

Table 11: Chemical Composition and Structural Formulas for Analyzed Primary Amphiboles.

	1	2	3	4 (1)	5 (2)	6
SiO_2	46.73	45.91	45.70	49.69	49.45	39.74
TiO_2	3.45	2.66	3.34	3.44	0.42	4.16
Al_2O_3	8.95	9.15	11.27	9.40	9.19	10.62
Fe as FeO	9.90	7.67	7.81	6.39	5.65	9.74
MnO	0.09	0.17	0.15	0.10	0.09	0.32
MgO	15.50	15.19	18.32	16.35	18.93	16.92
CaO	11.68	10.60	11.42	11.57	13.36	13.35
Na_2O	2.28	1.52	2.12	2.25	1.82	1.81
K_2O	0.56	0.37	0.16	0.49	0.29	0.33
Cr_2O_3	0.37	1.28	0.10	0.93	0.18	0.32
NiO	0.10	0.05	0.07	0.08	0.09	0.07
	99.61	94.57	100.46	100.69	99.47	97.18
Fe	18.80	15.80	14.10	12.80	10.00	17.10
Ca	28.50	28.10	26.60	29.30	30.30	30.00
Mg	52.70	50.10	59.30	57.90	59.70	52.90
Ti/Al	0.25	0.19	0.19	0.24	0.03	0.25
	Structural Formula Based on 23 oxygens					
Si	6.66	6.77	6.37	6.84	6.88	5.91
Al	1.34	1.23	1.63	1.16	1.12	1.86
	8.00	8.00	8.00	8.00	8.00	7.77
Al	0.17	0.36	0.22	0.36	0.39	---
Ti	0.37	0.29	0.35	0.36	0.04	0.46
Fe	1.18	0.95	0.91	0.74	0.66	1.21
Mg	3.29	3.34	3.81	3.35	3.93	3.75
Mn	0.01	0.02	0.05	0.01	0.01	0.02
Cr	0.04	0.15	0.03	0.10	0.02	0.04
Ni	0.01	0.01	0.02	0.01	0.01	0.01
	5.07	5.12	5.39	4.93	5.06	5.49
Na	0.63	0.44	0.57	0.60	0.49	0.52
Ca	1.78	1.68	1.71	1.70	1.99	2.13
K	0.10	0.07	0.03	0.08	0.05	0.06
	2.51	2.19	2.31	2.38	2.53	2.71

(1), Red Amphibole Core; (2), Red Amphibole Margin.

322-323). The amphibole therefore appears intermediate in comparison between the two and could be termed a kaersutitic pargasite.

As previously discussed, the amphibole commonly shows a color zoning from red cores to clear margins. This change in color appears to be the result of a decrease in TiO_2 (3.44 wt.% core to 0.43 wt.% margin) outwards from the center of the grain. A decrease in Cr_2O_3 was also noted outwards towards the margin (0.93 wt.% core to 0.18 wt.% margin). The Cr_2O_3 shows a range from 0.10 to 1.28 wt.% in the other amphiboles analyzed.

Plagioclase

Plagioclase, in the samples examined, is generally too altered to allow accurate compositional determinations to be made. Norms calculated from the available rock analyses show that the plagioclase probably becomes more sodium-rich with differentiation.

Two analyses were obtained from a skeletal plagioclase grain from Unit C (plagioclase chill) of the chilled margin of the Cedar Lake sill (Figure 44 a). Broad beam microprobe scans across the plagioclase grain show it to consist of alternating calcium-rich and potassium-rich lamellae (see Figures 44 b and c). In terms of K:Na:Ca ratios the calcium-rich lamellae show ratios of 0.8:28.5:70.7 while the potassium-rich lamellae show ratios of 63.7:22.6:13.7 (Figure 45). Even though the plagioclase

Key to Figures

Figure 44 a. Photomicrograph showing hollow plagioclase crystals from Unit C of the layered sill chilled margins. Sample SES-22.

Figure 44 b. Potassium microprobe scan over a portion of the feldsar in Figure 44 a. White areas are K_2O rich while black areas are K_2O poor.

Figure 44 c. Calcium microprobe scan of the same area as in Figure 44 b. Note that areas which are K_2O poor in Figure 44 b are calcium rich.

44a

0 100 μ

44b

0 20 μ

44c

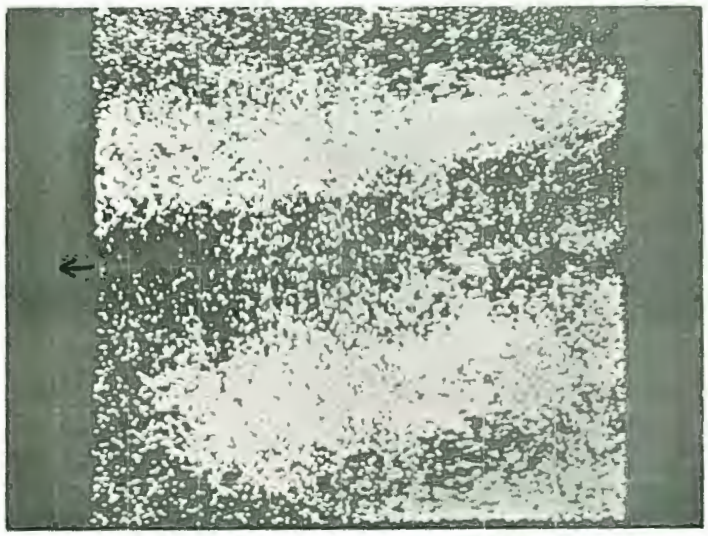

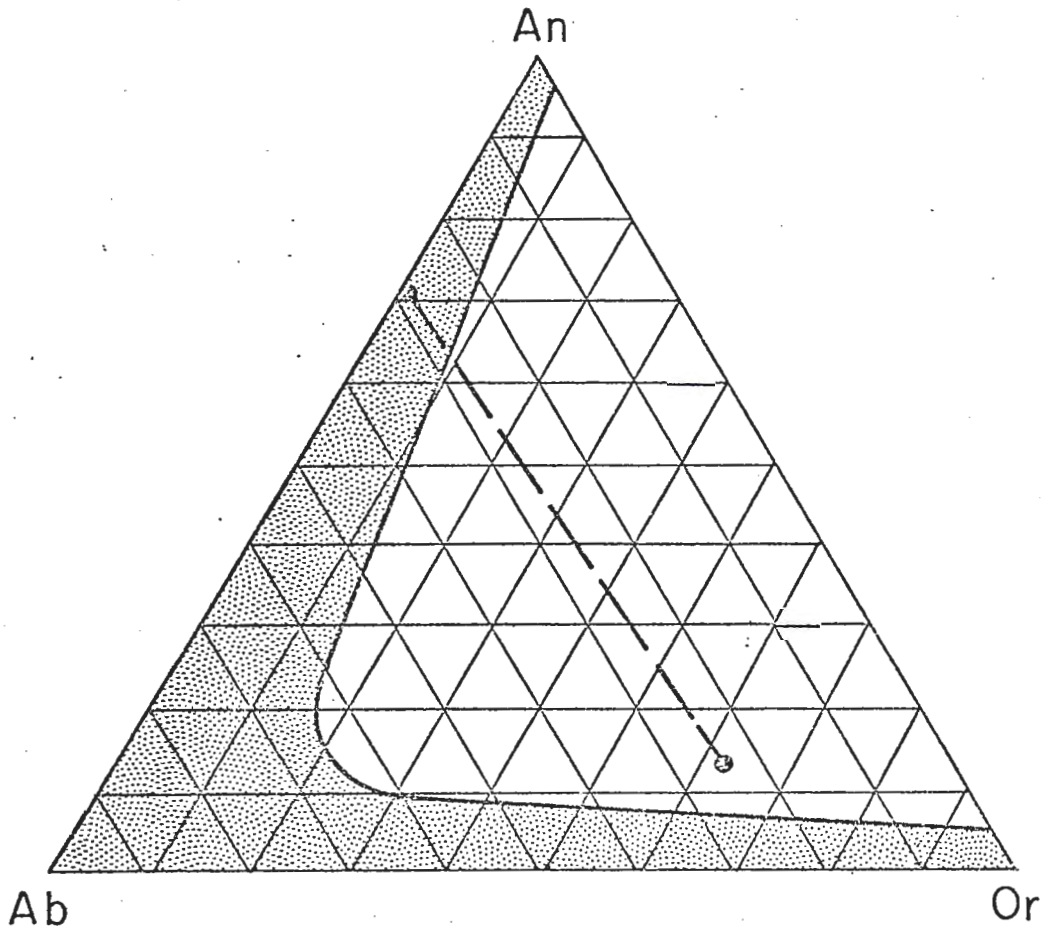

Figure 45. Ab-An-Or diagram showing position of the lamella compositions determined for the plagioclase of the layered sill chilled-margin. The shaded area indicates the area of maximum feldspar solid solution at high temperatures (after Franco and Schairer, 1951).

grains show slight alteration the ratios must clearly reflect original compositions. The origin of the alternating lamellae of sodium and calcium-rich feldspar is probably related to initial rapid cooling under supercooled conditions in the chilled margins followed by subsolidus cooling slow enough to permit exsolution.

Major Element Geochemistry of the Layered Sills

Cedar Lake Sill

Chemical analyses for eight rock samples from the layered sills of the Newton Lake Formation are presented in Table 12. Samples 2, 3, 4, 5, and 6 are from the Cedar Lake sill and represent samples from peridotite, pyroxenite, bronzite gabbro, gabbro and upper chilled zone (Unit C) respectively. Samples 7 and 8 are from chilled zones of two separate sills while sample 1 is from the peridotite portion of the Picketts Lake sill (sample locations for all analyses are shown on Plate 1).

As all the rocks analyzed were partially or completely altered (metamorphosed at low grades) some question may exist as to how nearly the analyses represent the original igneous compositions. In the case of the peridotites, alteration has mainly affected the olivine. Viljoen and Viljoen (1969) have known that for serpentinized rocks with less than 10% H_2O and where carbonation has been slight the chemical analysis still shows distinctive chemistry of the igneous rock. Many authors

have also shown that the chemistries of regionally metamorphosed mafic rocks are still distinctive (see MacRae, 1969; Naldrett and Mason, 1968; Williams, 1972; Williams and Hallberg; 1973). It is concluded that at least the relative amounts of the different elements in each sample were not significantly changed during alteration, although H_2O and in some cases minor CO_2 were added. This conclusion is supported by the general agreement between "primary" modes (as determined from relict textures, etc.) and C.I.P.W. norms. In order to reduce the effects of alteration all analyses have been recalcualted to exclude H_2O and CO_2. In the serpentinized peridotites Fe_2O_3 has been set at 1.25 wt.% following MacRae (1969) with the remaining iron recalculated as FeO to reduce effects of oxidation during serpentinization. The recalculated analyses are presented in Table 13 with their C.I.P.W. norms presented in Table 14.

To illustrate the variations in chemistry in the layered sills, major oxides are plotted against height for the Cedar Lake sill (sill units to scale with the total sill thickness ~1000 feet) (Figure 46). Chemical trends are evident from the figure (lines depict inferred variations) and can be correlated with proportion and composition of the mineral phases in each of the sill units. This relationship is reviewed for each of the major oxides in the discussion below. The chilled-margin analyses and the Picketts Lake sill peridotite are discussed

Key to Analyses

Table 12

1. Peridotite, Picketts Lake sill, SW 1/4, SW 1/4, Sec. 6, T.63N., R.11W., Sample No. SEP-8.
2. Peridotite, Cedar Lake sill, SE 1/4, NE 1/4, Sec. 7, T.63N., R.11W., Sample No. E-46 b.
3. Pyroxenite, Cedar Lake sill, NE 1/4, NW 1/4, Sec. 18, T.63N., R.11W., Sample No. SES-26.
4. Bronzite Gabbro, Cedar Lake sill, same as No. 3., Sample No. SES-27.
5. Gabbro, Cedar Lake sill, same as for No. 3., Sample No. SES-29.
6. Chilled Margin, Cedar Lake sill, same as for No. 3., Unit C of chilled margin. Sample No. SES-22.
7. Chilled Margin, NE 1/4, NW 1/4, Sec. 1, T.63N., R.12W., Sample No. SEN-271.
8. Chilled Margin, Bass Lake sill, NE 1/4, SW 1/4, Sec. 9, T.63N., R.12W., Sample No. E-159 a.

Table 12. Chemical anayses from Newton Lake layered sills.

	SEP-8 (1)	E-46a (2)	SES-26 (3)	SES-27 (4)	SES-29 (5)	SES-22 (6)	SEN-271 (7)	E-159a (8)
SiO_2	37.50	36.65	44.10	46.20	49.35	48.55	48.40	51.05
Al_2O_3	5.67	3.93	7.22	9.64	13.04	9.88	11.05	12.58
Fe_2O_3	5.39	5.76	1.62	1.53	3.28	1.82	2.30	1.78
FeO	12.48	10.84	9.96	7.40	9.84	12,56	11.32	10,60
MgO	24.85	31.93	21.85	15.45	7.41	11.05	10.72	7.95
CaO	3.85	2.78	9.93	13.78	9.48	8.15	9,61	6.80
Na_2O	0.08	0.19	0.16	1.31	2.19	2.57	1.65	4.03
K_2O	0.06	0.08	0.04	0.06	0.10	0,73	0.19	0.63
H_2O	8.87	6.92	4.35	3.59	3.48	2.82	3.46	2.32
CO_2	0.27	0.22	0.27	0.14	0.18	0.28	0.17	0.72
TiO_2	0.61	0.20	0.21	0.28	0.91	1.11	0.70	0.92
P_2O_5	0.17	0.13	0.09	0.07	0.19	0.18	0.21	0.15
MnO	0.21	0.20	0.20	0.17	0.18	0.19	0.20	0.17
S	---	0.03	---	---	---	---	---	0.44
Total	99.90	99.85	99.99	99.61	99.63	99.89	99.98	99.92

Table 13: Recalculated Chemical Analyses from Newton Lake Layered Sills.

	1	2	3	4	5	6	7	8
SiO_2	41.40	39.53	46.24	48.19	51.42	50.16	50.23	52.69
Al_2O_3	6.36	4.24	7.57	10.05	13.59	10.21	11.47	12.99
Fe_2O_3	1.25	1.25	1.70	1.60	3.42	1.88	2.39	1.84
FeO	17.92	16.15	10.44	7.72	10.25	12.98	11.75	10.94
MgO	27.45	34.44	22.91	16.11	7.72	11.42	11.13	8.21
CaO	4.25	3.00	10.41	14.37	9.88	8.42	9.97	7.02
Na_2O	0.09	0.20	0.17	1.37	2.28	2.66	1.71	4.16
K_2O	0.07	0.09	0.04	0.06	0.10	0.75	0.20	0.65
TiO_2	0.67	0.22	0.22	0.29	0.95	1.15	0.73	0.95
P_2O_5	0.19	0.14	0.09	0.07	0.20	0.19	0.22	0.15
MnO	0.23	0.22	0.20	0.17	0.19	0.20	0.21	0.18
S	---	0.03	---	---	---	---	---	0.45
$\frac{CaO}{Al_2O_3}$	---	---	---	---	---	0.82	0.87	0.54

Samples same as in Table 12.

Table 14: CIPW Norms for Recalculated Chemical Analyses from Newton Lake Layered Sills.

	1	2	3	4	5	6	7	8
Q	---	---	---	---	3.50	---	---	---
Ne	---	---	---	0.15	---	---	---	---
Or	0.41	0.53	0.24	0.35	0.59	4.43	1.18	3.84
Ab	0.76	1.69	1.44	11.31	19.29	22.51	14.47	35.20
An	16.74	10.41	19.77	21.10	26.55	13.70	23.03	14.85
Di	2.50	2.86	25.03	39.81	17.35	21.97	20.43	15.60
Hy	17.27	0.63	18.78	---	25.49	14.76	32.64	13.39
Ol	58.74	80.81	31.64	24.35	---	17.30	3.11	11.57
Mt	1.83	1.81	2.46	2.32	4.96	2.73	3.23	2.67
Il	1.27	0.42	0.42	0.55	1.80	2.18	1.39	1.80
Pr	---	---	---	---	---	---	---	0.84
Ap	0.44	0.33	0.21	0.16	0.46	0.44	0.51	0.35

Samples same as in Table 12.

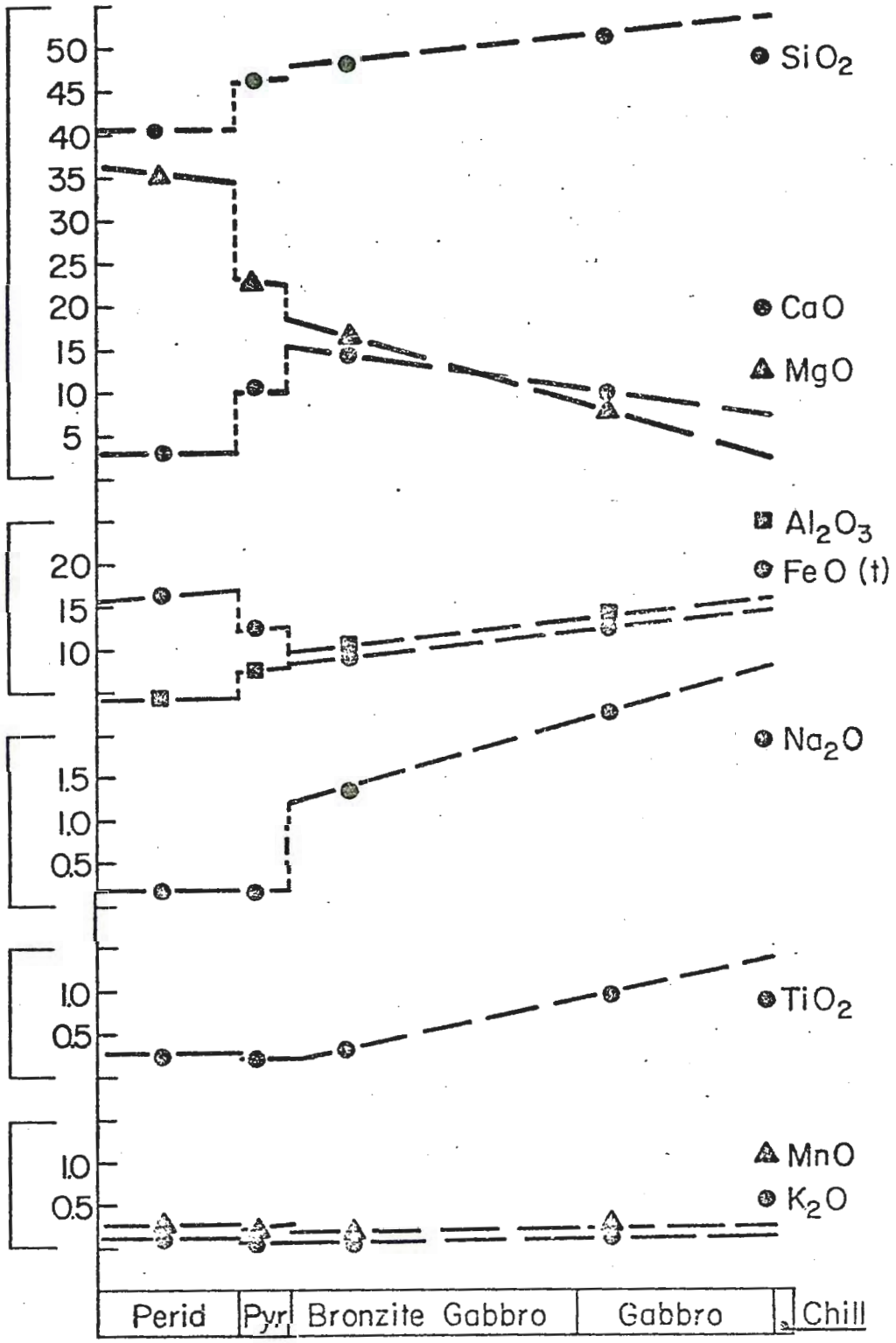

Figure 46. Major element variation for the Cedar Lake sill (in wt.%). $FeO_{(t)} = FeO + Fe_2O_3$

separately in following sections.

Silica: The silica content, as is to be expected, is low in the peridotite (39.5 wt.%) where olivine (SiO_2 40 wt.%) forms the major mineral phase (~65%). There is an abrupt increase in silica content in the pyroxenite (46 wt.%) where olivine is no longer present. Silica continues to show a gradual increase upwards through the rest of the sill to approximately 51 wt.% in the upper gabbro. This increase reflects the increase of interstitial quartz upwards through the sill (see Tables 5 - 7).

Aluminum: Variation in the Al_2O_3 content with height in the Cedar Lake sill is largely controlled by the amount of plagioclase and to a lesser extent, pyroxene, present in the individual units. The Al_2O_3 content of the peridotite is about 4 wt.% and reflects the presence of a small amount of plagioclase (~13%). The pyroxenite contains about 7.5 wt.% Al_2O_3 with increased plagioclase (≤27%) and pyroxene present. The aluminum shows a gradual increase upwards from the pyroxenite to 10 wt.% in the bronzite gabbro and 13.5% in the upper gabbro. This increase reflects an increase in plagioclase and clinopyroxene (which contains higher Al_2O_3 than the orthopyroxene).

Iron (Total Fe_2O_3 + FeO): The total iron content of the peridotite is high (~17%) because of the high olivine, pyroxene and magnetite-chromite content. The total iron drops to approximately 12 wt.% in the pyroxenite, reflecting

the disappearance of olivine and chromite and to ~9 wt.% in the bronzite gabbro as orthopyroxene content decreases from 57 to 17 volume percent. In the upper gabbro the total iron content is again higher (~14 wt.%) because of the presence of ferroaugite and primary iron-titanium oxides.

Magnesium: The trend of magnesium, which is one of the main components of olivine and pyroxene, clearly reflects the differentiation trend of the Cedar Lake sill. The MgO content of the peridotite is high (~34 wt.%) because of the high content of olivine (Mg 77 wt.%) and orthopyroxene (Mg 81 wt.%). The pyroxenite shows an abrupt drop to 23 wt.% MgO reflecting the absence of olivine and a lower En content in the orthopyroxenes (Mg 75 wt.%). There is a further drop in the MgO content through the rest of the sill with the bronzite gabbro containing 16 wt.% MgO and the upper gabbro about 8 wt.% MgO. This continued decrease is related to the disappearance of orthopyroxene upwards and the probable increase in the Fe/Mg ratio of the clinopyroxene.

Calcium: The major calcium bearing minerals present in the Cedar Lake sill are plagioclase and clinopyroxene and their variation largely controls the observed calcium variation. The peridotite shows a low calcium content of 3 wt.% reflecting the low plagioclase (13%) and clinopyroxene (4%) contents. The calcium content of the pyroxenite (10.5 wt.%) and the bronzite gabbro (14 wt.%) shows an abrupt increase from the peridotite resulting

from the increase in clinopyroxene and plagioclase in these units. The upper gabbro shows a somewhat lower CaO content (10 wt.%) than the bronzite gabbro probably because of a change to more sodic plagioclase compositions.

Sodium: Sodium occurs mainly within plagioclase and the variation of sodium with height in the Cedar Lake sill clearly reflects the plagioclase crystallization trend. Sodium is low in the peridotite (0.2 wt.%) and pyroxenite (0.17 wt.%) as a result of the low plagioclase content in these units and also the probable high An content of the plagioclase which is present. The higher Na_2O of both the bronzite gabbro (1.4 wt.%) and the upper gabbro (2.3 wt.%) appears due to both an increase in the abundance of plagioclase and an increase in the sodium content of the plagioclase in these successive units.

Potassium: The K_2O content is extremely low in all the units of the Cedar Lake sill, averaging about 0.07 wt.% for the layered sequence. This low value is to be expected in view of general lack of micas and potassium feldspar which are the principle potassium bearing phases.

Titanium: The titanium content is low in the peridotite (0.22 wt.%), pyroxenite (0.22 wt.%) and bronzite gabbro (0.3 wt.%) units because of the general lack of any titanium bearing minerals except pyroxene in these units. The TiO_2 content of the upper gabbro is 0.95 wt,% reflecting the presence of about 3% iron-titanium oxide.

Manganese: Manganese does not appear to show any significant

trend upwards through the Cedar Lake sill. There does appear to be a slight enrichment of MnO in the peridotite and pyroxenite (0.22 and 0.20 wt.% respectively) units, probably because manganese is primarily found in the pyroxenes and olivines of igneous rock in about equal amounts.

Phosphorus: The phosphorus content of the various units is low, ranging from 0.07 to 0.20 wt.%. The peridotite and upper gabbro units show the highest P_2O_5 content (0.14 wt.% and 0.20 wt.% respectively) reflecting the presence of minor apatite in these units.

Picketts Lake Sill Peridotite

It is uncertain whether the Picketts Lake peridotite is part of a layered sill or just a peridotite lens (see page 85). The chemical analyses obtained from the peridotite (No. 1, Table 13) reflects a difference in mineralogy from the peridotite of the Cedar Lake sill.

The Picketts Lake peridotite appears to have less olivine (47%) and more plagioclase (22%) than the Cedar Lake sill peridotite (see Table 4). This difference in mineralogy is reflected by slightly higher SiO_2, Al_2O_3, CaO and lower MgO in the Picketts Lake peridotite. Its higher total iron content reflects a larger content of magnetite and chromite.

Differentiation Trends

The differentiation trends in the layered sills, based on the whole-rock analyses are seen by plotting (FeO_t - MgO - CaO), Alk - FeO_t - MgO) and oxides versus MgO) which are illustrated in Figures 47, 48 and 49. The rock analyses corresponds, at best, to the composition of fractionated crystals plus trapped interstitial liquid and thus may not accurately portray the differentiation trend. Calculations of liquid compositions (see discussion page 147), however, have shown that the two trends are very similar and indicate the same general trend of differentiation.

FeO_t - MgO - CaO Variation

Figure 47 is an FeO_t - MgO - CaO (wt.%) diagram for the analyzed rocks from the Newton Lake layered sills. The broken line shows the trend for samples from the Cedar Lake sill. The trend of both the ultramafic and gabbroic rocks reflects the variation in their mineralogy with peridotite plotting near the FeO_t - MgO join, pyroxenite plotting away from peridotite towards the CaO corner, and the gabbros extending in the direction of increasing FeO_t:(MgO + CaO) ratios.

An interesting feature of the above trend is the initial increase in CaO with slightly decreasing FeO_t. A similar trend was noted by Naldrett and Mason (1968) for the Dundonald sill of the Abitibi region, Canada.

A similar plot for the calculated liquid compositions suggests however, that this trend may be less pronounced and of an almost constant CaO/FeO_t ratio (Figure 50).

Alk - FeO_t - MgO Variation

In Figure 48 the whole rock analyses have been plotted on a Alk - FeO_t - MgO (wt.%) diagram. Samples from the Cedar Lake sill are connected by a broken line. The indicated trend is one of iron enrichment. As can be expected, both the peridotite and pyroxenite plot very near the FeO_t - MgO join with the gabbros showing a gradual enrichment in alkalies. This trend is in contrast to that obtained by MacRae (1969) for similar sills in the Abitibi region of Canada which showed a more marked increase in alkalies with increasing FeO (see MacRae, 1969, Figure 12). If analyses were available of the late stage leucocratic veins found in the Newton Lake layered sills the trend would show a marked increase in alkalies for the final crystallizing liquids.

Oxides versus MgO

Major oxides have been plotted in Figure 49 with decreasing MgO used as a differentiation index, this being its typical variation in magmatic differentiation (Wright and Fiske, 1971). The solid line shows the trend for samples from the Cedar Lake sill. For comparison, oxide trends from the Dundonald sill (Naldrett and Mason, 1968) and the Ghost Range sill (MacRae, 1969)

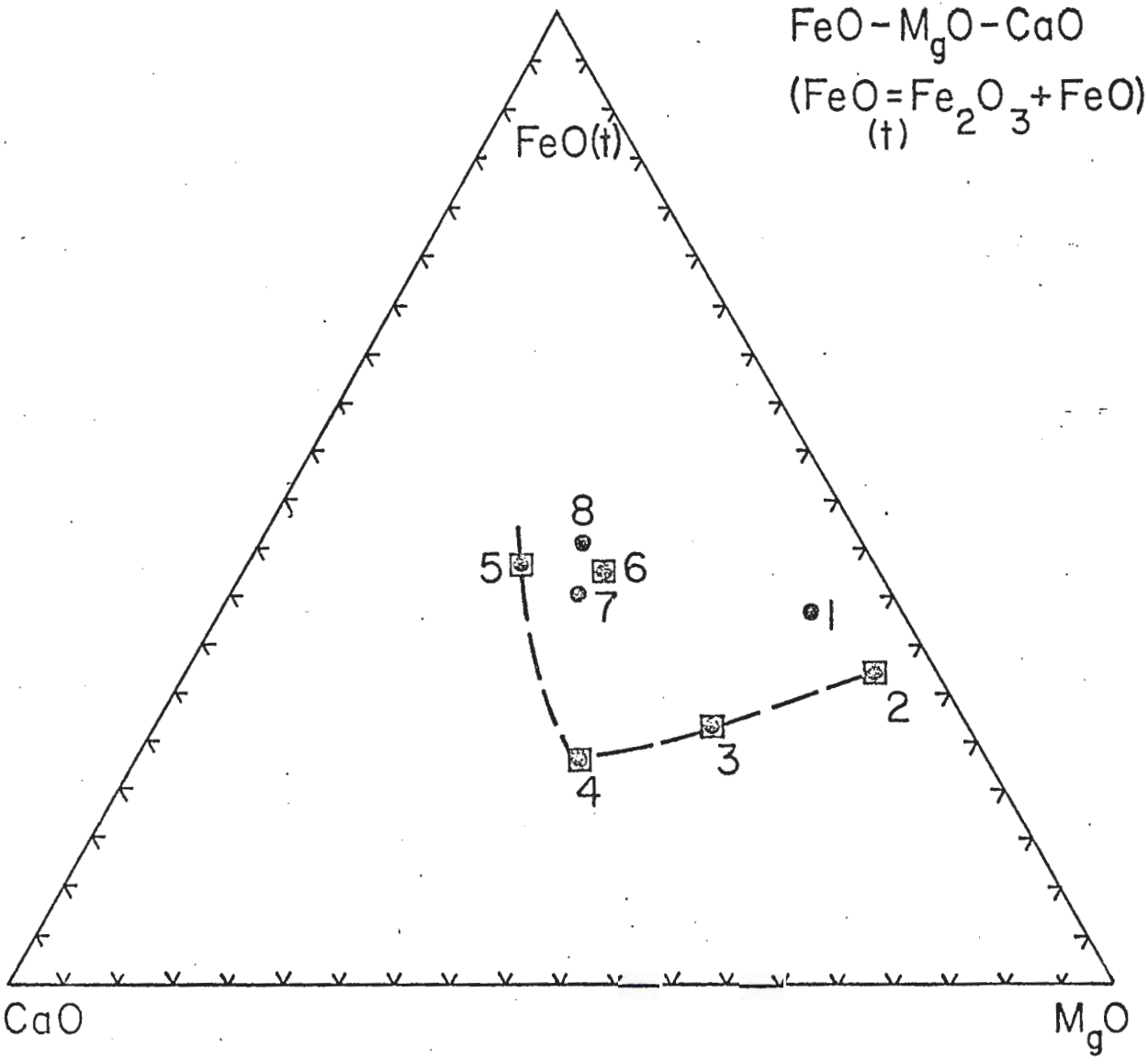

Figure 47. FeO_t - MgO - CaO (wt.%) diagram for samples from the Newton Lake layered sills. FeO_t is FeO + Fe_2O_3. Broken line shows the trend for samples from the Cedar Lake sill (points shown by ⊡). See page 132 for sample numbers.

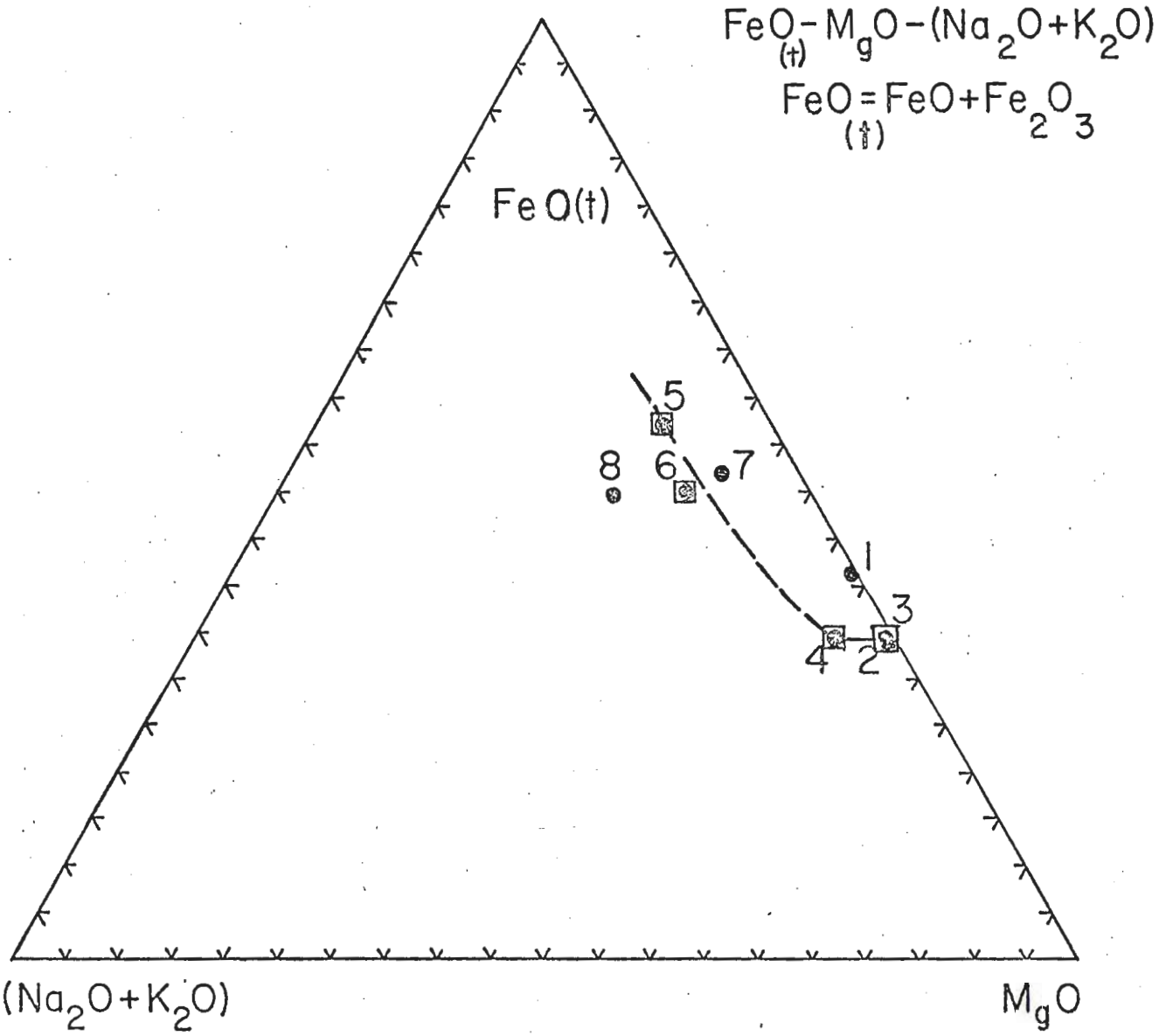

Figure 48. FeO_t - MgO - Alk (wt.%) diagram for samples from the Newton Lake layered sills. Broken line shows the trend for the Cedar Lake sill samples (points shown by ▣). Sample numbers refer to Table 13, p.132.

Figure 49. A plot of major oxides vs MgO for samples from the Newton Lake layered sills, Garrison sill (MacRae, 1969) and Dundonald sill (Naldrett and Mason, 1968). Sample numbers same as in Table 13, p 132

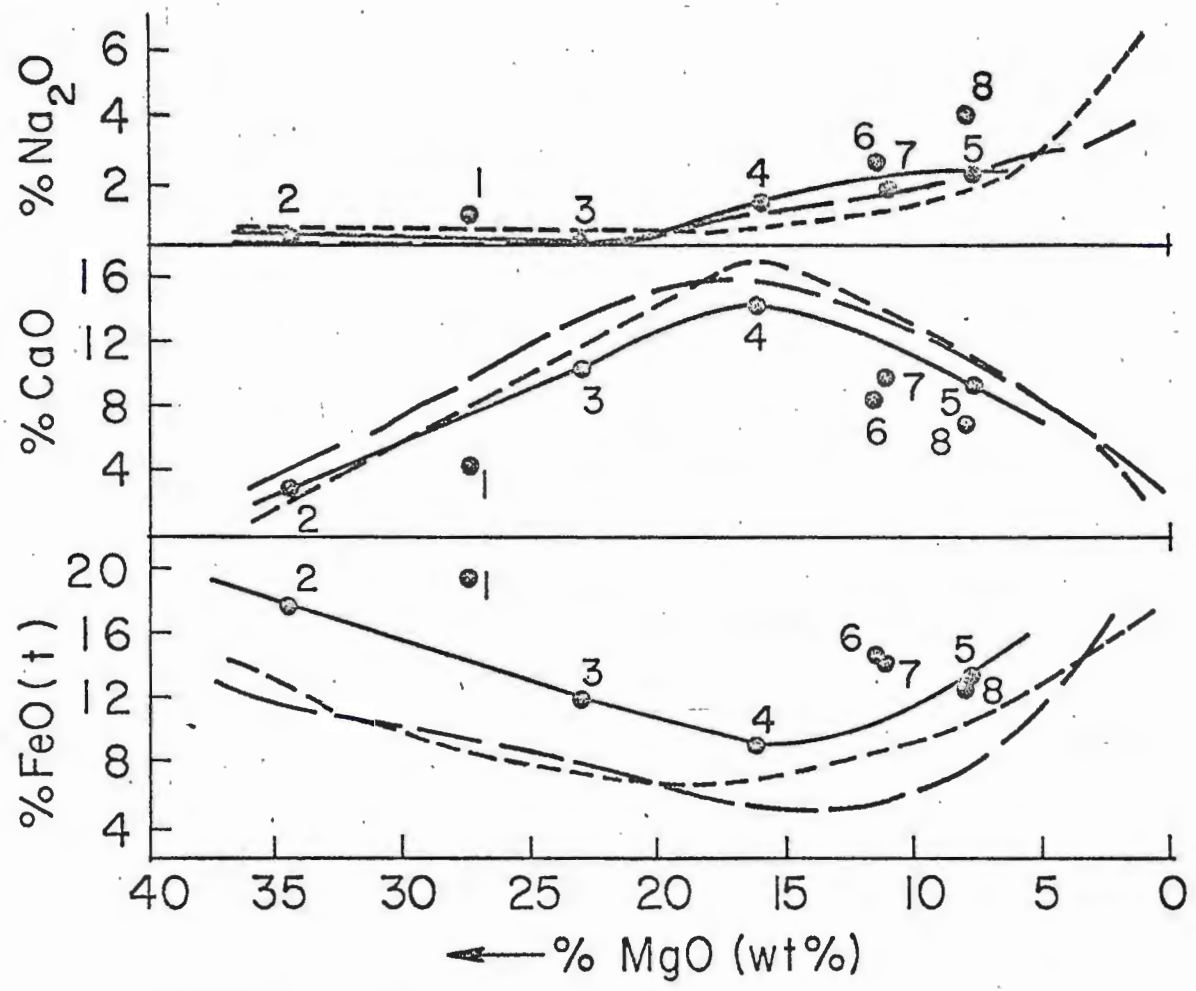

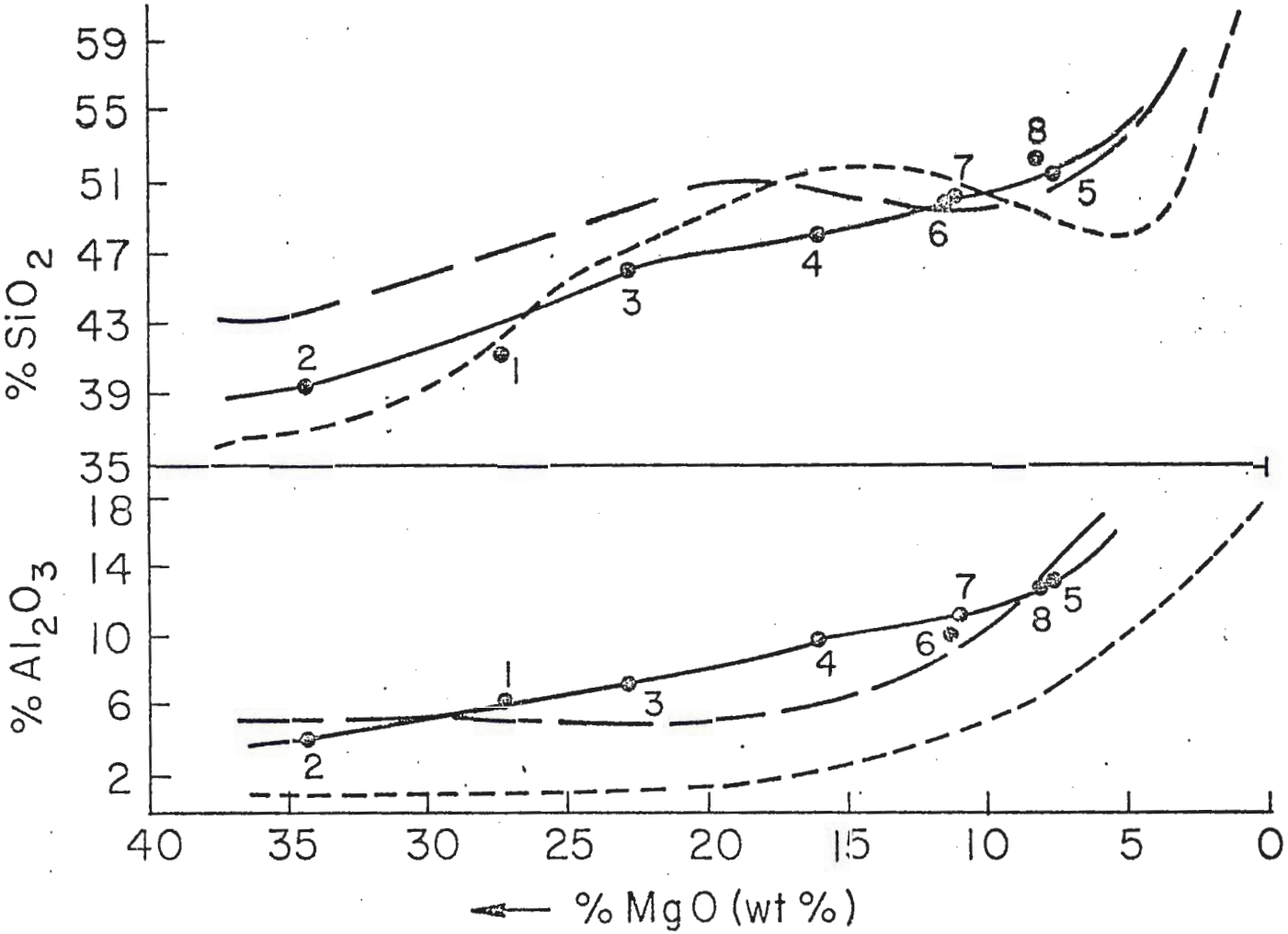
59
55
51
47
43
39
35
% SiO2
18
14
10
6
2
% Al2O3
1
2
3
4
5
6
7
8
40
35
30
25
20
15
10
5
0
← % MgO (wt %)
Newton Lake Layered Sills
Garrison Sill, Canada (MacRae, 1969)
Dundanold Sill, Canada (Naldrett & Mason, 1968)

have also been plotted. The plots of CaO and FeO_t also show a decreasing FeO_t content with increasing CaO in the initial stages of differentiation as was obtained in Figure 47. It should be noted that the trend for the Cedar Lake sill is very similar to the two from the Canadian sills.

Successive Magmatic Liquid Compositions in a Differentiated Layered Sill

Though only four analyses were available from the layered sequence of a Newton Lake sill (the Cedar Lake sill) an attempt was made to calculate the liquid composition at various stages of crystallization and also the initial bulk composition. The absence of strong rhythmic layering and cyclic units in the sills makes them amenable to such calculations. In carrying out the calculations it has been assumed that the layered sequences at their present level of erosion, are representative of the total sill, and that the volume of each unit is proportional to its thickness. For each unit the analyses are assumed to be representative and are weighted according to the unit thickness determined from field mapping.

The liquid compositions so obtained are plotted in Figures 50, 51 and 52. In Figure 50 the calculated liquids are plotted on a FeO_t - MgO - CaO diagram. Plotted for comparison are calculated liquid trends for the Munro Lake sill of Canada (MacRae, 1969) and the Mt. Monger sill from Western Australia (Williams

and Hallberg, 1973). The compositions of olivine augite and chromite crystallizing from each of the Newton Lake liquids are also plotted along with the chilled margin analyses from each of the sills shown. A comparison of Figure 47 with Figure 50 shows that the rock trend is similar to the liquid trend, but is more exaggerated. The extent of the magnesium enrichment of the proxenes and olivine over the liquid is also shown in Figure 50. In the early stages of crystallization the FeO:MgO ratio increases only slightly for both calculated liquids (Fig. 50) and whole rock samples (Fig. 47). This trend can be produced by olivine + orthopyroxene crystallization. The marked increase in the FeO:MgO ratio in the bronzite gabbro (Fig. 47) is a result of substantial crystallization of clinpyroxene in addition to orthopyroxene (Fig. 50).

Figure 51 shows a $FeO_{(t)}$ - MgO - $(Na_2O + K_2O)$ plot of the Newton Lake calculated liquids, liquid trends from the Canadian and Australian sills, and their respective chilled margin compositions. The liquid trend for the Newton Lake liquids is again similar to the rock trend (Figure 48) and the liquid trend of the Australian sills. It should be noted that the liquids from the Abitibi sills of Canada (MacRae, 1969) which are quite similar to the Skaergaard liquid trend (see MacRae, 1969, page 299, Figure 18), show a more marked alkali enrichment

Figure 50. $Fe_{(t)}$ - MgO - CaO plot for calculated Cedar Lake sill liquids. Also plotted are the calculated liquid trends for the Mt. Monger sill, Australia (Williams and Hallberg, 1973) and the Munro Lake sill, Canada (MacRae, 1969). The crystallizing phases for each of the Cedar Lake liquids are also shown. Note that the Cedar Lake and Mt. Monger liquid trends are very similar though the chilled margin compositions for each are quite different. The Mt. Monger chilled-margin composition is very similar however to the Cedar Lake calculated initial liquid. See text for discussion.

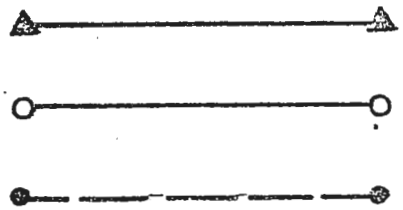

Cedar Lake sill (this report)

Mt. Monger sill (Williams and Hallberg, 1973)

Munro Lake sill (MacRae, 1969)

1, Cedar Lake sill chilled-margin. 2, Chilled-margin of sill in Sect. 1, T.63N., R.12W.

O 3 Mt. Monger chilled-margin sample

● 4 Munro Lake chilled-margin samples

●--- Crystallizing phases for each of the Cedar Lake liquids

X Deer Lake Complex pyroxenes (Ripley, 1973)

Figure 50.
$FeO_{(t)}$ - MgO - CaO

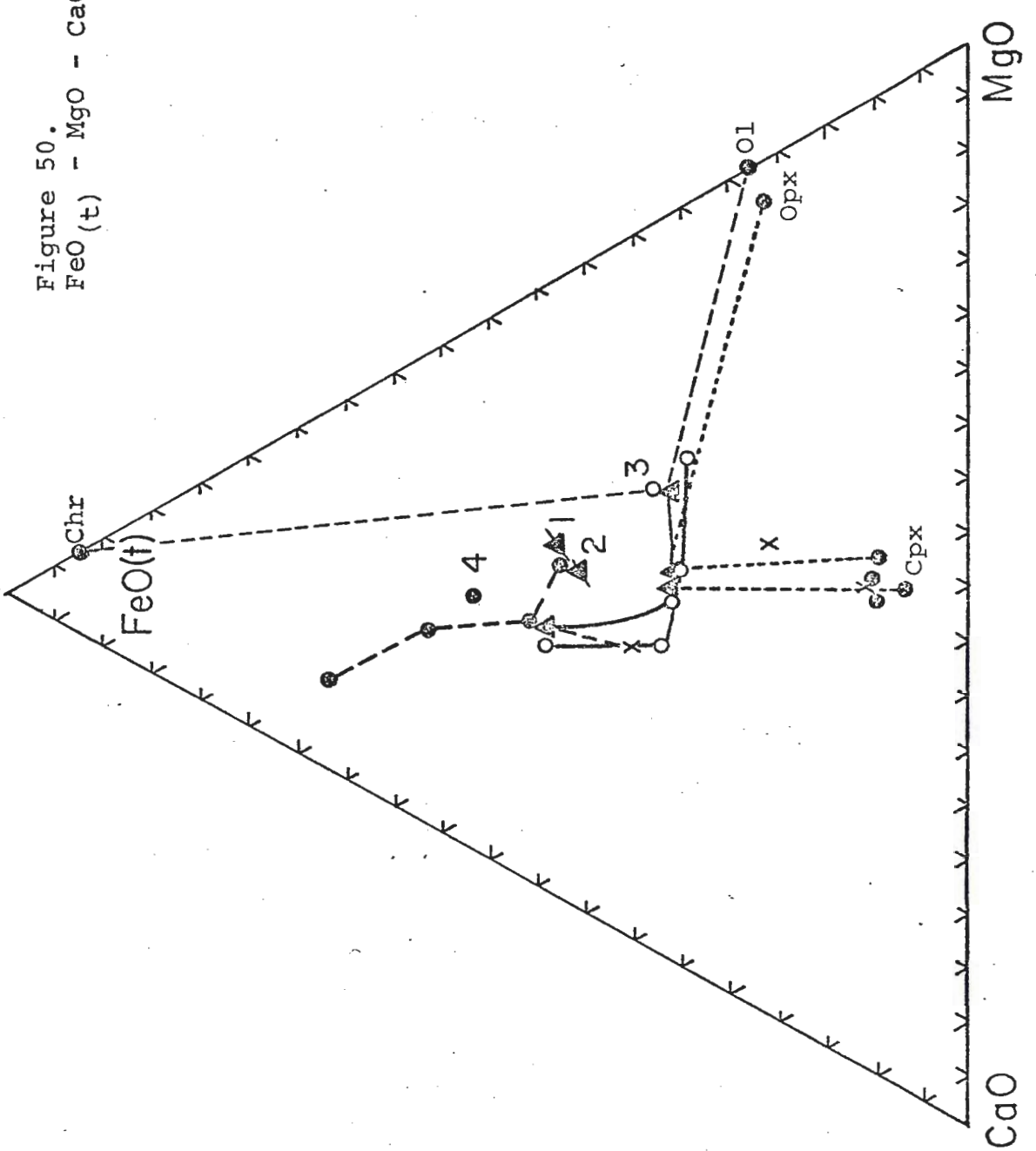

Figure 51. $FeO_{(t)}$ - MgO - Alk variation diagram indicating the trend for the calculated Cedar Lake sill as compared to the Munro Lake liquid trend (MacRae, 1969) and the Mt. Monger liquid trend (Williams and Hallberg, 1973). Symbols are the same as in Figure 50.

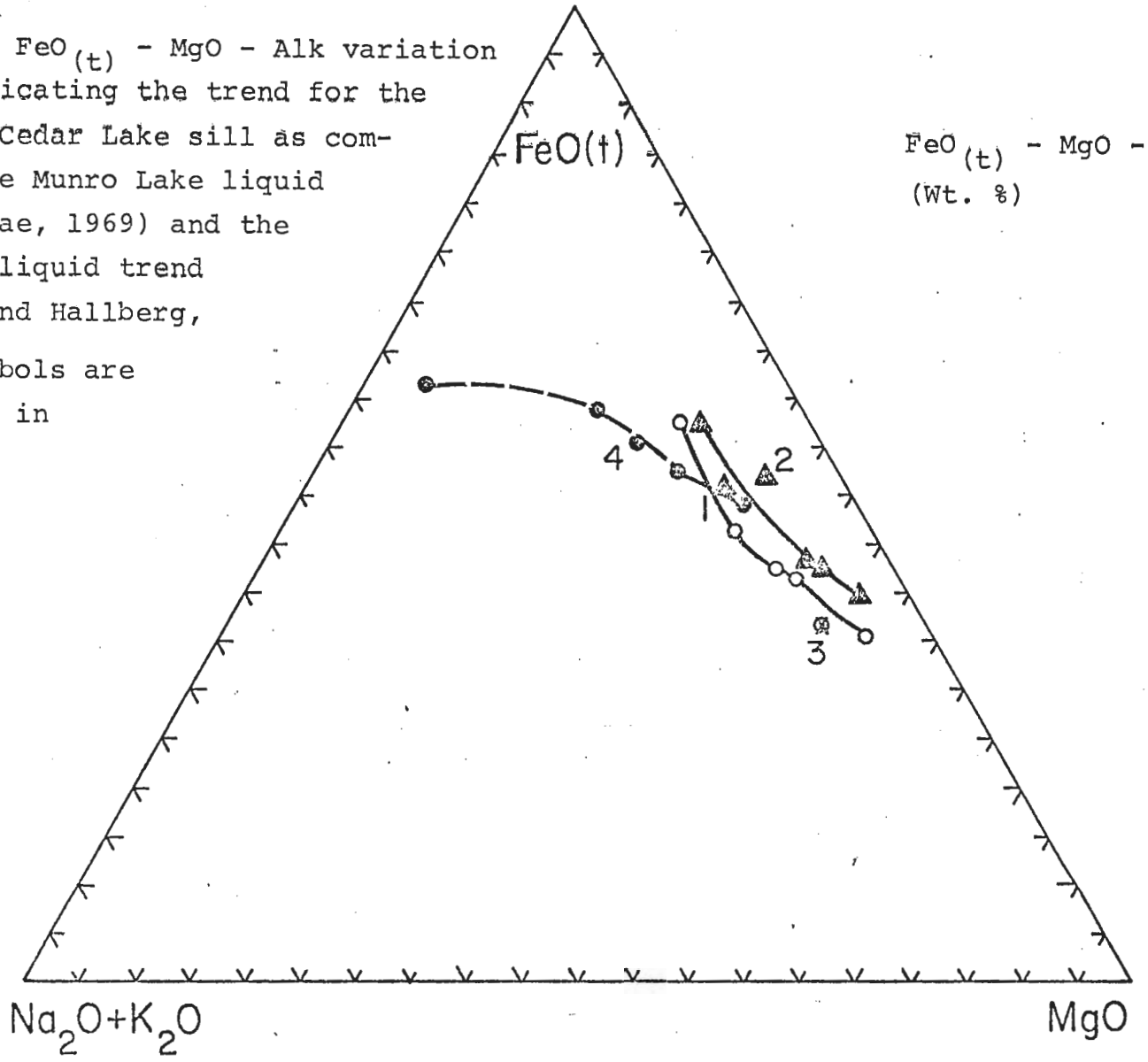

$FeO_{(t)}$ - MgO - Alk
(Wt. %)

Figure 52. Major oxide vs. MgO variation diagram for calculated liquids from the Cedar Lake sill and the Munro Lake sill, Canada (MacRae, 1969). $FeO_{(t)}$ = FeO + Fe_2O_3.

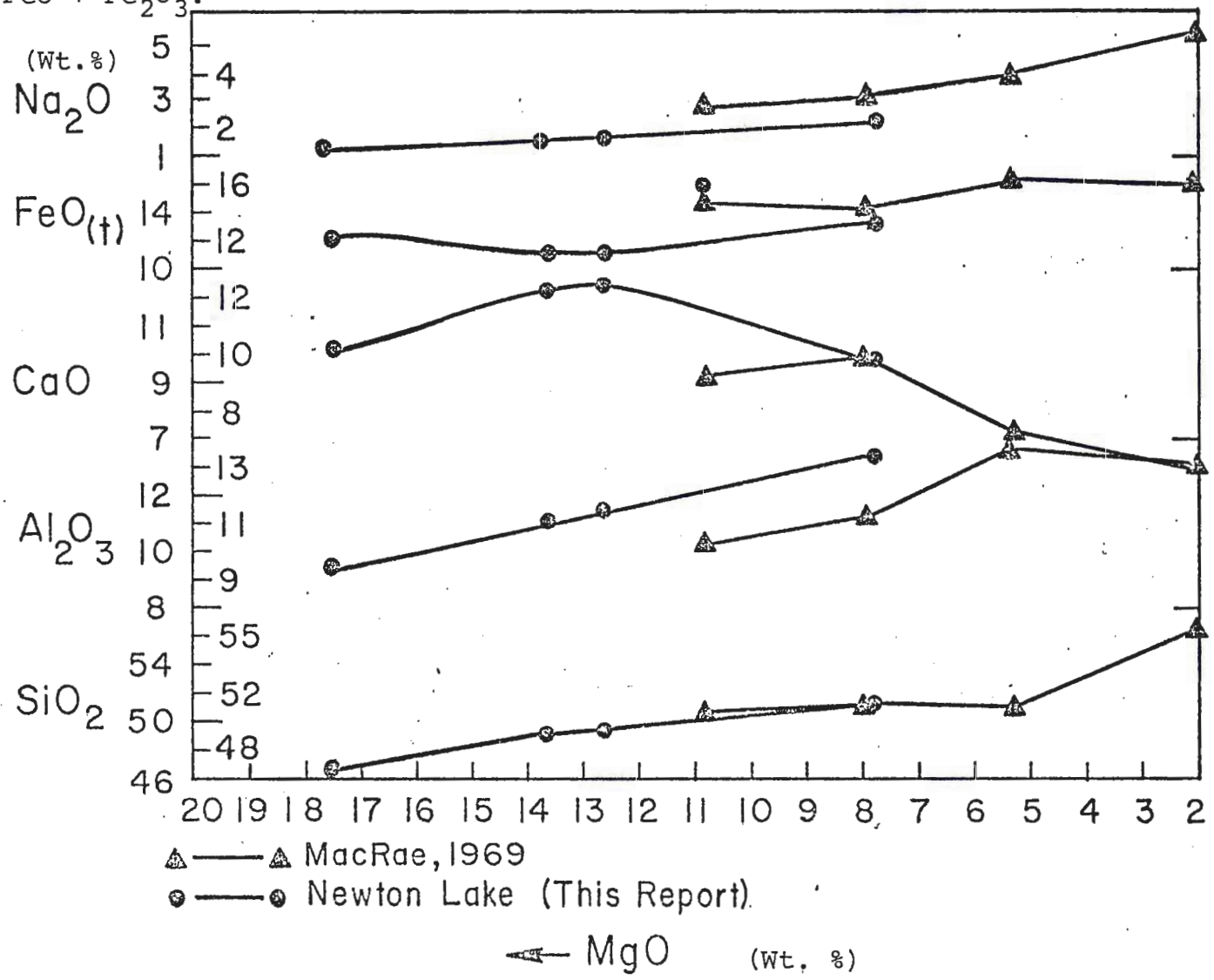

than either the Newton Lake or Australian sills.

Figure 52 shows an oxide versus MgO plot for the calculated Newton Lake magmatic liquids. The trends shown are again similar to the rock trends (Figure 49) though less exaggerated. It should be noted that the Abitibi liquids are generally poorer in MgO than the Newton Lake liquids. This is opposed to the rock trends (Figure 49) which appear quite similar.

Bulk Composition of the Layered Sills

Chilled-margins were found for many of the Newton Lake layered sills and three chilled-border samples were analyzed (Table 12, Table 13, recalculated anhydrous and Table 14, C.I.P.W. norms for recalculated compositions). Sample 6 was selected from Unit C (plumose plagioclase unit) of the Cedar Lake sill chilled-margin; Sample 7 from Unit B (plumose pyroxene unit) of the chilled-margin of a sill south of Low Lake; Sample 8 from a possible chilled-margin from the upper contact of the Bass Lake gabbro sill. It should be noted that an analysis of Unit A of the chilled margins was not obtained and the possibility exists that the analyses obtained from the two inner units may not accurately represent the initial liquid. The close similarity between the two layered sill chilled-margin analyses (see below) and the modal similarity between Units A and B suggests that any chemical differences between them may be restricted to the minor elements.

A comparison of the three chilled-margin analyses shows that the two from the layered sills (Samples 6 and 7) are very similar in major oxide content even though they are from two different units of the chilled zone. There is also a marked difference between the above analyses and that obtained from the Bass Lake gabbro sill (Sample 8). This difference is especially evident in the SiO_2, Al_2O_3, MgO and CaO contents. The SiO_2 and Al_2O_3 content is higher in Sample 8 than in 6 or 7, whereas the MgO and CaO contents are significantly lower. Sample 8 is, however, very similar to the upper gabbro composition of the Cedar Lake sill (Table 13, No.5). This supports the interpretation that at least some gabbro sills could be the crystallization product of intrusive magmas similar in composition to Sample 8 rather than in-place crystal fractionation products of more primative magmas.

As a check on the chilled-margin compositions the bulk composition of the Cedar Lake sill was calculated utilizing the method outlined in the previous section. Using the following relative percentage for the Cedar Lake sill units; peridotite 20%, pyroxenite 7.5%, bronzite gabbro 42.5% and gabbro 30%, the following bulk composition was obtained:

SiO_2 = 47.29	CaO = 10.45
Al_2O_3 = 9.77	Na_2O = 1.31
TiO_2 = 0.46	K_2O = 0.08
$FeO_{(t)}$ = 12.45	MnO = 0.18
MgO = 17.78	P_2O_5 = 0.13

The calculated composition above has lower SiO_2, Al_2O_3, Na_2O, K_2O, TiO_2 P_2O_5, higher CaO and considerably higher MgO than either of the analyzed chilled-margin samples. These differences can be seen graphically in Figures 50, 51 and 52. In Figure 50 (FeO_t - MgO - CaO plot) the two chilled-margin analyses plot well away from the calculated liquid trend and bulk composition, being richer in FeO_t and poorer in CaO. In this regard it is interesting to note that the chilled-margin samples from the Canadian and Western Australian sills also show a similar anomaly with respect to their calculated liquid trends.

This discrepancy between calculated initial liquids and those obtained from chilled-margin analyses suggests that the inferred ratio of ultramafic to gabbroic rocks may be too high or possibly that more Fe-rich, CaO poor portions of the sills have not been sampled and analyzed. In the case of the Newton Lake sills, analyses were not available of the upper portion of the gabbro unit or of the late stage quartz-feldspar veins cutting the upper portions of the sills. It appears likely that if they were taken into account, SiO_2, Al_2O_3, K_2O and P_2O_5 would be higher than presently calculated. Also it has been noted (page 85) that the Cedar Lake sill is deficient in normal gabbro compared to the other sills of the Newton Lake Formation. Recalculation of the initial liquid using the unit ratios of the Little Long Lake sill (see Figure 4) has shown, however that the resulting bulk

composition is not greatly changed with respect to the major elements.

MacRae (1969) has suggested three possible mechanisms for the observed discrepancy between calculated and analyzed bulk compositions: 1) the chilled-margin was contaminated and does not represent the initial liquid; 2) a large portion of the mafic minerals were carried in suspension at the time of intrusion; 3) the sill may not have remained closed during solidification, but lost some of its residual magma. Of the three possibilities MacRae favors the first, calling upon contamination with andesitic metavolcanics to account for the discrepancy observed in the Abitibi sills of Canada. Williams and Hallberg (1973) also use contamination by pelitic sedimentary rocks to account for observed discrepancies in the Western Australian sills.

In the Newton Lake sills contamination of the chilled portions does not appear likely to have occurred to any significant degree. This conclusion is based on the following points:

1. The two sills from which chilled-margin analyses were obtained appear intrusive into different rock types (Plate 1) yet have similar bulk compositions.
2. The formation of the chilled-margins by rapid chilling or quenching suggests little time was available for reaction with or assimilation of

surrounding rocks.

3. No xenoliths of the surrounding rocks have ever been observed in the chilled-margin zones though possible xenoliths have been observed in the gabbro unit of some sills.
4. The metavolcanics into which the sills were intruded are basaltic in composition and not andesitic; assimilation of them would not appreciably change the FeO_t/CaO ratio of the magma even if there were superheat available to accomplish it.

To evaluate the possibility of mafic minerals being carried in suspension at the time of intrusion, preliminary tests have been made using the least-squares analysis technique of Wright and Doherty (1970). These tests indicate that an addition of about 17% olivine ($Fo_{84.5}$) and 3.0% chromite to the chilled-margin composition will give a good fit to the calculated initial composition. The data also suggests that some olivine should have crystallized after intrusion. This is supported by the chilled-margin analyses plotting in the olivine field of Irvine's (1970) phase diagrams for the ol-pyrox-plag-qtz system (see discussion page 167). From the preliminary tests it appears that at least some olivine and chromite were in suspension in the Newton Lake sill magmas at the time of intrusion. This is also supported by the presence of the ultramafic lenses. They consist of a peridotite core surrounded by a complex chilled mar-

gin of the same type (and therefore presumably the same composition) as found with the layered sills. It appears that these lenses could have been intruded as an olivine bearing magma in which olivine (and chromite) were concentrated through flowage differentiation.

It is difficult, with the data now available, to evaluate whether or not the sills were closed systems (remained self-contained) during solidification. It appears that some of the sills might represent magma chambers which were occasionally tapped to form gabbro sills or flows. First of all sills, are present which show differing unit thicknesses for the same apparent bulk composition. Secondly, the presence of gabbro sills with chilled-margin compositions very similar to the gabbro of the layered sills and basaltic flows also having similar compositions strongly suggests that occasional tapping did occur. The presence of ultramafic lenses also supports this interpretation. MacRae (1969) from his study of the Abitibi sills of Canada also felt that some of the sills may have occasionally been tapped as rift chambers in an actively growing volcanic pile.

The nature of the initial magma for the Newton Lake sills and the observed discrepancy between the calculated and analyzed compositions clearly requires further investigation. From the preliminary data presently available, however, it appears that a combination of mafic minerals in suspension and occasional tapping of residual

gabbroic liquid can account for the difference between observed and calculated compositions.

Comparison of the Bulk and Chilled-Margin Compositions with other Mafic Rock Types

The chilled-margin analyses from the layered Newton Lake sills show some distinctive chemical features when compared to known basalt types (Table 15). These include low Al_2O_3 and alkalies, high MgO, a high CaO/Al_2O_3 ratio and similar Al_2O_3, CaO and MgO values (~10%). The C.I.P.W. norms calculated from these analyses (Table 14) show both hypersthene and olivine suggesting a tholeiitic affinity for the parent magma. This is supported by plotting alkalies verses silica (Figure 53) in which two of the analyses fall within the field of tholeiitic basalts as determined by MacDonald and Katsura (1964). The third (border of a gabbro sill) plots on the field boundary. The calculated initial liquid composition also plots in the tholeiite field.

In Figures 54 and 55 the Newton Lake chilled-margin analyses and calculated initial liquid are compared to some relevant igneous rock types including the bulk compositions given for similar sills from the Archean of Canada and Australia. Examination of the figures and Table 15 reveals that the chilled-margin analyses from the Newton Lake layered sills, while being tholeiitic in nature, have higher MgO and CaO/Al_2O_3 ratios than either the average Archean basalt or continental tholeiite.

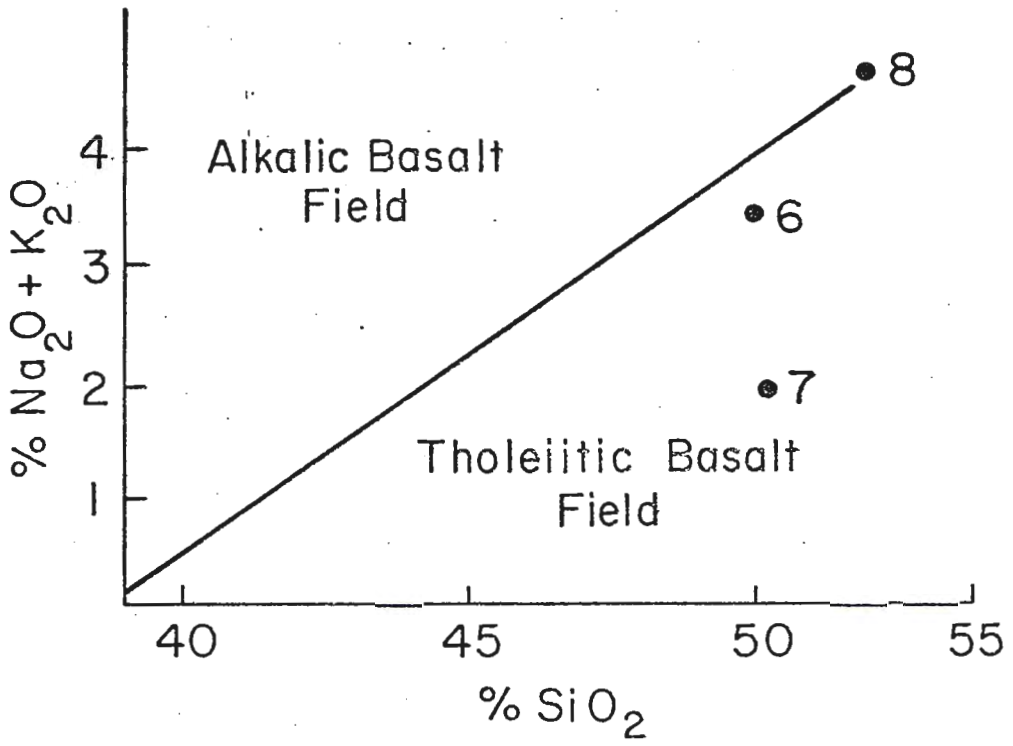

Figure 53. Alkali-Silica plot for the three chilled margin analyses from Newton Lake sills, (Field boundary after MacDonald and Katsura, 1964). Sample numbers same as in Table 13.

Figure 54.
Plot $MgO-CaO-Al_2O_3$(wt %)
For Newton Lake Chill Margin Analyses and Analyses From Table 15.

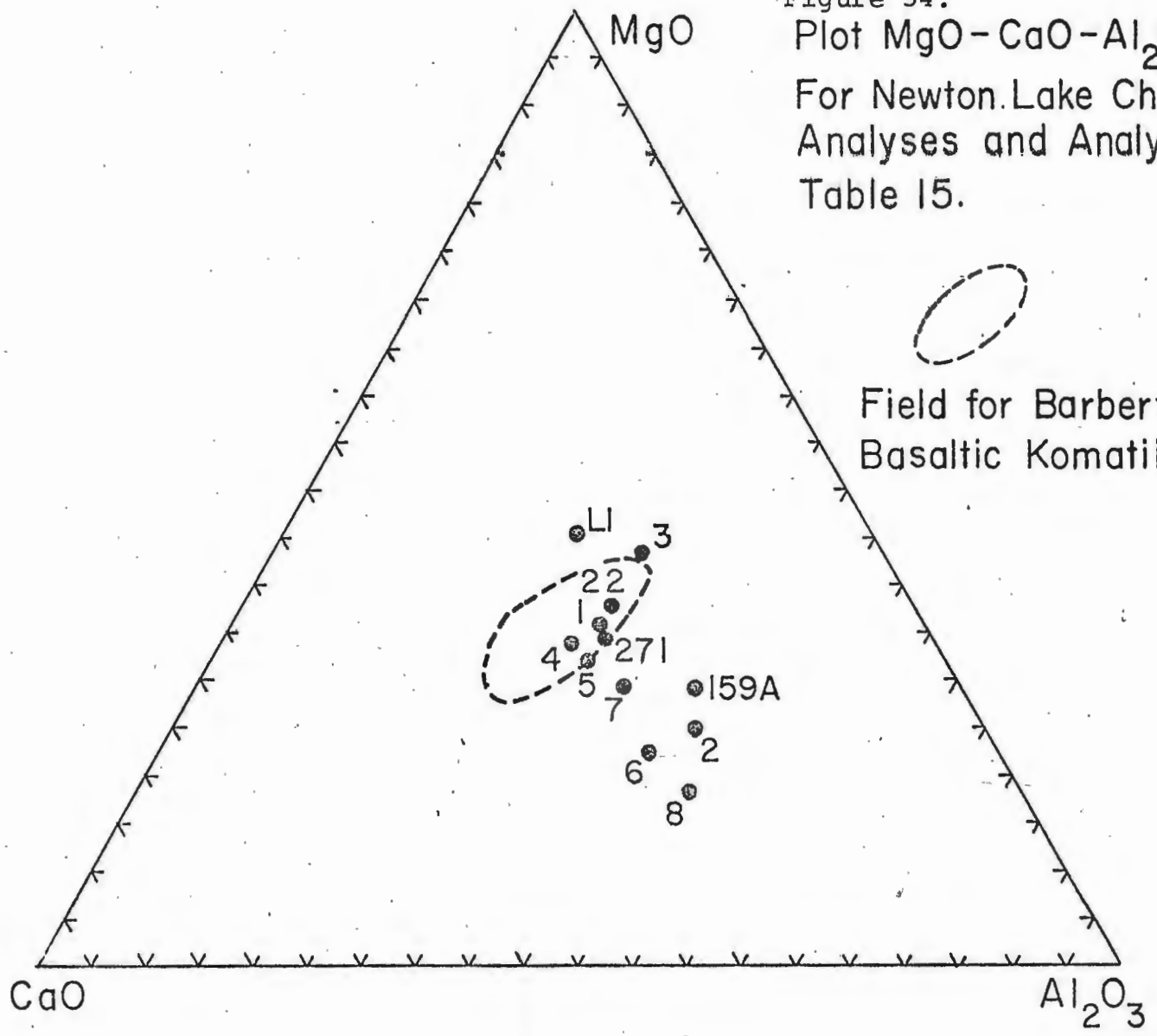

Field for Barberton Type Basaltic Komatiites.

Key to Figure 55

1 = Field of Noranda volcanics
2 = Field of Oceanic tholeiites
} (from Naldrett,1970).

3 = Field of high lime liquids of Drever and Johnston (1969).

A = Mt. Monger sill liquid composition (Williams and Hallberg, 1973).

B = Average tholeiitic olivine basalt (McCall and Leishman, 1971).

D = Dundonald sill liquid composition (Naldrett and Mason, 1969).

M_1= Munro Lake sill liquid composition (MacRae, 1969).

M_2= Garrison sill chilled margin analysis (MacRae, 1969).

N_1 & N_2 = Newton Lake layered sill chilled margin analyses (this report).

L_1= Calculated Cedar Lake bulk composition (this report).

K = Average Barberton basaltic komatiite (Viljoen and Viljoen, 1969 b).

+ = Average Archean basalt (Wilson and others, 1965).

X = Barberton basaltic komatiites (Viljoen and Viljoen, 1969 b).

• = Ely and Newton Lake volcanics (Green, 1970 a).

o = Australian high-MgO basalts (Williams, 1972).

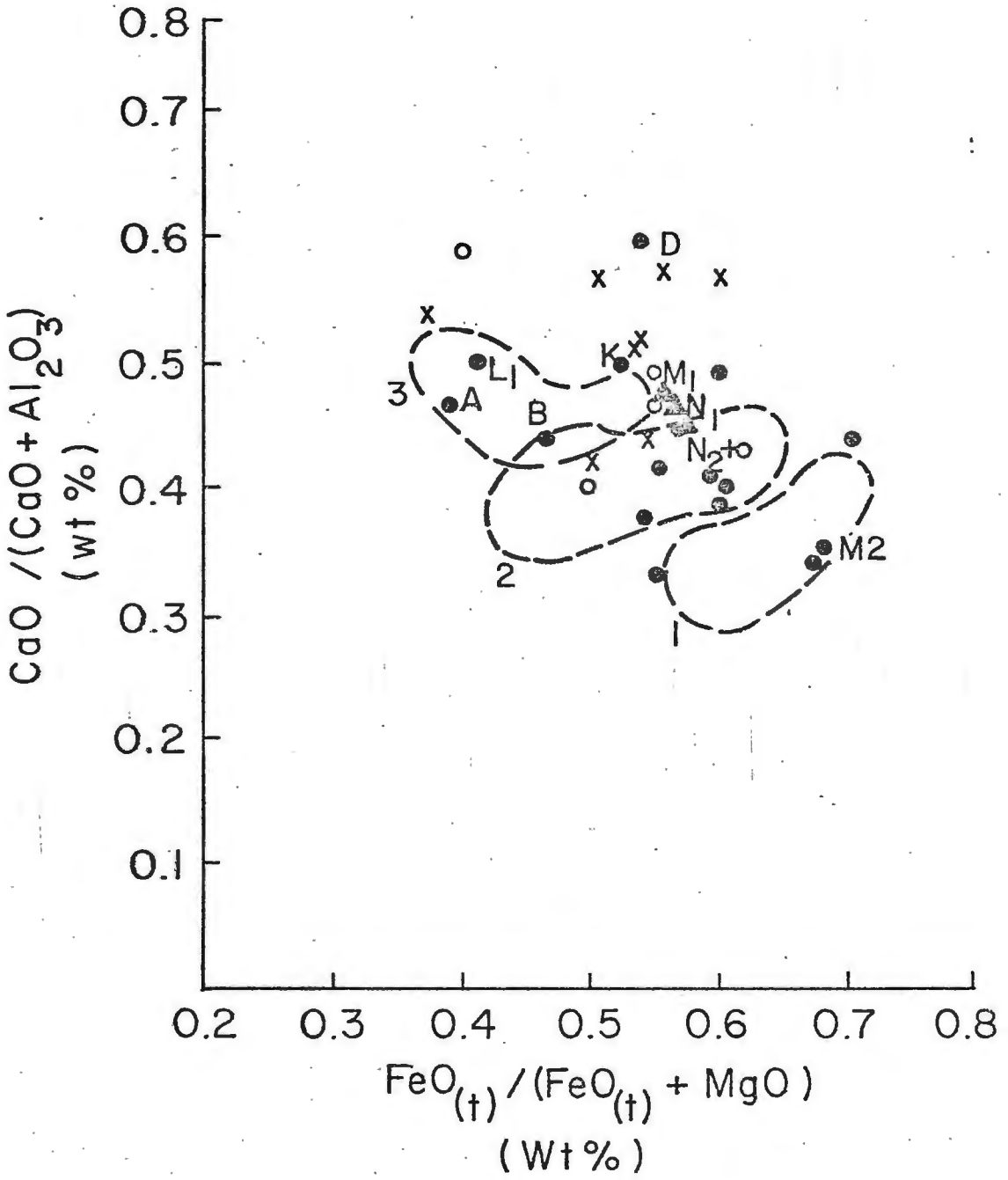

Figure 55. Plot of wt. percent CaO | $(CaO + Al_2O_3)$ against wt. percent $FeO_{(t)}$ | $(FeO_{(t)} + MgO)$ for a number of rock types including those of the Newton Lake Formation.

Key to Anaylses

Table 15

1. Calculated initial liquid composition for Munro Lake sill (MacRae, 1969).
2. Garrison chill analyses (MacRae, 1969).
3. Calculated initial liquid composition for Mt. Monger sill (Williams and Hallberg, 1973).
4. Average Barberton type basaltic komatiite (Viljoen and Viljoen, 1969 b).
5. High-Mg basalt, Western Australia (Williams, 1972).
6. Average Archean metabasalt of Superior Province, Canada (Wilson and others, 1965).
7. Average olivine basalt, Hawaii (MacDonald, 1949).
8. Average continental tholeiite (Mansen, 1967).

Table 15: Bulk Analyses from other layered sills and average analyses for some relevant igneous rock types.

	1	2	3	4	5	6	7	8
SiO_2	50.41	51.28	51.9	53.75	52.0	49.83	48.35	51.50
Al_2O_3	10.25	13.19	12.4	10.02	10.90	14.64	13.18	16.30
Fe_2O_3	2.61	1.20	9.7	1.25	12.00	3.03	2.35	2.80
FeO	12.21	13.70		9.90		8.77	9.08	7.90
MgO	10.84	6.82	15.7	10.30	10.20	7.36	9.72	5.90
CaO	9.23	7.24	8.1	10.18	10.60	10.46	10.34	9.80
Na_2O	2.75	4.04	1.21	2.70	2.69	2.02	2.42	2.50
K_2O	0.22	0.32	0.34	0.47	0.17	0.23	0.58	0.86
TiO_2	1.19	1.79	0.41	0.87	0.62	0.94	2.77	1.20
P_2O_5	0.08	0.14	0.06	---	0.08	---	---	---
MnO	0.21	0.28	0.17	0.22	0.20	0.21	0.14	0.17
$\frac{CaO}{Al_2O_3}$	0.90	0.54	0.65	1.00	0.97	0.71	0.79	0.60

All analyses Recalculated anhydrous.

The average olivine tholeiite, while having a similar CaO/Al_2O_3 ratio is also low in MgO and high in Al_2O_3 by comparison. The data also show the chilled-margin analyses from Newton Lake layered sills are very similar to the Barberton type basaltic komatiites and Australian high-Mg basalts. The calculated initial bulk composition can be seen to lie (Figure 55) in the field of high lime liquids of Drever and Johnston (1966) and falls close to the calculated bulk composition given for the Mt. Monger sill of Western Australia (Williams and Hallberg, 1973).

Recent work by Viljoen and Viljoen (1969 a and b) in the Barberton Mountain land of South Africa and by Williams (1972) in the Yilgarn Block of Western Australia has shown the existence in these areas of high-Mg basalts, characterized by high MgO, SiO_2, CaO and low Al_2O_3 and alkalies compared to known basalt types. Quite a range in MgO content (from 20% to 10%) has been observed in these rocks with skeletal crystal habits being common especially in the basalts having the lower MgO (~12-10%) content (Williams, 1972). In South Africa the name "konatiite" (Viljoen and Viljoen, 1969 a) has been applied to these rocks while those in Australia have been called high-Mg basalt (Williams, 1972).

In comparing the Newton Lake chilled-margin analyses with these high-Mg basaltic types it is apparent that for the same relative MgO content the CaO/Al_2O_3 ratio in the Newton Lake samples is lower than the Barberton

Mountain basalts but similar to the Australian rocks. It appears that the Newton Lake layered sill chilled-margin compositions (and calculated ?) may be intermediate between more normal tholeiites and the komatiites of the Barberton Mountain land.

The calculated initial composition for the Newton Lake layered sills is distinctly picritic in nature (see for example Clarke, 1970). Picrites, however, show a crystallization order of olivine-plagioclase-clinopyroxene (Clarke, 1970) while the Newton Lake sills and also the aforementioned high-Mg basalts show a crystallization order of olivine-pyroxene-plagioclase-quartz (see discussion below and Williams, 1972). It appears therefore that the Newton Lake layered sills were formed from magmas very similar in composition to those found in similar Archean sequences throughout the world.

Order of Crystallization in the Layered Sills

Textural and stratigraphic relationships previously described allow determination of the crystallization sequence for the layered sills. In the peridotite, olivine and chromite are the cumulus minerals with orthopyroxene, clinopyroxene and plagioclase forming as interstitial (post-cumulus) minerals. In the stratigraphically higher pyroxenite, clinopyroxene and orthopyroxene take the place of olivine and chromite as cumulus minerals, with plagioclase and occasional quartz forming interstitially.

In the gabbroic rocks plagioclase and iron-titanium oxide first become cumulus minerals along with clino- and ortho-pyroxene. Upwards in the gabbro orthopyroxene ceases as a "cumulus" phase with plagioclase, clinopyroxene and iron-titanium oxide crystallizing together. By this stage, evidence of actual crystal settling (cumulus textures) no longer is present. Assuming a continuous series, the order of crystallization of major minerals is;

1. chromite
2. olivine + chromite
3. clinopyroxene + orthopyroxene
4. clinopyroxene + orthopyroxene + plagioclase + iron-titanium oxide
5. clinopyroxene + plagioclase + iron-titanium oxide,

Phase relations in the system olivine-clinopyroxene-plagioclase-silica (ol-cp-pl-q) have recently been discussed by Irvine (1970). He has developed a phase model for this system (Figure 56) showing liquidus volumes for olivine, clinopyroxene, orthopyroxene (or pigeonite) and tridymite (or quartz). Irvine compared the crystallization order obtained by plotting chilled border analyses of various layered complexes in the tetrahedron, with that observed in their respective rock sequence. The liquidus boundaries used in the model are based on the melting relations of "average" basaltic rocks at a pressure of 1 atmosphere. Irvine found that the predicted crystallization order given by the model agreed fairly well with the observed

rock sequences. He also found that the four minerals listed above may have as many as 30 different crystallization orders in basaltic magmas, with cumulus sequences depending on the exact path of the liquid. Slight variations in starting compositions for a magma (e.g, Fe/Mg ratio), slightly different pressures (e.g. load or fO_2) are all that are required to change the crystallization path followed by the liquid (Irvine, 1970; Walker and others, 1973).

The Newton Lake chilled-margin samples are higher in MgO and slightly lower in Al_2O_3 than average basalts, however, they are hypersthene-normative and contain no more normative olivine than most of the average basalts used by Irvine in the tetrahedron. The Newton Lake samples have therefore been plotted in the tetrahedron to examine their theoretical crystallization order. Figure 57 shows the olivine and clinopyroxene projections of the tetrahedron as presented by Irvine (1970) with the two layered sill chilled-margin compositions (1 and 2) as well as the computed liquid for the Cedar Lake sill (L) being plotted. In the clinopyroxene projection all three compositions plot in the olivine field area and are predicted to differentiate toward the orthopyroxene boundry surface. The calculated composition (L) appears to project very close to the plagioclase-orthopyroxene eutectic, at least at 1 atmosphere. In the olivine projection compositions 1 and 2 plot on the clinopyroxene-

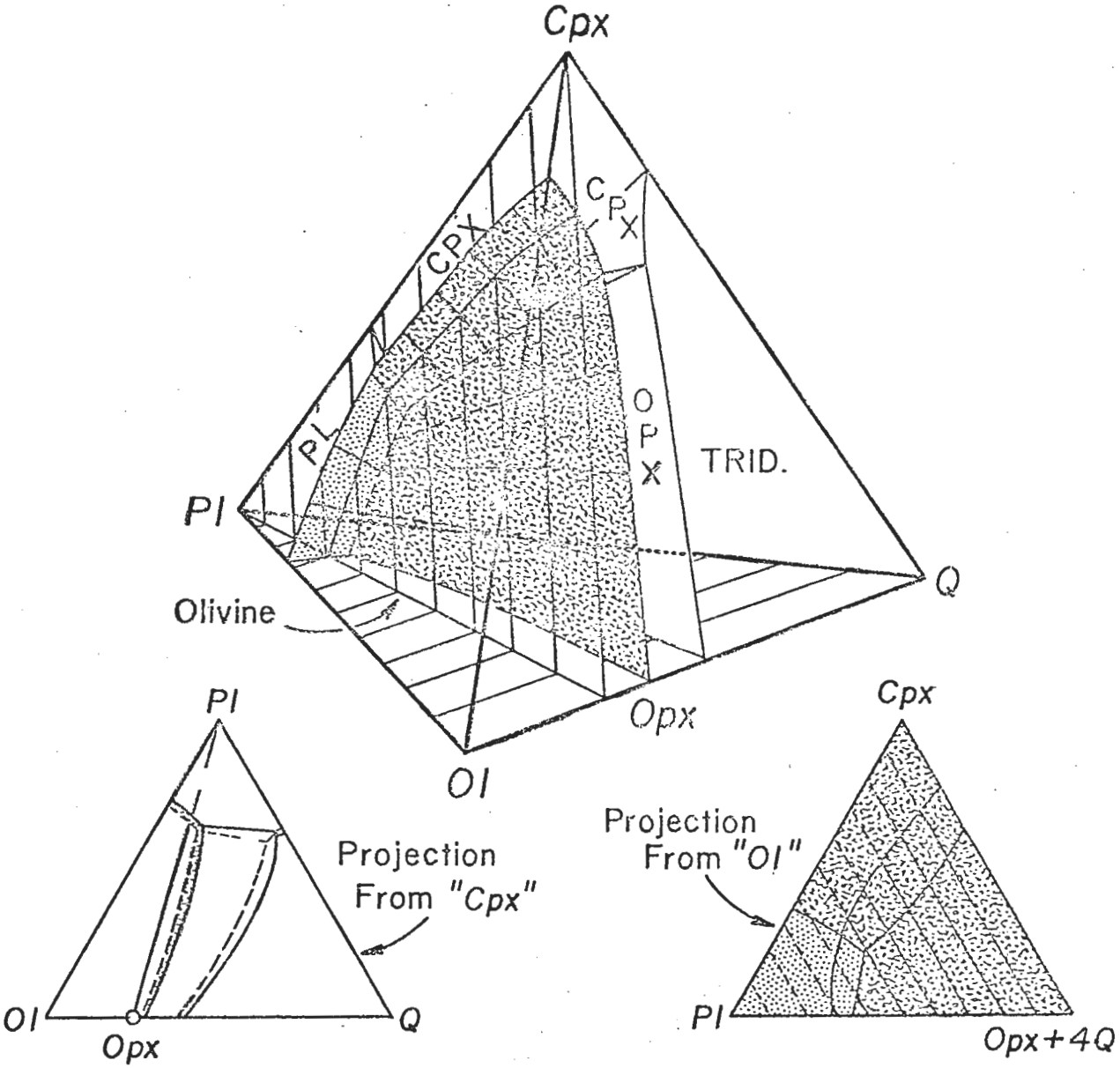

Figure 56. Phase diagram model and projections of the "system" Ol (olivine) - Cpx (clinopyroxene) - Pl (plagioclase) - Q (silica), showing liquidus volumes for Ol, Cpx, Opx (or pigeonite) and tridymite (or quartz). (After Irvine, 1970).

orthopyroxene join at 1 atmosphere. The calculated composition L plots well in the clinopyroxene field and should migrate toward the clinopyroxene-plagioclase join. It should be noted that with increasing pressure the orthopyroxene field expands at the expense of the plagioclase field. Thus at pressures of about 4 1/2 kb, compositions 1 and 2 lie well within the orthopyroxene field while composition L at 4 1/2 kb would migrate to the clinopyroxene-orthopyroxene join. At 9 kb all three compositions would lie in the orthopyroxene field.

The full crystallization order indicated at 1 atmosphere pressure for compositions 1 and 2 (assuming equilibrium crystallization) is:

1. olivine
2. olivine + clinopyroxene + orthopyroxene
3. olivine + clinopyroxene + orthopyroxene + plagioclase

In the Newton Lake sills a reaction relation between olivine and clinopyroxene appears to have existed (see page 40 and Figure 17). This would eliminate cotectic crystallization of olivine and clinopyroxene and the resulting crystallization order in Figure 57 becomes:

1. olivine
2. clinopyroxene + orthopyroxene
3. clinopyroxene + orthopyroxene + plagioclase,

which is also the observed sequence of crystallization

in the Newton Lake sills. Pressures greater than about 1 kb would give the crystallization sequence (with the olivine-clinopyroxene reaction relation)(Irvine,1970,p463):

1. olivine
2. orthopyroxene
3. orthopyroxene + clinopyroxene
4. orthopyroxene + clinopyroxene + plagioclase.

As no orthopyroxenite units are present in the Newton Lake sills, it appears that the crystallization of these sills did not occur in a high pressure environment but rather at very low pressures (i.e. shallow depths).

It should be noted that the calculated liquid L shows the sequence at 1 atmosphere pressure:

1. olivine
2. olivine + clinopyroxene
3. olivine + clinopyroxene + plagioclase
4. olivine + clinopyroxene + plagioclase + orthopyroxene,

and with the olivine-clinopyroxene reaction relation:

1. olivine
2. clinopyroxene
3. clinopyroxene + plagioclase
4. clinopyroxene + orthopyroxene + plagioclase.

Pressures in the range of 7 kb are required to obtain the crystallization order observed in the Newton Lake sills. This pressure is considerable higher than that

Figure 57. Olivine and clinopyroxene projections from Figure 56 containing the analyses from the Newton Lake layered sills chilled-margin samples. Note that analyses 1 and 2 project from clinopyroxene to the orthopyroxene cotectic. The crystallization sequence shown by analyses 1 and 2 are the same as that observed in the sills indicating crystallization probably took place at very low pressures as the diagram is based on 1 atmosphere pressure. With increasing pressure the plagioclase field would contract, expanding the orthopyroxene field. (Adopted from Irvine, 1970).

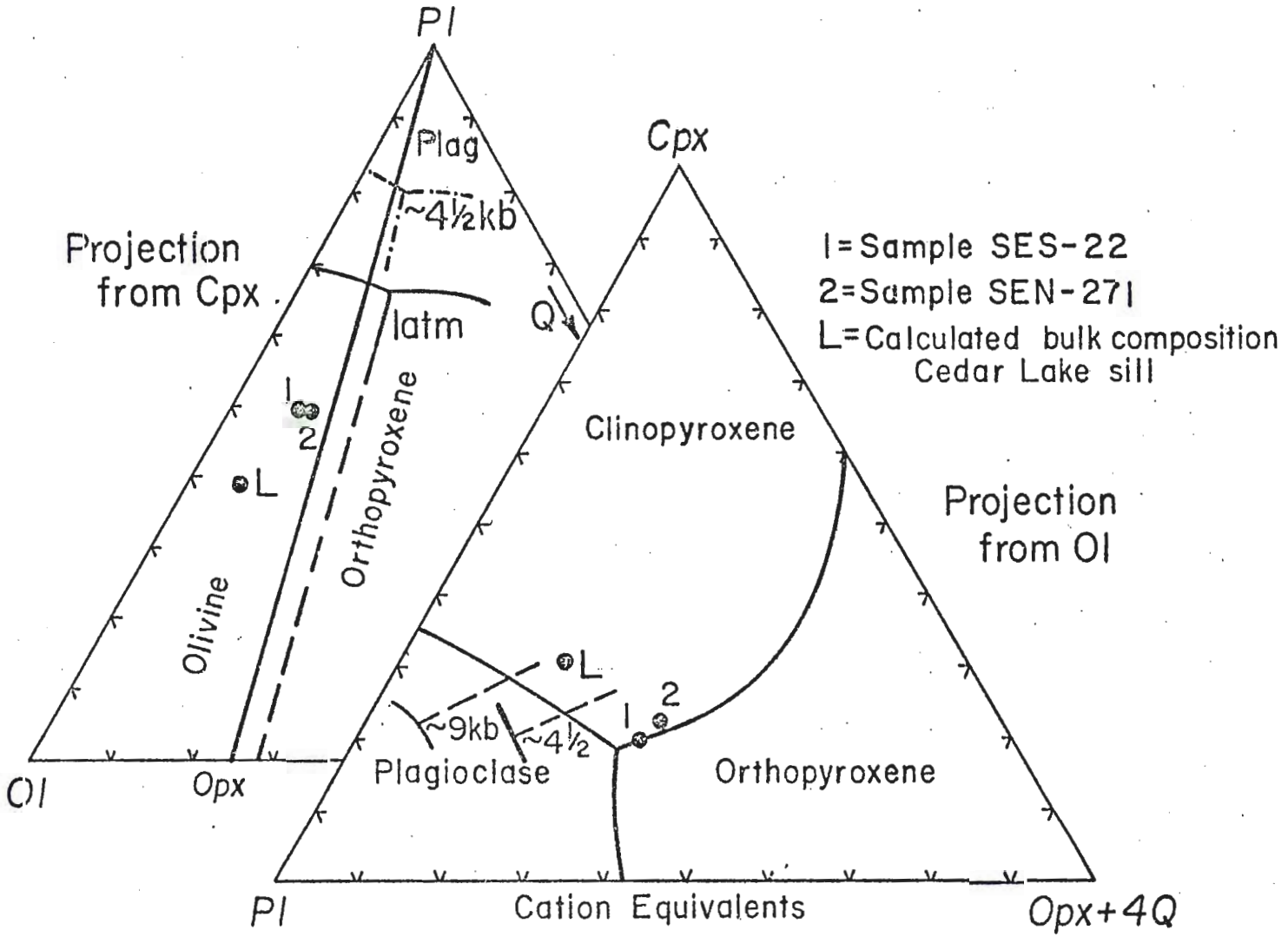
Pl
Plag
~4½kb
Projection
from Cpx
latm
Q
1
2
L
Olivine
Orthopyroxene
Cpx
1=Sample SES-22
2=Sample SEN-271
L=Calculated bulk composition
Cedar Lake sill
Clinopyroxene
Projection
from Ol
L
1
2
~9kb
~4½
Plagioclase
Orthopyroxene
Ol
Opx
Pl
Cation Equivalents
Opx+4Q

obtained by other methods (see discussion below). The data and interpretation discussed above support the idea that the chilled-margin compositions accurately represent the composition of the magma at the time of intrusion and suggest that crystallization took place at shallow depths.

Temperature and Pressure of Formation for the Layered Sills based on Mineral Composition and Textural Relations

Temperature

Temperature dependance on coexisting mineral compositions is an area of on-going research in petrology and current "thermometers" must be considered empirical estimates of temperature of equilibration at best. The problem is complex because inter- as well as intracrystalline equilibria must be considered (Grover and Orville, 1969). Because of the obvious problem that the greenschist facies metamorphism imposes on temperature determinations, estimates for the rocks studied in this investigation are based on the interpretation of the analytical data in light of only some of the current thermometers available.

Orthopyroxene-Clinopyroxene: The equilibrium distribution coefficient for Mg and Fe between coexisting orthopyroxene and clinopyroxene assuming ideal solid solution is given by the expression:

$$K_D = \frac{X_{Mg}^{cpx} \; X_{Fe}^{opx}}{X_{Mg}^{opx} \; X_{Fe}^{cpx}}$$, where

X_{Mg}^{cpx} and X_{Fe}^{cpx} are the mole fractions of the end members $CaFeSi_2O_6$ and $CaMgSi_2O_6$ in clinopyroxene and X_{Mg}^{opx} and X_{Fe}^{opx} are the mole fractions of the end members $FeSiO_3$ and $MgSiO_3$ in orthopyroxene (Kretz, 1963). At equilibrium, K is a constant at a fixed composition. The two-pyroxene distribution coefficient has not been calibrated by experimental techniquies; however Kretz (1963) and Bartholome (1962) have demonstrated the K_D values range from appoximately 1.4 for pyroxene crystallizating from mafic magmas to 1.8 for pyroxenes in crustal metamorphic rocks, a variation considered to correlate with decreasing temperature. These empirical values may be useful for comparative purposes, but a more quantitative application must take into account intracrystalline equilibrium (Grover and Orville, 1969). The K_D value obtained for one orthopyroxene pair from the Cedar Lake sill (pyroxenite unit, Sample SES-26) is 1.5. This value while lower than the 1.4 value obtained for pyroxenes from mafic intrusions by Kretz (1963), is still indicative of normal igneous temperatures as it was derived from pyroxenes which show some subsolidus equilibration (i.e. exsolution).

Olivine-Chromian Spinel: Jackson (1969) has derived a general expression for estimating the temperature of formation of olivine-chromian spinel pairs that formed in equilibrium. The temperatures so obtained must be

considered as nominal values only and not absolute for the following reasons:

1. Because of the lack of data on the activity - concentration relationships of chromian spinels, Jackson (1969) assumed ideal solid solution behavior.
2. There are uncertainties in the free-energy values.
3. In the Newton Lake spinels there is an uncertainty in the calculation of ferrous and ferric iron assuming a spinel stoichiometry.
4. The high TiO_2 content makes it imperative that the activity of TiO_2 (ulvospinel) be considered in deriving the equation (Evan and Wright, 1972).

However, using Jackson's (1969) expression a temperature of 865°C was obtained for a olivine-chromite pair from a Newton Lake layered sill peridotite sample (Sample SEN-310). This temperature is considerably lower than that obtained by Jackson (1969) from olivine-spinel pairs in the Stillwater Complex (900° to 1400°C). It appears that the uncertainties in the expression and the limitations noted above may account for the descrepancy. It is interesting to note that the Newton Lake spinels show compositional variations very similar to those described by Evans and Wright (1972) for chromite from the Kilauea volcano, Hawaii and by Thompson (1973) for Snake River Plain basalt chromites. Evans and Wright (1972) also found large descrepancies between the calculated

temperatures from their olivine-spinel pairs and those of Jackson (1969).

Ca/Ca + Mg ratios in Pyroxenes: The pyroxenes from the peridotite and pyroxenite have compositions close to the join $Mg_2Si_2O_6$ - $CaMgSi_2O_6$. Davis and Boyd (1966) have shown that below 1400°C the amount of solid solution of $MgSiO_3$ in clinopyroxene, and the diopside solvus of the system $MgSiO_3$ - $CaMgSi_2O_6$ can be used as an equilibration temperature indicator for coexisting ortho- and clinopyroxenes. Using the solvus of Boyd and Schairer (1964) equilibration temperatures of apporximately 1055°C and 1090°C were obtained for clinopyroxene and orthopyroxene, respectively from two peridotite samples (Figure 58). Temperatures obtained with clinopyroxenes from two pyroxenite samples were slightly lower, approximately 940°C (Figure 58).

Evaluation: The temperatures obtained above for equilibration of pyroxenes in the peridotite unit are similar to those obtained by Ripley (1973) for pyroxenes from the peridotites of the Deer Lake Comples sills. It must be remembered however, that these temperatures do not represent that at the time of intrusion. At best they are temperatures of equilibration of pyroxenes with trapped liquid in the peridotite unit of the sills. They indicate however, that the initial temperature was above this minimum temperature.

An examination of the literature dealing with mafic

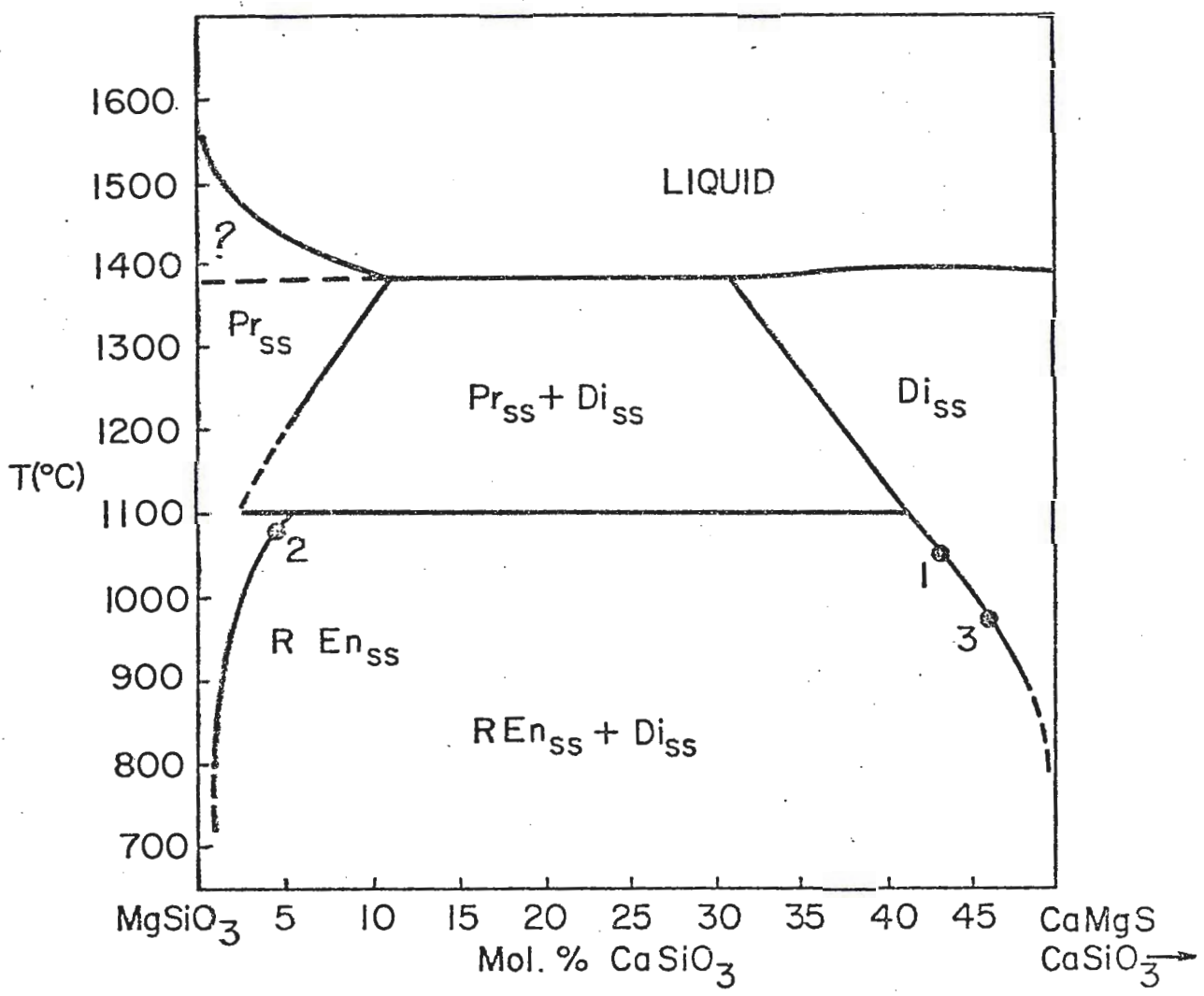

Figure 58. Equilibrium relations along the join $MgSiO_3$-$CaMgSi_2O_6$. Sample points 1, 2 and 3 represent the approximate location for Newton Lake peridotite, pyroxenite pyroxenes. (Adapted from Boyd and Schairer, 1964).

intrusives and extrusives shows that many had initial magmatic temperatures in the range of 1200°C. Hess (1960) in his discussion of the Stillwater intrusion suggested an initial temperature of about 1225°C. Recent measurements made by the U.S. Geological Survey found initial temperatures in the Makaopuhi Lava Lake, Hawaii to be at a maximum of 1200°C (Wright and Weiblen, 1967). Recent interpretation of data on peridotitic lavas in South Africa (Viljoen and Viljoen, 1969 a) and Canada (Naldrett, 1972) suggest temperatures of about 1350°C at the time of extrusion. The above values may serve as an upper limit for the initial temperature of the magmas which were emplaced in the Newton Lake Formation. It should be remembered however, that the presence of water in a mafic magma can lower the melting temperature. That water was present in the Newton Lake sill magmas is indicated by the presence of primary amphibole in the peridotite and amygdules in the chilled margins, however the absolute amount is unknown. It is concluded from the available data that an initial temperature between 1200°C and 1100°C is not unreasonable for the magmas which formed the Newton Lake sills.

Pressure

The determination of the pressure (depth) which prevailed during the formation of the Newton Lake sills is hampered by a lack of experimental data on systems having similar high MgO compositions. Some estimate may be made

however, using the phase diagrams of Irvine (1970) and by noting critical textures in the chilled-margin rocks.

Several textural features noted in the chilled-margin rocks suggest shallow levels of intrusion for the Newton Lake sills (and lenses). These features include the following:

1. The presence of skeletal textures similar to those produced in rapidly chilled basalts or slags;
2. the presence of amygdules (3-4%) indicating pressures were low enough to allow vesiculation to occur upon intrusion. This also suggests relatively rapid ascent of the magma from depth to fairly shallow levels.

For vesiculation to occur in a magma the confining pressure must be less than the saturated vapour pressure at a particular temperature. One mechanism for reducing the confining pressure is ascent of the magma. This is especially common in volcanic rocks which ascend to the surface resulting in separation of a volatile gaseous phase and vesiculation (MacDonald, 1972). The amount of vesiculation which occurs is clearly pressure dependant and Moore (1965) has found a systematic variation in the percent vesicles and depth of extrusion in deep-sea basalt near Hawaii. Moore's data further shows that below an ocean depth of about 5 km (0.5 kb) vesiculation did not occur. Through utilization of Moore's (1965) data

it is estimated that vesiculation may have occurred at a depth of about 1 km (0.27 kb) in the Newton Lake sills and lenses (assuming a density of approximately 2.70 for the basaltic country rocks (Jackson, 1971). This value can only be taken as a very rough approximation as other factors also control vesiculation (temperature, water content and crystallization). This figure is compatible, however with the low pressure crystallization conditions suggested from Irvine's (1970) phase diagrams and also with inferences made from the geologic setting. It is concluded from the data presently available that crystallization of the Newton Lake layered sills (and ultramafic lenses) did not take place under pressures greater than about 1 kb (2.7 km) and may have been even lower.

METAMORPHISM OF THE NEWTON LAKE SILLS

A complete study of the metamorphic alteration which has affected the Newton Lake sills has not been attempted in this study. Examination of thin sections and preliminary x-ray and microprobe work does, however, allow some general statements to be made regarding the metamorphic conditions which prevailed after intrusion.

General Preservation of Textures

As has previously been noted igneous textures are generally preserved in all but the most sheared samples.

Cumulus textures, including sharp and consistent textural relations between cumulus and intercumulus phases are discernable in even completely altered rocks. This preservation of textural relations even in the peridotites suggests that the alteration process may have involved little change in volume (Williams, 1971). This is in contrast to typical greenschist metamorphism of pelitic rocks (Turner, 1968) which are generally recrystallized and well foliated.

Ultramafic Rocks

In the peridotites the major metamorphic effect is serpentinization of the olivine. In some cases however, orthopyroxene and clinopyroxene were also altered with bastite or talc + tremolite alteration after orthopyroxene and actinolite and magnetite forming from clinopyroxene (see Table 2, page 25, for list of common alteration products). Examination of the serpentine using standard x-ray diffraction methods for identification (ASTM x-ray powder data file) indicates that antigorite is the only or at least major serpentine mineral now present. Studies by Williams (1971) on the ultramafic sills of Western Australia found that the original serpentine minerals formed where chrysotile - lizardite and that progressive metamorphism converted these to antigorite. In some Newton Lake peridotites talc was also formed along with tremolite stringers in the more highly sheared peridotites. Necessary calcium for their

formation may have come from introduced carbonate or liberated from destruction of clinopyroxene and plagioclase.

The presence of abundant magnetite in the peridotites is also clearly related to serpentinization. This is shown by the occurrance of magnetite along the fractures cutting the peridotites and along which serpentinization occurred and their presence in the altered clinopyroxenes. The identification of magnetite is based on cursury reflected light examination of the peridotites and by the highly magnetic nature of the rock. Reflected light examination suggests several generations of magnetite may be present and that a detailed study of the oxide minerals in relation to alteration is essential to understanding this aspect of the Newton Lake sills. Coleman and Keith (1971) have shown that serpentinization minerals can accommodate only part of the iron released from alteration of olivine and pyroxene and that with sufficient silica serpentine + magnetite form from pyroxene rich ultramafic rocks. With out sufficient silica serpentine + brucite would tend to form with the iron being largely accommodated in the brucite (Coleman and Keith, 1971).

The replacement of plagioclase in the peridotites is also at least partially related to serpentinization. As previously noted no fresh plagioclase has been observed in the peridotites; however, a fine dense aggregate of chlorite is commonly present. The interpretation that chlorite has replaced plagioclase is based on descriptions

of replaced plagioclase from other ultramafic sills (e.g. MacRae, 1969; and Williams, 1971) and on the close agreement between normative plagioclase and modal chlorite in the peridotites. The formation of chlorite after plagioclase is probably the result of MgO expelled from olivine (and orthopyroxene?) during serpentinization (Williams, 1971).

The process by which serpentinization takes place is still a major problem in geology. Examination of the Newton Lake peridotites has led to the following general conclusions concerning their serpentinization.

A common feature in the Newton Lake peridotites is fine parallel microfractures which appear unrelated to any igneous fabric. These fractures can be seen in thin section cutting olivine grains with occasional olivine kernels still present surrounded by serpentine and magnetite (Figure 16). It appears that the fractures controlled the alteration and the path taken by the altering fluids. The importance of the fracture controlled alteration is that it indicates serpentinization took place only after solidification of the peridotite and that it was not a deuteric alteration. This observation was first made by Green (1970 b).

A major point of controversy in studies of serpentinized rocks has been the question of whether it occurred as a constant-volume or constant-chemical composition process. Both sides of the argument have proponents (e.g. Coleman and Keith, 1971, constant-composition; Thayer, 1966,

constant-volume) and from the evidence collected it appears that serpentinization can occur in response to a variety of different processes. It appears that the geological setting may be of major importance in this regard (Williams, 1972).

In the Newton Lake peridotites little evidence has been found to support a volume increase with serpentinization. The almost perfect preservation of igneous textures in all but the most altered sheared samples appears to require a constant volume process. Field relations also support this conclusion, although simple thickening of units may not form any recognizable features, As little compositional variation appears to have occurred (with the exception of H_2O and CO_2) it is likely that water and minor CO_2 where the main components added to the peridotites with redistribution of elements occurring so as to preserve the relative amounts of the different elements.

The stable mineral assemblage in the peridotites appears to be serpentine + talc + chlorite + pargasite + magnetite (see note above). It appears that clinopyroxene was also generally stable under the metamorphic conditions. The absence of brucite suggests that the assemblage serpentine-brucite was not stable. The presence of antigorite as the major serpentine species suggests higher temperatures than lizardite-bearing assembalges (Martin, 1971). Figure 59 shows experimentally determined equilibrium curves for the pertinent reactions in the

$MgO - SiO_2 - H_2O$ system under conditions of prevailing water pressure equal to the pressure acting on the solid phases. Anhydrous peridotite is stable on the high-temperature side of curve (a) in the figure. On crossing (a), the rock could begin to produce talc. On crossing (b), the rock could begin to produce serpentine. The mineral assemblage noted above for the Newton Lake peridotites is stable in the temperature-pressure field between curves (b) and (c). Martin (1971) has pointed out that equilibrium temperatures should probably be lower as aluminum and iron are present in the relevant silicates. Also if the prevailing water pressure were lower than the pressure acting on the solid phases, the temperatures of the beginning of formation of talc, serpentine and brucite would be lower than the curves shown in Figure 59 (Miyashiro and others, 1969). The presence of olivine relicts in the peridotite as well as common relicts in other units of the sills suggests that the H_2O and CO_2 available was insufficient for complete reaction (Williams, 1972).

The pyroxenites appear not to have been greatly effected by the serpentinization of the peridotites. The orthopyroxene phenocrysts are generally altered to a lameller intergrowth of talc-tremolite or chlorite-tremolite. This alteration is very distinctive and reflects the original "Bushveld" type of exsolution in the orthopyroxenes. Preliminary microprobe analyses of the tremolite after orthopyroxene shows an average FeO:CaO:MgO

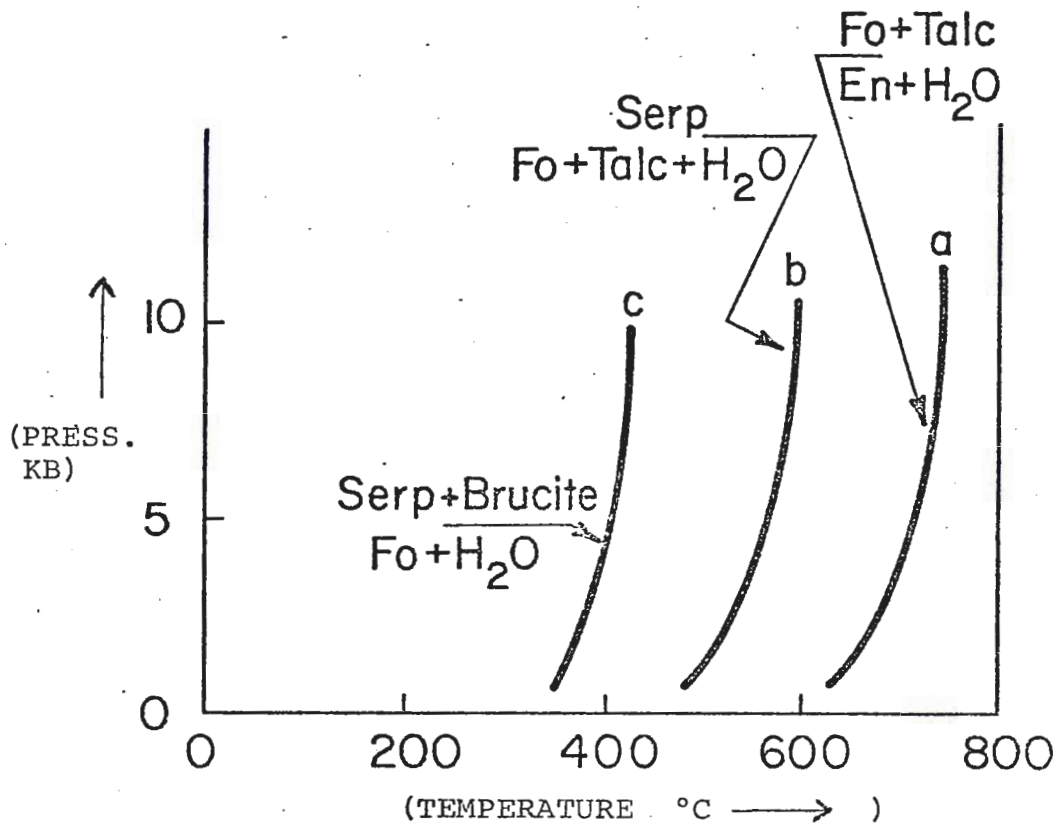

Figure 59. Experimentally determined equilibrium curves for the following reactions under $P_{H_2O} = P_S$ conditions. Reactions are from right to left:

a) enstatite + water = forsterite + talc

b) forsterite + talc + water = serpentine

c) forsterite + water = serpentine + brucite

(ater Miyashiro and others, 1969).

ratio of 17:26:57. Berkley (1972) reported antophyllite alteration from similar orthopyroxene in the Deer Lake Complex of Minnesota. Recent work by Ripley (1973) on the same rocks has not been able to verify the presence of anthophyllite in the Deer Lake Complex. Clinopyroxene is generally partially altered to actinolite while plagioclase is highly sausseritized.

Mafic Rocks

Metamorphic assemblages in the gabbroic portions of the sills are characterized by tremolite-actinolite and sausseritized plagioclase with minor chlorite, epidote, sphene, leucoxene (?) and rare relict pyroxene grains. The assemblages are very similar to those found in the surrounding mafic metavolcanics suggesting that both the Newton Lake sills and volcanics were altered under the same general set of metamorphic conditions. A plot of the chemical compositions of the sill rocks in the ACF diagram for the muscovite-chlorite subfacies of the greenschist facies (Figure 60) shows how the samples have approached equilibrium in the facies, insofar as the mineralogy is controlled by the chemical composition. The predicted mineralogy from the plotted points agrees fairly well with the observed metamorphic mineral assemblage except for the occasional relict pyroxenes still present. The presence of these relicts suggests that metamorphic reactions were retarded perhaps in relation

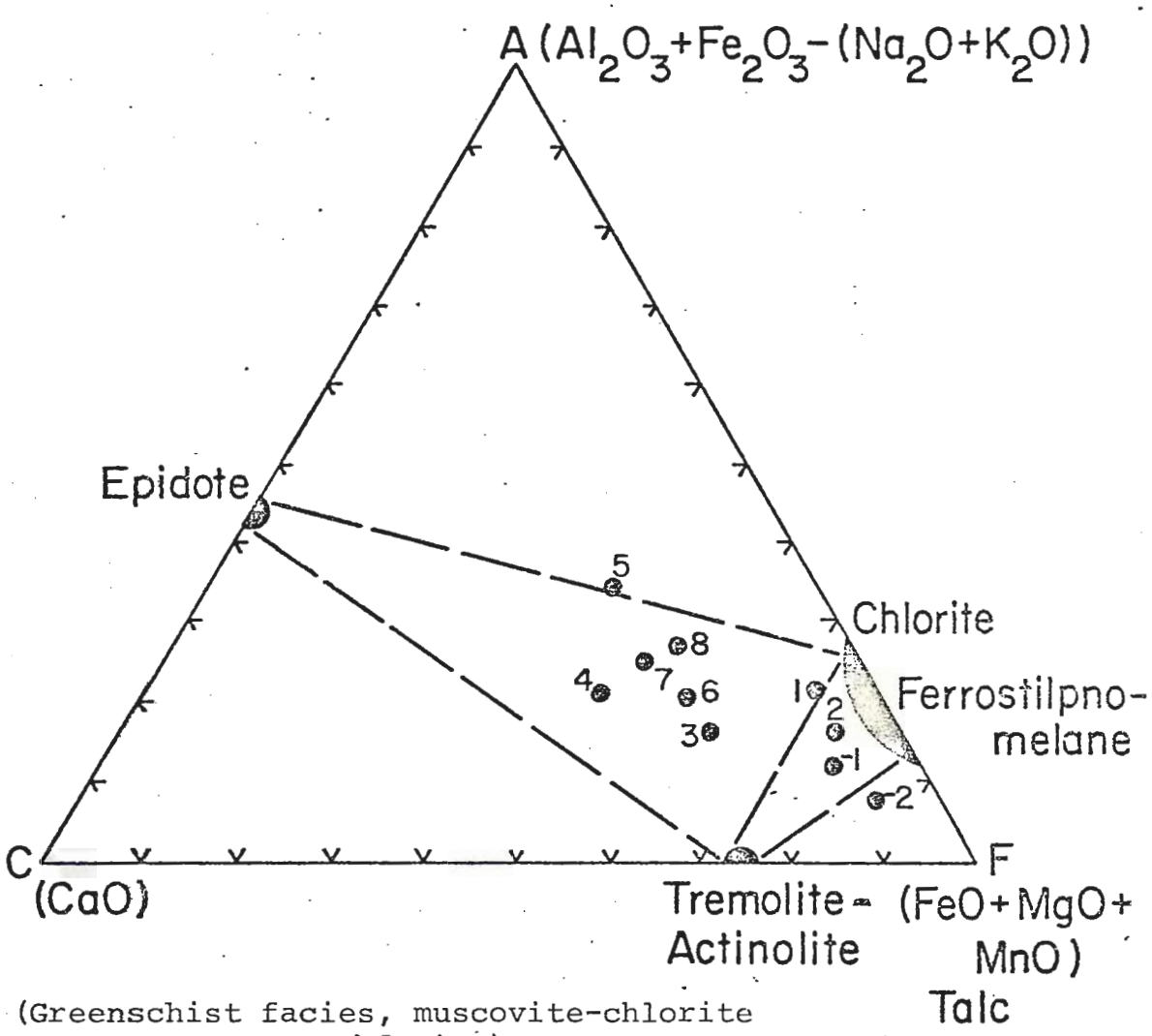

Figure 60. Figure shows the predicted mineral assemblage for the analyzed Newton Lake samples in the greenschist facies, insofar as the mineralogy is controlled by the chemical composition. Sample numbers same as in Table 13. (-1,-2 = Peridotite with Fe_2O_3 recalculated to 1.25%). (Adapted from Turner, 1968).

to low H_2O and CO_2 availability and low pressure (Williams, 1972).

Microprobe analyses of the amphibole after clinopyroxene shows it to be tremolite-actinolite with an FeO:CaO:MgO ratio of 35:27:38. Alteration of the clinopyroxene in chilled margins is similar to that observed in the gabbros, however the actinolite is richer in MgO having the ratio 25:24:51 for FeO:CaO:MgO.

PETROGENESIS AND GEOLOGIC HISTORY FOR NEWTON LAKE SILLS

Classification

Naldrett (1970) has suggested that ultramafic bodies in orogenic belts can be subdivided on the basis of the timing of their final emplacement with regard to the development of the orogen. Using this criterion three subdivisions are possible:

1. Ultramafic bodies emplaced and crystallized prior to major folding of the enclosing rock,
2. those emplaced during folding (i.e. "Alpine-type" ultramafic bodies),
3. those emplaced during the final stages of orogenis. This class includes the Alaskan concentrically zoned ultramafic bodies.

Naldrett (1970) has further established three different classes of ultramafic bodies common in Archean greenstone

belts, distinguished according to size and chemical composition. The three classes are:

1. large (20-50 miles long, greater than 20,000 feet thick) igneous complexes such as the Dore Lake complex (Allard, 1970). This class is largely mafic rather than ultramafic in overall composition.
2. Smaller (1-10 miles long, up to 5000 feet thick) gravity stratified sills such as the Dundonald sill described by Naldrett and Mason (1968).
3. Lenses of peridotite and pyroxenite (ranging from 10 X 200 feet to 4000 X 20,000 feet in surface dimensions) that show no evidence of gravity stratification.

The layered differentiated sills of the Newton Lake Formation and the ultramafic lenses appear to belong to classes 2 and 3 respectively of Naldrett's classes of Archean ultramafic bodies. At present no large differentiated complex meeting the description of class 1 is known. Both the layered sills and ultramafic lenses are broadly conformable to the enclosing rocks (Plate 1). In the layered sills, the gravity-formed layers are also parallel to the stratification in the surrounding rocks. These features along with the microfractures cutting the peridotite indicated intrusion prior to deformation for Newton Lake sills and lenses and places them in division 1 of the orogenic classification developed by Naldrett (see above). This conclusion, that the sills and lenses

were emplaced prior to major deformation has important bearing on the origin of the ultramafic bodies and the tectonic setting in which they lie. This is discussed in the following section.

Origin of the Newton Lake Sills and Lenses

The Newton Lake Formation, in the area investigated, consists of about 60% intrusive mafic-ultramafic sills and lenses and about 40% mafic metavolcanics and minor metasedimentary rocks. The close spatial association of the mafic-ultramafic bodies with the mafic metavolcanics and their absence in the felsic portion of the formation, the presence of pillowed flows having skeletal textures and compositions (Green, J.C., written communication) similar to the chilled margins of the layered sills and ultramafic lenses, the conformable nature of the bodies to the surrounding rocks, and the similarity in the type of metamorphic alteration of the sills and enclosing rocks is strongly suggestive of a penecontemporaneous origin for the sills and lenses and the mafic volcanics of the Newton Lake Formation. As mentioned earlier the theoretically determined order of crystallization in the layered sills is compatible with low-pressure crystallization (see page 175) and supports the concept of the sills being high-level intrusions roughly contemporaneous with volcanism. The deficiency of gabbro in some sills (see page 155) and similarity in composition

of the mafic volcanics and gabbros suggests that some sills may also represent cumulus rocks developed in magma chambers which fed surface volcanism.

The magma from which the layered sills and lenses formed appears to have been ultrabasic in nature (MgO~ 17%) and similar to those reported from Australia (Williams, 1972), South Africa (Viljoen and Viljoen, 1969 b) and Canada (Naldrett and Mason, 1968; Brooks and Hart, 1972). On its' ascent it appears to have crystallized chromite and olivine, fractionating to the composition of the chilled-margin rocks. Derivation of such a magma has generally been attributed to high degrees of partial melting at fairly shallow depth (Brooks and Hart, 1972; Williams, 1972).

Green (1970 a) and Sims (1972) have shown that the basalts of the Newton Lake Formation are low K_2O tholeiitic basalts with the formation as a whole showing a general calc-alkaline trend. The bulk composition of the sills and lenses and some flows also show tholeiitic affinities but are much higher in MgO and have higher CaO/Al_2O_3 ratios than the Newton Lake volcanics. The occurrence of high-Mg basalts with normal tholeiites in Western Australia has been accounted for by two possible relations (Williams, 1972):

1. the tholeiites may represent the end-product of a high-Mg basalts series evolved by fractional crystallization or

2. the MgO-rich and tholeiitic magmas were produced separately by differing degrees of partial melting in the mantle.

An unequivocal answer to the relationship between the high-Mg basalts and normal tholeiites is not possible at this stage of investigation. Detailed examination of minor and trace-element distributions and mass balance calculations using a method as presented by Wright and Doherty (1970) are essential to the resolution of the problem. As an example of the problems in interpretation which exist; the occurrence of the high-Mg basalts (as sills and flows) within the tholeiites as penecontemporaneous units might suggest that the tholeiites did not form by simple crystal fractionation from the same magma as the former. However, if replentishment of the magma chamber occurred both basaltic types could be directly related by simple fraction.

A derivation of the two magma types by differing degrees of partial melting has been proposed by Williams (1972) and Brooks and Hart (1972) to explain similar occurrences of high-Mg and normal basalts. Brooks and Hart (1972) have suggested that Archean tholeiites represent fairly high degrees of mantle melting at shallow depths with the high-Mg magmas representing even more extensive melting especially of the clinopyroxene components. They envision the volcanics as occurring in an island arc type of environment with

melting occurring in the sub-arc mantle controlled by adiabatic decompression during upwelling of mantle diapirs. It appears that a model similar to that of Brooks and Hart (1972) may be applicable to the Newton Lake sequence. The general calc-alkaline trend indicated by the volcanics, similar to that of island arcs, is support for such a model. The mafic portion of the Newton Lake Formation may represent the lower part of such an active volcanic system .

Summary of the Geologic History of the Newton Lake Formation

In the discussion below a geologic history is attempted for the Newton Lake Formation based on this study and the work of Green (1970 a).

After deposition of the Knife Lake Group, volcanism commenced abruptly in the area with deposition of dominantly andesitic and dacitic lavas, tuffs, and breccias east of Fall Lake and basalts to the west. The preserved metavolcanics from this period have been named the Newton Lake Formation. Extrusion of the lavas was largely subaqueous, according to the abundance of pillow structures throughout the formation.

Contemporaneously with the outpourings of tholeiitic basalt in the western portion, magmas having high-Mg compositions were intruded as sills and lenses at shallow depths within the volcanic pile. The magmas forming the

intrusions were probably derived from a separate magma source from that of the tholeiites and brought rapidly towards the surface and supercooled on intrusion. Intrusion appears to have occurred along stratigraphic contacts without great disruption of the volcanic strata. Normal tholeiite magma was also probably intruded to form some of the gabbroic sills.

Stable conditions appear to have existed during crystallization of the sills as a regular layering was produced in them by gravity settling. The presence of cherty limestone and limy chert conglomerate suggests stable conditions did prevail locally (Green, 1970 a). Most of the sills remained closed, crystallizing a sequence of peridotite-pyroxenite-gabbro. Occassional tapping of some sills may have occurred resulting in gabbro sills and some ultramafic lenses. Some small intrusions of olivine bearing magma also appear to have occurred forming the ultramafic lenses with the distinctive complex chilled-margins.

The Newton Lake Formation contains the youngest Archean supracrustal rocks remaining in this area and as the Vermilion batholith lies in fault contact with the upper portion it is not known how thick a volcanic sequence was formed. The next event which apparently affected these rocks was the Algoman orogeny in which large, isoclinal folds were formed and faulting occurred prior to the intrusion of the Vermilion and Giants Range

batholiths. This in turn was followed by more major faulting. Metamorphism also probably accompanied orogenesis with generally low-grade greenschist facies assemblages formed except near granitic intrusions where the amphibolite facies was attained.

Since the Algoman orogeny the area has experienced various degrees of erosion and tectonism with erosion and deposition of sediments during Middle Precambrian time and minor influence from the Penokean orogeny. Direct influence of Keweenawan volcanism in the area is not known. Since Keweenawan time the area has probably remained above sea level and undergoing erosion, except for possible Early Paleozoic and Cretaceous transgressions. Pleistocene glaciation moved across an erosion surface which had cut across Lower, Middle and Upper Precambrian rocks and removed nearly all weathered material, especially along zones of weakness. Glaciation has left a cover of ground moraine and local glaciofluvial stratified drift over much of the area.

ECONOMIC GEOLOGY

Considerable time and effort have recently been spent by various mining companies in the examination of the Newton Lake layered sills described above for copper-nickel mineralization. Similar attention has also been given to the Deer Lake Complex of Itasca County, Minnesota (Berkley, 1972; Ripley, 1973). To date no economic

mineralization has been reported from either area.

Examination of the literature on the occurrence of copper-nickel sulfide mineraliztion in ultramafic rocks (see for example McCall, 1972; Naldrett, 1973) shows that almost all known economic mineralization has occurred with the ultramafic lenses rather than the layered mafic-ultramafic sills. McCall (1972) has suggested that this relationship is related to the magnesium content of the parent magma and also the sub-volcanic environment of emplacement. Chemical studies of the ultramafic lenses associated with the copper-nickel ores has shown them to have formed from magmas rich in MgO (25 - 34%) whereas the layered sills appear to have formed from magmas with 12 to 18% MgO. This is attributed to almost complete melting of the mantle to form the magmas of the ultramafic lenses while those forming the layered sills formed from differentiated melts or partial melts of the mantle (Viljoen and Viljoen, 1969 b). It appears that the MgO rich ultrabasic magmas contained an immiscible sulfide liquid in association with the silicate melt (Naldrett, 1973) and that it settled upon intrusion (and extrusion) toward the base of the lenses.

As has already been shown the Newton Lake layered sills and probably the lenses formed from parent magmas having between 12-18% MgO. These values while high for normal basalts are still significantly lower than for the known ore bearing ultramafic lenses. If McCalls (1972) sug-

gestions regarding nickel mineralization in ultramafic rock are correct it may mean that the lower MgO parent magmas indicated for the Newton Lake sills contained less nickel possibly because of a lower degree of partial melting (?). The association of ore with ultramafic lenses also suggests more effort should be put into the study of and exploration for ultramafic lenses in Minnesota.

SUMMARY AND CONCLUSIONS

The Newton Lake layered sills formed by simple fractionation and gravity accumulation of crystals from a parent basaltic magma relatively rich in magnesium and which may have itself fractionated from an initial ultrabasic magma. The sills are envisaged as high-level injections contemporaneous with volcanism. The ultramafic lenses apparently represent small injections of olivine-bearing magma in which the olivines were concentrated towards the centers of the lens during initial injection with subsequent rapid cooling of the remaining crystal free liquid to form the nonporphyritic border zones. It is possible that some sills also formed by tapping of sills before solidification, with the gabbroic portion tapped off to form the unlayered gabbro sills or possibly surface flows. Some of the unlayered gabbro sills may not be differentiated products of the layered sequence of sills but have formed directly from undifferentiated magma.

Serpentinization and regional metamorphism have largely altered most of the primary igneous minerals, however, textural preservation has remained excellent in all but the most altered or sheared rocks. This has made it possible to determine the crystallization sequence in the layered sills and the mechanism of differentiation. Notable features of layered sills are given below.

1. The sills show a marked simplicity of layering despite the limited thickness, with basal peridotite followed upwards by pyroxenite, bronzite gabbro and gabbro. This succession results from the crystallization sequence:

   1) Chromite
   2) Olivine + Chromite
   3) Clinopyroxene + Orthopyroxene
   4) Clinopyroxene + Orthopyroxene + Plagioclase + Iron-titanium oxides
   5) Clinopyroxene + Plagioclase + Iron-titanium oxides

   Residual granophyre and felsic veins are also present in very minor amounts. Complex chilled margins, showing skeletal crystals of pyroxene and plagioclase and amygdules are generally present at both upper and lower contacts with the upper zone generally thicker (30 ft) than the lower. Textures in the chilled margins indicate an origin by rapid cooling or quenching.

2. Cumulus textures are well developed in all but the upper gabbros, indicating fractionation by gravity settling. The peridotite appears to be a heteradcumulate, the pyroxene an adcumulate and the lower bronzite gabbro a mesocumulate. Crystal settling has resulted in phase and cryptic layering being well developed but rhythmic layering is rare suggesting little current action during crystallization. Repetition of units in a cyclic manner is generally absent.
3. Differentiation followed a general tholeiitic trend, with an increasing Fe/Mg ratio upwards and an accompanying increase in total alkalies. Analyses from the chilled-margins indicate a parent magma composition high in MgO (11-12%) and low in Al_2O_3 (9-10%) compared to normal basalt types but quite similar to high-Mg basalts described from Archean greenstone belts in South Africa, Australia and Canada. Calculation of an initial liquid using available analyses and assuming the volume of the units is proportional to their thickness gives a liquid richer in MgO (17%) than the chilled-margin analyses. Preliminary studies suggest that some chromite and olivine may have crystallized prior to intrusion as sills.
4. The presence of the high-Mg magmas contemporaneously with normal tholeiites suggests the possibility of different magma sources for each. It may also indicate

differing degrees of partial melting in the mantle.

The ultramafic lenses appear to have formed from small injections of the same olivine-bearing magma that formed the larger layered sills. The olivines were apparently concentrated towards the center of the lens through flowage differentiation with the surrounding crystal free liquid being rapidly cooled or quenched. Some lenses may also represent the residue from which the gabbroic portion was tapped off to form unlayered gabbro sills.

As this is the first examination to be done in any detail on the sills and lenses of the Newton Lake Formation more work is clearly required to fully decipher their history. Some areas of further research that should be pursued are:

1. A further examination by microprobe methods of the compositional variation of cumulus phases in the sills.
2. A detailed study of the chemistry of the parent liquid to the sills and lenses.
3. A detailed study of the ultramafic lenses to determine their chemical composition and relation to the layered sills.
4. A further examination of the complex chilled-margins associated with both the layered sills and lenses to more fully understand their development.
5. A study of the metamorphic alteration which has

affected the intrusive rocks of the Newton Lake Formation.

6. A study of the controls on sulfide mineralization in sills of this nature.

REFERENCES

Anderson, Daniel H., 1965, Uranium-Thorium-Lead ages of zircons and model lead ages of feldspars from the Saganaga, Snowband, and Giants Range Granites of northeastern Minnesota: Unpublished Ph. D. Thesis, Univ. of Minnesota.

Arth, G. J., Jr., 1973, Geochemistry of Early Precambrian igneous rocks, Minnesota-Ontario: Unpublished Ph. D. Thesis, State University of New York at Stony Brook.

Arth, J. G. and Hanson, G. N., 1972, Quartz diorites derived by partial melting of eclogite or amphibolite at mantle depths: Contr. Mineral. and Petrol., v. 37, p. 161-174.

Bartholome, P., 1962, Iron-magnesium ratio in associated pyroxenes and olivines: in Petrologic studies: Geol. Soc. America Buddington volume, p.1-20.

Bence, A. E. and Papike, J. J., 1972, Pyroxenes as recorders of lunar basalt petrogenesis: Chemical trends due to crystal-liquid interaction: Proc. Third Lunar Sci. Conf., Geochim. Cosmochim. Acta Suppl. 3, v. 1, p. 431-469, MIT Press.

Berkley, J. L., 1972, The geology of the Deer Lake Gabbro-Peridotite Complex Itasca County, Minnesota: Unpubl. Masters Thesis, Univ. of Missouri, 107p.

Boyd, F. R. and Schairer, J. F., 1964, The system $MgSiO_3$-$CaMgSi_2O_6$: Jour. Petrology, v. 5, p. 275-309.

Brooks, C. and Hart, S., 1972, An extrusive basaltic komatiite from a Canadian Archean metavolcanic belt: Canadian Jour. Earth Sci., v.9, p. 1250-1253.

Cameron, E. N., 1969, Postcumulus changes in the Eastern Bushveld Complex: American Mineralogist, v. 54, p. 754-779.

Clarke, D. B., 1970, Tertiary basalts of Baffin Bay: possible primary magma from the mantle: Contr. Mineral. and Petrol., v. 25, p. 203-224.

Clements, J. M., 1903, The Vermilion iron-bearing district of Minnesota: U. S. Geol. Survey Mon. 45, 463p.

Coleman, R. G. and Keith, T. A., 1971, A chemical study of serpentinization - Burro Mountain, California: Jour. Petrology, v. 12, p. 311-328.

Davis, B. T. C. and Boyd, F. R., 1966, The join $Mg_2Si_2O_6$-$CaMgSi_2O_6$ at 30 kilobars pressure and its application to pyroxenes from kimerberlites: Jour. Geophys. Research, v. 71, p. 3567-3576.

Deer, W. A., Howie, R. A. and Zussman, J., 1963, Rock Forming Minerals, v. 2, Chain Silicates; Langmans, Green and Co., London, 378p.

Drever, H. I. and Johnston, 1966, A natural high-lime silicate liquid more basic than basalt: Jour. Petrology, v. 7, p. 414-420.

Evans, B. W. and Wright, T. L., 1972, Composition of liquidus chromite from 1959 (Kilauea Iki) and 1965 (Makaopuhi) eruptions of Kilauea Volcano, Hawaii: American Mineral., v. 57, p. 217-230.

Franco, R. R., and Schairer, J. F., 1951, Liquidus temperatures in mixtures of the feldspars of soda, potash and lime: Jour. Geology, v. 59, p. 259-267.

Goldich, S. S., 1968, Geochronology in the Lake Superior region: Canadian Jour. Earth Sci., v. 5, p. 715.

Goldich, S. S., Nier, A. O., Baadsgaard, H., Hoffman, J. H., and Krueger, H. W., 1961, The Precambrian geology and geochronology of Minnesota: Minnesota Geol. Survey, Bull. v. 41, 193p.

Goldich, S. S., Hanson, G. N., Halliford, C. R. and Mudrey, M. G., Jr., 1972, Early Precambrian rocks in the Saganaga Lake - Northern Light Lake area, Minnesota-Ontario: Part I. Petrology and Structure, p.151; Part II. Petrogenesis, p.179, Geol. Society America Memoir 135.

Grant, J. A. and Weiblen, P. W., 1971, Retrograde zoning in garnet near the second sillimanite isograd; American Jour. Sci., v. 270, p. 281-296.

Green J. C. 1970a, Lower Precambrian rocks of the Gabbro Lake quadrangle, northeastern Minnesota: Minnesota Geol. Survey Spec. Pub. SP-13, 96p.

--------, 1970b, Ultramafic bodies in the Vermilion District near Ely, Minnesota (abs.): Ann. Inst. Lake Superior Geol., 16th, Thunder Bay (Ontario), p. 17.

Green, J. C., Phinney, W. C. and Weiblen, P. W., 1966, Gabbro Lake quadrangle, Lake County, Minnesota: Minn. Geol. Survey Misc. Map M-2.

Griffin, W. L., 1969, Embarrass quadrangle, St. Louis County, Minnesota: Minn. Geol. Survey Misc. Map M-6.

Griffin, W. L., and Morey, G. B., 1969, The geology of the Isaac Lake quadrangle, St. Louis County, Minnesota: Minn. Geol. Survey Spec. Pub. SP-8, 57p.

Grout, F. F., 1926, The geology and magnetite deposits of northern St. Louis County, Minnesota: Minn. Geol. Survey Bull. 21, 220p.

Grover, J. E. and Orville, P. H., 1969, The partitioning of cations between coexisting single and multi-site phases with application to the assemblages: orthopyroxene - clinopyroxene and orthopyroxene - olivine: Geochim. Cosmochim. Acta, v. 33, p. 205-226.

Gruner, J. W., 1941, Structural geology of the Knife Lake area of northeastern Minnesota: Geol. Soc. America Bull., v. 52, p. 1577-1642.

Hanson, G. N., Goldich, S. S., Arth, J. G. and Yardley, D. H., 1971, Age of the Early Precambrian rocks of the Saganaga Lake-Northern Light Lake area, Ontario-Minnesota: Canadian Jour. Earth Sci., v. 8, p. 1110-1124.

Hart, S. R. and Davis, G. L., 1969, Zircon U-Pb and whole rock Rb-Sr ages and early crustal development near Rainy Lake, Ontario: Geol. Soc. America Bull., v. 80, p. 595-616.

Hess, H. H., 1960, Stillwater igneous complex, Montana: Geol. Soc. America, Memoir 80.

Irvine, T. N., 1965, Sedimentary structures in igneous intrusions with particular reference to the Duke Island Ultramafic Complex: Am. Assoc. Petroleum Geologists Bull., Spec. Pub. 12, p. 220-232.

--------, 1967, Chromian spinel as a petrologic indicator, Part 2. Petrologic aplications: Canadian Jour. Earth Sci., v. 4, p. 71-

--------, 1970, Crystallization sequences in the Muskox intrusion and other layered intrusions: Olivine - Pyroxene - Plagioclase relations: Geol. Soc. S. Africa Spec. Pub. 1, p. 441-476.

Irvine, T. N. and Findlay, T. C., 1972, Alpine-type peridotite with particular reference to the Bay of Islands complex: Earth Physics Branch Pub., Dept. Energy, Mines and Resources, Ottawa, v. 42, p. 97-128.

Jackson, E. D., 1961, Primary textures and mineral associations in the ultramafic zone of the Stillwater complex, Montana: U. S. Geol. Survey Prof. Paper 358, 106p.

----------, 1969, Chemical variation in coexisting chromite and olivine in chromite zones of the Stillwater complex: Econ. Geol. Monograph 4, p. 41-71.

----------, 1971, The origin of ultramafic rocks by cumulus processes: Fortschritte der Mineralogie, v. 48, p. 128-174.

Jahn, Bor-ming and Murthy, V. R., 1971, Rb-Sr isotopic studies of the Vermilion greenstone belt, northeastern Minnesota (abs.): Geol. Soc. America Abs. with Programs, v. 3, p. 611.

Kretz, R., 1963, Distribution of magnesium and iron between orthopyroxene and calcic pyroxene in natural mineral assemblages: Jour. Geology, v. 71, p. 773-785.

Lewis, J. F., 1973, Petrology of the ejected plutonic blocks of the Soufriere Volcano, St. Vincent, West Indies: Jour. Petrology, v. 14, p. 81-112.

Lofgren, G. E., 1972, Crystallization studies of plagioclase (abs.): Trans. American Geophys, Union, v. 53, p. 549.

----------, 1973, Experimental evidence bearing on the origin of "Comb (Willow Lake) Layering" (abs.): Geol. Soc. America Abs. with Programs, v. 5, p. 716.

MacDonald, G. A., 1949, Hawaiian petrographic province: Geol. Soc. America Bull., v. 60, p. 1541-1596.

----------, 1972, Volcanoes: New Jersey, Prentice-Hall, Inc., 510p.

MacDonald, G. A. and Katsura, T., 1964, Chemical composition of Hawaiian lavas: Jour. Petrology, v. 5, p. 82-133.

MacRae, N. D., 1969, Ultramafic intrusions of the Abitibi area, Ontario: Canadian Jour. Earth Sci., v. 6, p. 281-299.

Manson, V., 1967, Geochemistry of basaltic rocks - major elements: in Hess and Poldervaart, Basalts, v. 1, Interscience Publishers, John Wiley, New York, p. 215-270.

Martin, B., 1971, Some comments on the processes of serpentinization from experimental and otjer work: Geol. Soc. Australia Spec. Pub. 3, p. 301-310.

McCall, G. J. H., 1972, The nickel-sulphide bearing ultramafic rocks and their environments in the Archean of Western Australia: 24th Inter. Geol. Congress, Montreal section 1, p. 354-362.

McCall, G. J. H. and Leishman, J., 1971, Clues to the origin of Archean eugeosynclinal peridotites and the nature of serpentinization: Geol. Soc. Australia Spec. Pub. 3, p. 281-300.

Miyashiro, A., Shido, F. and Ewing, M., 1969, Composition and origin of serpentinites from the Mid-Atlantic Ridge near 24° and 30° north latitude: Contr. Mineral. and Petrol., v, 23, p. 117-127.

Moore, J. G., 1965, Petrology of deep sea basalt near Hawaii: Am. Jour. Sci., v. 263, p. 40-52.

Morey, G. B., Green, J. C., Ojakangas, R. W. and Sims, P. K., 1970, Stratigraphy of the Lower Precambrian rocks in the Vermilion district, northeastern Minnesota: Minn. Geol. Survey Rept. Inv. 14, 33p.

Naldrett, A. J., 1972, Archean ultramafic rocks: Earth Physics Branch Pub., Dept. Energy, Mines and Resources, Ottawa, v. 42, p. 141-151.

----------, 1973, Nickel sulphide deposits - Their classification and genesis, with special emphasis on deposits of volcanic association: Canadian Inst. Mining Bull., v. 66, p. 45-63.

Naldrett, A. J. and Mason, G. D., 1968, Contrasting Archean ultramafic igneous bodies in Dundonald and Clerque Townships, Ontario: Canadian Jour. Earth Sci., v. 5, p. 111-143.

Nesbitt, R. W., 1971, Skeletal crystal forms in the ultramafic rocks of the Yilgarn Block, Western Australia: Evidence of an Archean ultramafic liquid: Geol. Soc. Australia Spec. Pub. 3, p. 331-350.

Peterman, Z. E., Goldich, S. S., Hedge, C. E. and Yardley, D. H., 1972, Geochronology of the Rainy Lake region, Minnesota - Ontario: Geol. Soc. America Memoir 135.

Poldervaart, A. and Hess, H. H., 1951, Pyroxenes in the crystallization of basaltic magma: Jour. Geol., V, 51, p. 4 - 72.

Prince, L. A. and Hanson, G. N., 1971, Geochronology of the Giants Range Granite (abs.): Ann. Inst. Lake Superior Geol., 17th, Duluth (Minn.), p. 57.

Pyke, D. R., Naldrett, A. J. and Eckstrand, O. R., 1973, Archean ultramafic flows in Munro Township, Ontario: Geol. Soc. America Bull., v. 84, p. 955-978.

Ripley, E. M., 1973, The ore petrology and structural geology of the Lower Precambrian Deer Lake mafic - ultramafic complex, Effie, Itasca County, Minnesota: Unpublished M. S. Thesis, Univ. of Minn. - Duluth, 142p.

Roedder, E. and Weiblen, P. W., 1971, Petrology of silicate melt inclusions, Apollo 11 and Apollo 12 and terrestrial equivalents: Proceedings 2nd Lunar Science Conference, v. 1, p. 507-528.

Simkin, T. and Smith, J. V., 1970, Minor - element distribution in olivine: Jour. Geol., v. 78, p. 304-325.

Sims, P. K., 1972, Metavolcanic and associated synvolcanic rocks in Vermilion district: in Sims, P. K. and Morey, G. B., editors, Geology of Minnesota: A Centennial Volume, p. 63-75.

Sims, P. K., Green, J. C., Morey, G. B. and Ojakangas, R. W., 1972, Geology of the western part of the Vermilion metavolcanic - metasedimentary belt, northeastern Minnesota: in Lower Precambrian volcanic - sedimentary rocks of the Vermilion district, Minnesota, Field Trip Guidebook, Minn. Geol. Survey Guidebook Series No. 2., p. 1-20.

Taubeneck, W. H. and Poldervaart, A., 1960, Geology of the Elkhorn Mountains, northeastern Oregon: Part 2. Willow Lake Intrusion: Geol. Soc. America Bull., v. 71, p. 1295-1322.

Travis, G. A., Woodall, R. and Bartram, G. D., 1971, The Geology of the Kalgoorlie Goldfield: Geol. Soc. Australia Spec. Pub. 3, p. 175-190.

Thayer, T. P., 1966, Serpentinization considered as a constant volume metasomatic process: American Mineral., v. 51, p. 685-710.

Thompson, R. N., 1973, Titanium chromite and chromian titanomagnetite from a Snake River Plain basalt, a terrestrial analoque to lunar spinels: American Mineral., v. 58. p. 826-830.

Turner, F. J., 1968, Metamorphic Petrology: New York, McGraw Hill, 403p.

Viljoen, M. J. and Viljoen, R. P., 1969a, Evidence for the existence of a mobile extrusive peridotite magma from the Komati Formation of the Onerwacht Group: Geol. Soc. S. Africa Spec. Pub. 2, p. 87-112.

---------- and ----------, 1969b, The geology and geochemistry of the lower ultramafic unit of the Onerwacht Group and a proposed new class of igneous rock: Geol. Soc. S. Africa Spec. Pub. 2, p. 55-85.

Viljoen, R. P. and Viljoen, M. J., 1970, The geology and geochemistry of the layered ultramafic bodies of the Kaapmuiden area, Barberton Mountain Land: Geol. Soc. S. Africa Spec. Pub. 1, p. 661-688.

Wadsworth, W. J., 1973, Magmatic sediments: Minerals Sci. and Engineering, v. 5, p. 25-35.

Wager, L. R., Brown, G. M. and Wadsworth, W. J., 1960, Types of igneous cumulates: Jour. Petrol., v. 1, p. 73-85.

Wager, L. R. and Brown, G. M., 1968, Layered Igneous Rocks: W. H. Freeman and Company, 555p.

Weigand, P. W. and Hollister, L. S., 1973, Basaltic Vitrophyre 15597: An undifferentiated melt sample: Earth and Planetary Sci. Letters, v. 19, p. 61-74.

Willemse, J., 1969, The geology of the Bushveld Igneous Complex, the largest repository of magmatic ore deposits in the world: Econ. Geology Monograph 4, p. 1-22.

Williams, D. A. C., 1971, Determination of primary mineralogy and textures in ultramafic rocks from Mt. Monger, Western Australia: Geol. Soc. Australia Spec. Pub. 3, p. 259-268.

----------, 1972, Archean ultramafic, mafic and associated rocks, Mt. Monger, Western Australia: Jour. Geol. Soc. Australia, v. 19, p. 163-188.

Williams, D. A. C. and Hallberg, J. A., 1973, Archean layered intrusions of the Eastern Goldfields region, Western Australia; Contr. Mineral. and Petrol., v. 38, p. 45-70.

Wilson, H. D. B., Andrews, P., Moxham, R. L. and Ramlal, K., 1965, Archean volcanism in the Canadian shield: Canadian Jour. Earth Sci., v. 2, p. 161-175.

Wood, J. A., Marvin, U. B., Reid, J. B. Jr., Taylor, G. J., Bower, J. F., Powell, B. N. and Dickey, J. S. Jr., 1971, Mineralogy and petrology of the Apollo 12 lunar sample: Smithsonian Astrophys. Observatory Spec. Report 333.

Wright, T. L. and Weiblen, P. W., 1967, Mineral composition and paragenesis in the tholeiitic basalt from Makaopuhi lava lake, Hawaii (abs.): Geol. Soc. America Abs. with Program, v.78, p. 242-243.

Wright, T. L. and Doherty, P. C., 1970, A linear programming and least squares computer method for solving petrologic mixing problems: Geol. Soc. America Bull., v. 81, p. 1995-2008.

Wright, T. L. and Fiske, R. S., 1971, Origin of the differentiated and hybrid lavas of Kilauea Volcano, Hawaii: Jour. Petrol., v. 12, p. 1-65.

Yoder, H. S. Jr., 1954, Synthetic basalt: Carnegie Inst. Washington, Yearbook 53, p. 106-107.